# Simulation Modelling for In-field Planning of Sequential Machinery Operations in Cropping Systems

by Kun Zhou

AARHUS
UNIVERSITY

# Simulation Modelling for In-field Planning of Sequential Machinery Operations in Cropping Systems

# Simulation Modelling for In-field Planning of Sequential Machinery Operations in Cropping Systems

---

**PhD Thesis by**

**Kun Zhou**

*Aarhus University Department of Engineering, Denmark*

AARHUS
UNIVERSITY
DEPARTMENT OF ENGINEERING

River Publishers

# Preface

This thesis is submitted to the Graduate School of Science and Technology (GSST), Aarhus University, in partial fulfilment of the requirements for the degree of Doctor of Philosophy (PhD). It documents the results of my research that was carried out from January 2012 to January 2015 at the Operations Management group at the Department of Engineering, Aarhus University. The research was funded by the Chinese Scholarship Council (CSC) (Grant No: 2011635157) and Department of Engineering.

The thesis is supported by the following collection of published articles and submitted manuscripts:

1) **K. Zhou**, A. Leck Jensen, D.D. Bochtis, C.G. Sørensen, 2013. *A web–based tool for comparing field area coverage practices.* (Presented orally and published in conference proceedings at the CIOSTA XXXV Conference, 3 to 5 July 2013 , Billund, Denmark).

2) **K. Zhou**, A. Leck Jensen, C.G. Sørensen, P. Busato, D.D. Bochtis, 2014. *Agricultural operations planning in fields with multiple obstacle areas.* Computers and Electronics in Agriculture, 109, 12-22. (Published)

3) **K. Zhou**, A. Leck Jensen, D.D. Bochtis, C.G. Sørensen, *Quantifying the benefits of alternative fieldwork patterns in potato cultivation system.* (In review at the peer-reviewed journal：Computers and Electronics in Agriculture. Under review.).

4) **K. Zhou**, A. Leck Jensen, D.D. Bochtis, C.G. Sørensen, *Simulation model for the sequential in-field machinery operations in the potato production system.* (Submitted to the peer-reviewed journal：Computers and Electronics in Agriculture. Under review).

5) **K. Zhou**, A. Leck Jensen, D.D. Bochtis, C.G. Sørensen, *Performance of machinery in potato production in one growing season.* (Submitted to the peer-reviewed journal: Spanish journal of agricultural research. Under review).

# Acknowledgements

First and foremost, my sincerest gratitude goes to my principal supervisor Dr. Allan Leck Jensen for his continuous support of my PhD study and research, for his patience, encouragement, enthusiasm, and broad knowledge. His guidance helped me in all the time of research and writing of this thesis. I could not have imagined having a better supervisor for my PhD study.

I would like to express my sincerest gratitude to my co-supervisor Dr. Dionysis Bochtis, who offered his continuous advice and help throughout the course of my PhD research. I thank him for the systematic guidance to train me in the scientific field. My thanks also extend to Dr. Claus Aage Grøn Sørensen for his valuable help and discussion on the PhD research.

I deliver my thanks to all the colleagues and friends that I have met in this beautiful country, Denmark, for their support and kindness. Without you, this journey would not have been possible.

Furthermore, special thanks to the Jens Peter Skov Jensen, Inge Skafte Jensen, Niels Frederik Skov Jensen, Jens Christian Skov Jensen, and Anne Luise Skov Jensen for their cooperation of gathering GPS data and warm hospitality.

I am especially grateful to my grandparents and parents, who supported me emotionally and financially. I always knew that you believed in me and gave the best for me. Thank you for teaching me that my role in life is to learn, to be happy, and to know and understand myself and to be kind and generous to others. Thanks also to my dear sister and relatives for their great love and care.

Finally, I thank with love to my girlfriend Yue Yuan who has been my best friend and great companion, loved, supported, encouraged, understood. I do not know what the future holds, but I do know that I hope to get through all the moments not matter if it is tough or happy holding you.

– Zhou Kun, Foulum, 20th January, 2015

# Abstract

In highly mechanized agriculture farmers are facing many challenges in the strongly competitive agricultural market. The challenges are economical (e.g. higher labor costs, higher fuel prices, increasing investment in larger and larger and more and more specialized machinery) as well as environmental (e.g. regulative provision and effects of climate changes). In order to maximize the profits farmers have to reduce the production cost while maintaining high product quality. The annual cost of machinery management and operation is a significant part of the annual production cost. Therefore, the development of technologies to improve the machinery productivity and operational efficiency is of key importance.

This PhD research focuses on improving the machinery performance of agricultural field operations through generation of optimized coverage planning and simulation models of the operations and the machinery. As a prerequisite for the operation modelling and validation, a range of field operations were monitored using deployed GPS equipment. In order to analyze and decompose the recorded GPS data into various time and distance elements, an automatic GPS analysis tool for a complete set of operations in potato production was developed. In terms of optimized coverage planning, a three-stage planning method that generates feasible area coverage plans for agricultural machines executing non-capacitated operations in fields inhabiting multiple obstacle areas was developed. As a spin-off from this development, a functional prototype of web-based field coverage planning was developed. In terms of simulation model development, a targeted simulation model that simulates all in-field sequential operations in potato production was developed. The model includes all key parameters for the evaluation of user selected scenarios. In order to demonstrate the capability of this simulation model as a decision support system (DSS), it has been applied as a way to assess the potential savings by simulating non-working distance and time using pre-determined motifs of field coverage track sequences and compare with user selected ones. The assessment results can be used by machine operators to select a realizable field work pattern that improves the overall field efficiency for a specific combination of field and machinery characteristics.

# Sammenfatning på dansk

Landmænd står over for mange udfordringer i vores højt mekaniserede landbrug og i det meget konkurrenceprægede landbrugsmarked. Udfordringerne er både økonomiske (f.eks. stigende lønomkostninger, stigende brændstofpriser, øget behov for investeringer i maskiner, der bliver stadigt større og mere specialiserede) og miljømæssige (f.eks. miljømæssige reguleringer og effekter af klimaforandringer). For at maksimere deres fortjeneste er landmændene nødt til at reducere produktionsomkostningerne og samtidig opretholde en høj produktkvalitet. De årlige udgifter til drift og vedligehold af maskiner er en betragtelig del af de samlede produktionsomkostninger. Derfor er udviklingen af metoder og teknologier til forbedring af maskinernes produktivitet og til en smartere anvendelse af dem af afgørende betydning.

Denne PhD-afhandling fokuserer på at forbedre produktiviteten for landbrugsmaskiner til markoperationer. Dette gøres dels ved at udvikle metoder til planlægning af, hvordan maskinerne skal køre i markerne, så hele markarealet dækkes på bedst mulig måde (en *dækningsplan*), dels ved at udvikle simuleringsmodeller af markoperationerne og maskinerne. Som en forudsætning for modelleringen af markoperationerne og for validering af de udviklede modeller blev de vigtigste markoperationer i en række kartoffelmarker overvåget vha. GPS udstyr installeret i de anvendte maskiner. For at analysere de indsamlede GPS data blev der udviklet et analyseværktøj, der automatisk kan opdele de indsamlede GPS data i sekvenser, hvor hver sekvens er et stykke ensartet arbejde, produktivt eller uproduktivt (f.eks. en vending i forageren), målt i kørt distance og forbrugt tid. Samlet set giver sekvenserne et mål for den opnåede effektivitet af maskinen i markoperationen. Med hensyn til optimering af kørslen i marken blev der udviklet en metode til at udvikle en dækningsplan i marker med forhindringer. Metoden foregår i tre trin, hvor første trin består i at repræsentere marken og forhindringerne geometrisk som polygoner, hvorefter forhindringerne klassificeres efter størrelse og beliggenhed. Forhindringer, der ligger tæt på hinanden i forhold til maskinens bredde og kørselsretning, smeltes sammen, og forhindringer, der er smalle i forhold til kørselsretningen bliver negligeret i den efterfølgende behandling. Næste trin er at opdele marken i delarealer uden betydende forhindringer, og sidste trin at finde den optimale måde at forbinde delarealerne på. Som et afledt resultat

blev der udviklet en funktionel prototype af et web-baseret værktøj til at udvikle og præsentere en dækningsplan for en mark udvalgt af brugeren. Med hensyn til udvikling af simuleringsmodeller blev der udviklet en samlet model, der kan simulere alle de vigtigske sekventielle markoperationer i kartoffelproduktionen. For at demonstrere muligheden for at benytte simuleringsmodellen som et beslutningsstøttesystem blev den anvendt til at simulere en række scenarier og derved få et mål for effekten af at ændre på forskellige parametre, så som kørselsretning, arbejdsbredde. Modellen blev desuden brugt til at sammenligne forskellige, almindeligt anvendte kørselsmønstre, dvs. en fast metode til at vælge rækkefølgen af rækker, der skal køres efter. Ved at vælge det bedste mønster for en given mark kan operatøren udføre arbejdet hurtigere, med mindre brændstofforbrug, med mindre jordkomprimering og/eller med mindre spild ved dobbelt eller manglende behandling.

# Contents

# Chapter 1

# General introduction

# 1   General introduction

## 1.1   Background

In crop production, usually several sequential operations are required through an entire growing season, and in general the common operations are: cultivation, seeding, fertilizing, crop protection and harvesting. All these operations are accomplished by dedicated machines, either by a tractor attached with one or more implements or by self-propelled agricultural machines. According to the recognized definitions introduced by Bochtis and Sørensen (2009), agricultural machines can be classified into *primary units* (PUs) that execute the main task and *service units* (SUs) that reload or unload the PUs. For instance, in a grain harvesting operation, usually a harvester (PU) is unloaded by transport carts (SUs) that move the grain out of the field to the storage places. In addition, agricultural operations, according to the direction of material flow, can be categorized as "*neutral material flow*" operations (e.g. ploughing, bed preparation), "*input material flow*" operations (e.g., spraying, and fertilizing) and "*output material flow*" operations (e.g., harvesting).

Although the increased average size of machinery has led to increased productivity, this trend also has unwanted environmental and biological side effects (e.g. soil compaction). Therefore, more efforts are being contributed to the development of advanced Information and Communication Technology (ICT) systems and decision support models to achieve higher operational efficiency and machinery productivity (Sørensen and Bochtis, 2010). Currently, commercial auto-steering and GPS systems have been widely adopted. However, the potentials of such systems are not fully realized because they still partially rely on the users' decisions, for example in the case of determining the direction of tracks, which is normally done unsupported, according to user's experience and knowledge. This strategy may be not optimal. In order to fully utilize the advantages of navigation aiding systems and improve the operation's efficiency, a significant amount of research has been dedicated to the problem of field coverage planning (*cf.* Bochtis *et al.*, 2014) which can provide plans either for PUs or SUs to execute field operations based on one or multiple optimization criterions that include the minimization of the total distance traversed, the non-working turning distance and

time, or the total operational time. Yet, there is still room for further development of complete methods that can provide optimized coverage plans for fields with obstacles. Furthermore, field operation simulation models also have received significant interest because such models can be used to evaluate and quantify the operational efficiency and performance of machinery based on user-defined scenarios. A model simulation of a scenario is a much more time efficient and less costly way of gathering experience than having to test each scenario under real life conditions, obviously under the assumption that the simulation model is reliable. Nevertheless, it is impossible to make a universal model capable of simulating all the operations in any crop production as each operation has its own unique operational features for a given crop; harvesting of barley is very different from harvesting of corn or potatoes, and completely different machinery is required. Therefore, for simulating a specific operation or multiple sequential operations in a crop production, a dedicated simulation model has to be developed for the particular crop production.

## 1.2 Monitoring and analysis of field operations

Monitoring and analysis of field operations are considered a key step for machinery management and model development and validation. Machinery performance estimation is an important aspect of machinery management, and the estimation processes can be divided into *offline* or *online* according to the time of the recorded data processing take place. The offline estimation is often done after the field operation to evaluate it, or before the operation to plan it, based on the data from the previous operations. In contrast to this, the online estimation takes place during the operation. In the following measures of machine performance is described, and a survey of the literature for offline and online estimation is presented.

### 1.2.1 Machinery performance

Traditionally, machinery performance has been carried out based on manual observations using stopwatch and clipboard, but this method is time demanding and laborious for researchers during the operation (Renoll, 1981; Sørensen and Møller, 2006; Sørensen and Nielsen, 2005). In the past decade, extensive use of GPS (Global Positioning System) and dedicated sensors have provided farm managers with new opportunities to measure machinery performance based on automatically acquired and high accuracy data. These collected

data of the machinery motions can be analyzed offline by decomposing them into various task time/distance elements, and afterwards aggregate the elements into information about the fieldwork pattern, the turning types and subsequently about the performance, expressed as the field efficiency and the field capacity.

*Field efficiency* is calculated as the ratio of the time a machine is effectively working to the total time committed by the machine during the whole operation, while *field capacity* is defined as the area processed per unit of time for a particular field operation. The knowledge gained from such recorded data analysis enable farm managers to make better management decisions to explore potential improvement in machine productivity, efficiency and potential benefits for the environment.

### 1.2.2    Offline estimation of the machinery performance

Grisso *et al.* (2002) gathered data for planting and harvesting within two crop productions from five fields representing both contour and straight traffic pattern to estimate the operational speed, time and field efficiency. Both operations were recorded using GPS. The analysis results showed that the machine had higher average travel speeds in straight rows than contour rows by about 1.6 km h$^{-1}$. The straight rows had 10% and 20% higher field efficiency comparing to contour rows'. However, in this paper, the effect of non-productive time elements, such as turning, refilling/ unloading travelling on field efficiency were not investigated. As a continued effort to investigate the effect of steering angle on field efficiency, Grisso *et al.* (2004) recorded geo-referenced data from five fields for soybean and corn planting and harvesting operations using yield monitors and GPS loggers. The study results indicated that the average steering angle had strong correlation with the field efficiency. Taylor *et al.* (2002) collected data of harvesting in 23 fields over six years including some fields with identical operations (same crop harvested by identical machines) in different years. A computer program was employed to decompose recoded data into various in-field activities: effective harvesting, turning, unloading, stopped and overnight based on heuristic time thresholds. The results showed that the time-based field efficiency significantly varied in different fields, and even on the same field with identical operations in different years. The author stated that optimizing the fieldwork pattern is a promising method to increase the field efficiency by minimizing turn time/distance. Bochtis *et al.* (2010) recorded slurry applications using two types of traffic systems: controlled traffic system (CTF) and

14

uncontrolled traffic system (UCTF) in two fields to investigate the effect of CTF on field efficiency. The comparison showed that implementation of CTF considerably increase the in-field transport distance, relative to the UCTF system. The increased in-field transport distance results in a reduction of field efficiency in the range from 4.68% to 7.41%. Ntogkoulis *et al.* (2014) monitored three in-field sequential operations: cutting, raking, and baling of cotton residue in 43 fields to evaluate the machinery performance. The measured field efficiencies and capacities were compared with calculated field efficiencies and capacities of identical machineries using ASABE (American Society of Agricultural and Biological Engineers) standard data for hay handling. The comparisons showed that the ASABE norms for hay handling operation cannot be applied to the handling of cotton residues where the measured field capacity were 15% lower, 21% lower and 2% higher than the corresponding estimated capacity based on ASABE data for cutting, raking, and baling, respectively. It can be found that all the above studies focused on estimation of the performance of a single machine or multiple machines that were involved in one field operation, while no research efforts have been contributed to estimate the performance of all machines in all field operations of a cropping system.

### 1.2.3    Online estimation of machinery performance

`The introduction of the on-board computer with advanced computer and electronic technology has offered opportunities for measuring, monitoring and estimating the performance of the machinery in real-time during the field operation. Yule *et al.* (1999) presented a data acquisition system to monitor in-field performance of an agricultural tractor. Transducers were used to measure various operational parameters such as the engine, wheel and ground speed with further devices to measure fuel consumption and field slope, and the force was also measured using a dynamometer system. The testing results from this field work showed that significant savings can be achieved by improving the machine set up according to the provided information. In this study, a saving of £4.70 ha$^{-1}$ was demonstrated while using a tined cultivator in stubble. Amiama *et al.* (2008) developed an online information and documentation system for the performance of a forage harvester. The recorded online information consisted of performance data (operation speed, location, harvested yield, etc.), machine settings (knife drum speed, etc.) and machine warnings (oil levels, oil pressure, oil temperature, etc.), which can be displayed on a monitor mounted in the cab for operator to make accurate and fast

decisions. The author stated that the implementation of this system would lead to savings of 1902€/ year for the co-operative. Yahya *et al.* (2009) developed a mapping system for monitoring the tractor-implement performance, which can in real-time measure, display and record the tractor's theoretical travel speed, actual travel speed, fuel consumption rate, rear drive wheel slippage, rear drive wheel torque, pitch and row angles, implement's PTO torque, drawbar force, three-point hitch forces, and tillage depth and position of the tractor. Kaivosoja *et al.* (2014) developed a system integrating different external sources data from CAN-bus and GPS to the task controller on the tractor. With the gathered data, spatial and/or temporal information, automatic operational control can be made during the work execution.

## 1.3  Agricultural field area coverage planning

In the past decade, commercial auto steering or navigation-aid systems (e.g. Trimble and John Deere) have been extensively introduced on agricultural machines with the benefits of reduction of input costs due to more accurate driving patterns, causing reduced overlaps and skips, reduced soil compaction, reduced operator's fatigue and improved machinery productivity. These systems enable machines to drive along parallel straight (Fig. 1.a) or curved tracks (Fig. 1.b) for complete field coverage with high accuracy. However, hardly any operational optimization has been taken into consideration in the current systems, which is relevant, especially in complex fields with inhabited obstacles (Jin, 2009). Area coverage planning is one of the promising solutions for these systems, which determines a path that passes over all points of a targeted spatial environment under the criterion of minimization of cost (such as time and distance) while avoiding obstacles. This subject has been extensively researched in the industrial robotics domain (Choset, 2001; Galceran and Carreras, 2013). Unfortunately, these developed approaches cannot be directly applied for agricultural machines and robotics due to the inherent features of field operations and agronomic restrictions, e.g. that driving and turning in the cropping area is restricted in order to reduce soil compaction and damage to the crop. However, these approaches have been used as an inspiration for the development of methods for area coverage by agricultural machines.
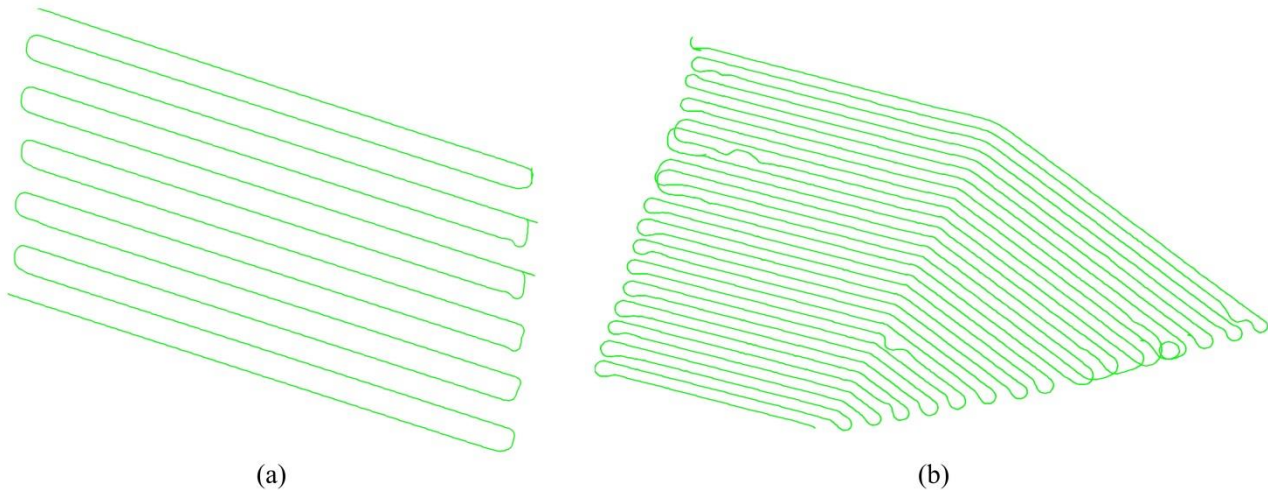
**Fig. 1 – Recorded trajectory using a Trimble auto steering system for (a) fertilizer spreading (operating width: 24 m) with straight tracks in 2013; for (b) tillage (operating width: 8m) with curved tracks in 2014. Both fields are from Lolland, Denmark.**

The approaches on field area coverage planning can be divided into three types, according to type of the outputted solution. The first type is the *spatial configuration planning* which concerns the process of generating a geometrical representation of a field using geometric primitives. The spatial configuration planning mainly comprises three tasks: 1) Decomposition of fields with complex geometry into simple shaped subfields; 2) determination of the driving direction in each subfield; 3) generation of fieldwork tracks according to the driving direction in each subfield. In general, the output of these methods is a set of line segments or polylines representing the fieldwork tracks and headland pass that can be followed by the machine. However, they do not give the answer how and in what sequence to traverse these fieldwork tracks. The second type is the *route planning*, which finds the optimal sequence of traversing these geometric entities, usually the fieldwork tracks that were generated by the spatial configuration planning method. The routing plans do not generate exact motion paths for the machines. This is done with the third type, the *reference trajectory*, which generates drivable smooth motion paths that fulfill the machines' kinematic constraints for agricultural machines. The most interesting part of reference trajectory is how the turnings are taken in the headland. In the following, the state-of-the-art of coverage methods is reviewed according to these three planning types, mentioned above, and combinations of them. The features of these planning approaches are summarized in Table 1.

## 1.3.1 Spatial configuration planning

In the past decade a number of methods have been developed that are capable of dealing with either two-dimensional or three-dimensional terrain fields with or without obstacle areas according to various optimization criterions. Palmer *et al.* (2003) presented a method to generate predetermined fieldwork tracks with objectives of minimization of the overlapped and missed area. The application results of this method in the case of spraying showed that the total travelled distance and material inputs can be reduced by 16% and 10%, respectively. Oksanen and Visala (2007) developed a field decomposition method based on the trapezoidal decomposition for agricultural machines to cover the field. After decomposition, the trapezoids are merged into blocks under the requirement that the blocks have exactly matching edges and the angles of ending edges is not too steep. The optimization criterion was a weighted sum of efficiency and total travelled distance. Jin and Tang (2010) developed an algorithm to decompose complex fields into subfields, followed by a determination of the optimal driving direction in each subfield with the criterion of reducing the turning cost. The results show that up to 16% in the number of turns and 15% in headland turning cost can be saved in comparison to the results derived by other researchers. Bochtis *et al.* (2010) proposed an approach to estimate the operational cost of machinery on an annual basis in CTF systems when adopting different tramlines for establishing driving directions. The main finding of this work is that the driving direction parallel to the longest field edge, which would be optimal in most cases in conventional traffic farming, does not hold true in the case of CTF systems. Hameed *et al.* (2010) presented an algorithmic method for the real time generation of both straight and curved field-work tracks, regardless of the field shape complexity. Later in the work by Hameed *et al.* (2013), this method was expanded for a three-dimensional field geometrical representation to find the optimal driving direction with the criterion of minimizing the direct energy requirements. The case study results indicated that the reduced energy requirement was up to 6.5% on average for all tested scenarios as compared with the case of assuming 2D field areas. Jin and Tang (2011) developed a method to handle three-dimensional field terrains where each field was decomposed into sub regions based on its terrain features. The test results showed that on average the 3D coverage planning method saved 10.3% of the turning cost, 24.7% on soil erosion, 81.2% on skipped area cost and 22.0% on the weighted sum of these costs as compared with 2D planning results.

18

### 1.3.2 Route planning

A typical vehicle route planning (VRP) problem concerns the task to determine a route with minimal cost, where a route visits each location of the domain exactly once. In the industrial sector, numerous applications of this problem have been developed for transportation, distribution and logistics. In agricultural field operations, this problem is also encountered by operators that have to make a decision on how to traverse the fieldwork tracks in order to minimize the non-working cost, which constitutes a VRP problem. Bochtis and Vougioukas (2008) did the first attempt to adopt the VRP methodology to solve the route planning problem for agricultural vehicles operating in one or multiple geographically dispersed fields, in which the field coverage is expressed as a traversal of a weighted graph. The problem of finding the optimal traversal sequence of fieldwork tracks is equivalent to finding the shortest route in a weighted graph and the problem was solved by applying algorithms for solving the travelling salesman problem (TSP). This new fieldwork pattern, the so called B-pattern, is defined as "algorithmically-computed sequences of field-work tracks completely covering an area and that do not follow any pre-determined standard motif, but in contrast, are a result of an optimization process under one or more selected criteria." (Bochtis *et al.*, 2013). Possible optimization criteria include minimization of the total non-working distance and time, total operational time and soil compaction. The implementation of B-pattern for an autonomous tractor was presented in Bochtis *et al.* (2009). The experimental results showed that the non-working distance can be reduced with up to 50% as compared with the conventional coverage plan. In the case of minimization of soil compaction, the risk factor of soil compaction was reduced by 23% and 61% in two experimental fields, respectively, by implementing the B-pattern coverage. In addition, in Bochtis *et al*. (2013) the assessment of the benefits of B-pattern showed that the total non-working distance can be reduced up to 58.65% and the increased area capacity up to 19.23% when comparing with different types of conventional standard fieldwork patterns. Ali *et al.* (2009) modeled the infield logistics planning for a grain harvester as a routing problem with an additional turn penalty when turning inside the fieldwork tracks. The optimization criterion was the minimization of the non-productive distance travelled by the combine harvester in the field. This problem was solved by implementing an exact branch-and-bound solver. The computational time was proven to be impractical for fields with an area of more than 5 ha.

### 1.3.3 Headland turning

For coverage planning, all the fieldwork tracks have to be traversed by the agricultural machines once in order to complete the entire operation. In other words, since the main track distance is not variable for a given spatial configuration plan of a field, two possible route plans only differ in the length and time required for their headland turnings. Therefore, the optimal route plan is determined by optimizing the headland turnings. The time spent on a headland turning depends on the turning length and speed. Some headland turning types are easy to operate at high speed, while others need reverse maneuvers with skillful driving, resulting in higher non-working distance and a lower mean speed. The headland turning cost (distance or time), counting as non-working cost, has a high effect on the field efficiency. So far, a number of advanced turn models have been developed to calculate the headland turning cost. Dubins (1957) proposed a kinematic car model, in which the shortest path, composed by circular arcs of maximum curvature and straight lines, can be generated in order to connect two oriented points. Oksanen (2007) used Bézier curves to approximate the headland turn paths, and the influence of angle deviation and headland width on turn paths was also investigated. In the work of Bochtis and Vougioukas (2008), a geometrical turn model was presented for calculation of the minimum length of the three most common types of headland turns: $T$-turn, $\Omega$-turn and $\Pi$-turn executed by an Ackerman-steering agricultural machine. Jin (2009) developed four types of turns, named: "U", "flat", "bulb", and "fishtail", for agricultural vehicles to estimation of the turn cost (e.g. distance or time) using arcs of circles and straight lines. Cariou *et al.* (2010) addressed the problem of headland turn path generation and motion control for autonomous maneuvering of a farm vehicle with an attached implement using clothoids, polynomial splines and cubic spirals. The presented method consists of two steps: First, the motion primitives are generated and connected, and then a kinematic model is used to generate the trajectories. Edwards and Brøchner (2011) developed a method for smoothed headland path generation for agricultural vehicles based on the constant average acceleration method. Sabelhaus *et al.* (2013) developed a method to generate headland turning paths using continuous-curvature paths both for field robotics and agricultural vehicles. Spekken *et al.* (2015) developed a modified turning model after Jin

(2009) to calculate the cost of boundary maneuvering in sugarcane for planting, cultivating, spraying and harvesting.

### 1.3.4 Integrated algorithms

Integrated algorithms may consist of all or some of the above described approaches. The work of Bochtis and Oksanen (2009) was a first attempt to combine spatial configuration and B-pattern to generate *optimal area coverage planning* for field operations. Hameed *et al.* (2011) developed a two-stage approach: In the first stage, a field spatial configuration method was used to obtain the optimal driving direction based on the minimization of the overlapped area; in the second stage, a sub-optimal route was derived based on the minimization of headland non-working distance. Bochtis et al. (2012) developed a DSS for the route planning for agricultural vehicles implementing time-depended loads with objective to reduce the risk of soil compaction. The results from the system implementation in two experimental fields showed that the risk of soil compaction based on a selected risk factor was reduced by 23% and 61%. Spekken and de Bruin (2013) developed a method, combining spatial configuration, turning models and B-pattern, for route planning based on minimization of turning time and time of loading or unloading of the machine. Hameed (2014) developed an approach for a multi-objectives optimal coverage planning on three-dimensional terrain for field operations, in which a combination of 3D spatial configuration and route planning approaches was used. However, the route planning in fields with multiple obstacles is still unsolved in these studies.

| Author(s) and year | Planning type | | | Geometric features | | | | Optimization | | Targeted operations |
|---|---|---|---|---|---|---|---|---|---|---|
| | Spatial configuration | Route planning | Headland turning | Dimensions (2D/3D) | Field decomposition | Curved track | In-field obstacles | Method | Criterion | |
| Palmer et al., 2003 | Yes | | Yes | 2D | No | No | Yes | Exhaustive search | Minimization of overlapped and missed areas | Spraying |
| Oksanen and Visala, 2007 | Yes | | | 2D | Yes | No | Yes | Greedy search for field decomposition and heuristic search for the determination of driving direction | Minimization of number of headland turnings | Non-capacitated operations |
| Bochtis and Vougioukas, 2008 | | Yes | Yes | 2D | No | No | No | B-pattern generation and solved by implementation of the Clarke-Wright algorithm | Minimization of the non-working distance | Non-capacitated operations |
| Bochtis and Oksanen, 2009 | Yes | Yes | Yes | 2D | Yes | No | Yes | B-pattern generation | Minimization of turning distance | Non-capacitated operations |
| Jin and Tang, 2010 | Yes | | Yes | 2D | Yes | No | Yes | Depth-first search for field decomposition; divide-and-conquer strategy for the optimal driving direction search in each subfield | Minimization of turning distance in the headland area | Non-specific |
| Bochtis et al., 2010 | Yes | | Yes | 2D | No | No | No | Exhaustive enumeration | Annual operational cost | Complete set of operations in CTF system |
| Bochtis et al., 2010 | Yes | Yes | No | 2D | No | No | No | Generation of B-pattern | Minimization of the risk of soil compaction | Capacitated operations |
| Hameed et al., 2010 | Yes | | | 2D | Yes | Yes | Yes | None | None | Non-specific |
| Jin and Tang, | Yes | | Yes | 3D | NO | Yes | No | Heuristic-based | Weighted sum | Non-capacitated |

| | | | | | | | | | | |
|---|---|---|---|---|---|---|---|---|---|---|
| 2011 | | | | | | | | | of the cost of headland turning, soil erosion and skipped area | operations |
| Hameed et al., 2011 | Yes | Yes | Yes | 2D | Yes | No | No | Two stages: Exhaustive search driving direction. A genetic algorithm for B-pattern generation. | Minimization of overlapped area and total travelled distance | Non-capacitated operations |
| Hameed et al., 2013 | Yes | | | 3D | No | No | Yes | Exhaustive search with an simulation model for capacitated operations | Minimization of fuel consumption | Capacitated operations |
| Bochtis et al., 2013 | | Yes | Yes | 2D | No | No | No | B-pattern generation | Minimization of turning distance | Non-capacitated operations |
| Spekken and de Bruin, 2013 | Yes | Yes | Yes | 2D | No | No | No | B-pattern generation | Minimization of non-working time including turning and servicing time | Non-capacitated and capacitated operations. |
| Hameed, 2014 | Yes | Yes | No | 3D | Yes | No | Yes | Two stages: Exhaustive search driving direction. A genetic algorithm for B-pattern generation. | Minimization of direct energy requirement | Capacitated operations |

## 1.4   Modelling and simulation of agricultural field operations

During one operation, there may be several factors affecting the overall performance of the machinery and the cost of the field operation, such as the driving direction, the fieldwork pattern, the operating speed, and the turning type and speed. Nevertheless, making an operational plan that addresses all these factors at once is rather complex, particularly in the case where some factors have opposing effects. For instance, the driving direction with the shortest total turning distance for complete field coverage may not be the same as the driving direction with the smallest double-covered area (the so called "overlapped area") in the headland area. However, simulation models and programs may provide famers opportunities to determine the relative importance of factors affecting the operational efficiency and machinery performance without conducting time consuming field experiments, subsequently to make better managerial or technical decisions. As a result, simulation models and programs, either online or offline, have been developed for various agricultural field operations. In the following, the literature is reviewed separately for offline and online (web-based) simulation models of field operations.

### 1.4.1 Offline simulation models

A discrete event simulation model regarding the in-field motion of machines was developed by Bochtis *et al.* (2009), which is capable of simulating the CTF operations taking the coordination of multiple machines in material handling operations into consideration. Two slurry operations were designed and monitored to validate the developed model, the validation showed that the model can adequately predict the in-field motion of the machine; the prediction errors in terms of total covered distance ranged from 0.24% to 1.41%. Hameed *et al.* (2012) developed an object-oriented model for detailed simulation of in-field machine activities in material input operations during the execution phase. This model encompasses all the key operational parameters for evaluating a user defined scenario in terms of in-field operational decisions (e.g. traffic system, driving direction, etc.) and machinery features (e.g. machine capacity, operating width, etc.). Benson *et al.* (2002) developed a simulation model of in-field harvest operations capable of handling

multiple combines, carts and road transport units co-operating on the same fields. Busato *et al.* (2013) developed an algorithmic approach for planning the operation of liquid organic fertilizer application using an umbilical application system. Busato (2015) developed a targeted simulation of rice harvesting considering in-field and out-field activities of both combine and transport units. The prediction errors ranged between 2.59% and 3.12% in the area capacity.

### 1.4.2 Online simulation models

Little research has been focused on web-based simulation tools for field operations. de Bruin *et al.* (2014) developed a web service for systematic planning and cultivation of agricultural fields. It can help farmers to optimize the spatial configuration of swath in the main cultivated area with the objective of maximizing the balance between the costs of losses of cropping area versus subsidy received for field margins. Busato and Berruto (2014) presented a web-based tool for simulating the production, harvest, and out-of-field transport of biomass in multiple-crop production systems taking individual characteristics, such as soil conditions, machineries and labor types, into consideration. The outputs of this tool are estimations of the total cost of operation and transport.

All the above mentioned simulation models only take the factors of a single operation into consideration, but in multiple sequential operations, the simultaneous optimization criteria become more complex. For example, for row crops the seeding direction affects the driving direction of subsequent operations. Especially for specialized farming systems, such as bed cropping system and controlled traffic system (CTF) there is interdependency between sequential operations. Taking the bed cropping system as an example, the working width of all the machines has to be a multiple of the basic module width, i.e. the width of a bed. In addition, after the seedbed preparation all subsequent operations have to follow the direction of the bed orientation for field coverage. There is a huge potential of optimization both on strategic level (investment in machinery, deciding working width), tactical level (planning of operations, notably driving direction) and operational level (deciding fieldwork pattern, loading/unloading locations etc.). Therefore, a balanced operational plan considering these factors is favorable.

## 1.5  Research objectives

The main objective of this research was to develop field area coverage planning algorithms and simulation models for agricultural field operations. The targeted users are farmers and agricultural advisers who are interested in reducing the operational cost and the environmental impact whilst maximizing the field efficiency. The specific objectives were to:

- Record and analyze the individual task elements of field operations, notably productive elements (performing the main task) and unproductive elements (turning, transport, stopping etc.), in order to understand the operational performance of the machinery as well as the farmers' practice as the basis for developing, validating and benchmarking algorithms and models of the operations. Potato production was chosen as the study case.

- Develop an algorithm to solve the field coverage problem for agricultural machines in fields with multiple obstacles.

- Develop a prototype of a web-based system for interactive field coverage planning.

- Develop a unified simulation model of all the typical in-field sequential operations in potato production and apply the model to simulate the outcome of alternative scenarios.

- Develop an approach to help farm managers to select the proper fieldwork pattern for field coverage.

## 1.6  Overview of contents

The research content of this thesis consists of five parts, corresponding to the five research objectives listed above: Analysis of recorded GPS data in one season of potato production (**Chapter 2**), operation planning for agricultural machines operating in fields with multiple obstacle areas (**Chapter 3**), development of a web-based field coverage planning system (**Chapter 4**)., modelling of in-field sequential operations in potato production (**Chapter 5**), an approach to assess benefits of using alternative fieldwork patterns (**Chapter 6**). These five parts potentially constitute four peer-reviewed articles and one conference paper.

In **Chapter 2**, all operations in two consecutive growing seasons (2013 and 2014) of potato production were recorded with GPS sensors mounted on all in-field machines. The GPS data were processed and analyzed, such that individual task elements of the operations could be measured in length and duration and the performance of the machines could be quantified. This gave a deeper understanding of the farmer's working practice as well as the field operations which was applied in the development of the simulation models. The analysis of the field operations is presented in the first manuscript "*Performance of machinery in potato production in one growing season*".

In **Chapter 3**, a field coverage planning method for agricultural machines operating in fields with obstacle areas was developed. The feasibility of the generated coverage planning was tested and the capabilities of the method for complicated fields with more than two obstacles were demonstrated. This work is presented in the second manuscript "*Agricultural operations planning in fields with multiple obstacle areas*".

In **Chapter 4**, a functional prototype of a web-based tool for field coverage path planning is presented. Through the web interface the user can draw the borders of the field with an integrated Google Maps facility, select operational parameters, e.g. working width, and activate a server-side model that generates the corresponding coverage plan. In real time (after a few seconds) the model returns the coverage plan and the corresponding performance measures to the client web browser, which produces a visualization of the coverage plan on Google Maps. This work led to a conference paper "*A web-based tool for comparing field area coverage practices*".

In **Chapter 5**, a simulation model of all the in-field machinery operations in potato production was developed and validated. The capabilities of using the simulation model as a decision support system (DSS) were demonstrated in terms simulating the consequences on machinery performance of field operational decisions (e.g. driving direction, fieldwork pattern, etc.) and machinery dimensions (e.g. working width, size of harvester's storage tank, etc.). This work is presented in the third manuscript "*Simulation model for the sequential in-field machinery operations in the potato production system*".

In **Chapter 6**, a novel approach to assess the benefits of using five alternative common fieldwork patterns against the operator's used fieldwork patterns was presented. This approach can help operators to quantitatively evaluate predetermined motifs of field coverage track sequences, subsequently make better decisions on selection of fieldwork pattern beforehand working in the field. This approach constitutes the fourth manuscript "*Quantifying the benefits of alternative fieldwork patterns in potato cultivation system*".

In **Chapter 7**, the general discussion is made and the future research perspectives are suggested.

# Chapter 2

# Performance of machinery in potato production in one growing season

K. Zhou, A. Leck Jensen, D.D. Bochtis, C.G. Sørensen

(Submitted)

**Abstract**

Statistics on the machinery performance are essential for farm managers to make better decisions. In this paper, the performance of all machineries used in the potato production system in one growing season was investigated. There are five main operations involved in potato production, which are bed forming, stone separation, planting, spraying and harvesting. In order to evaluate the performance of the machinery in these operations, geo-referenced data were gathered by using Global Positioning System (GPS) receivers mounted on each tractor in each operation from ten fields. The data analysis was performed using an automated analysis tool developed in the MATLAB® technical programming language. The field efficiency and field capacity were estimated for each operation. Specifically, the measured average field efficiency was 71.33% for bed forming, 68.53% for stone separation, 40.32% for planting, 69.68% for spraying, and 67.35% for harvesting. The measured average field capacities were 1.46 ha h$^{-1}$, 0.53 ha h$^{-1}$, 0.47 ha h$^{-1}$, 10.21 ha h$^{-1}$, 0.51 ha h$^{-1}$, for the bed forming, stone separation, planting, spraying, and harvesting, respectively. These results deviate from the corresponding estimations calculated based on norm data from the American Society of Agricultural and Biological Engineers (ASABE). The deviations indicate that norms provided by ASABE cannot be used directly for the prediction of performance of the machinery used in this work. Moreover, the measured data of bed forming and stone separation could be used as supplementary data for the ASABE which does not provide performance norms for these two operations. The gained results can help farm managers to make better management and operational decisions that result in potential improvement in productivity and profitability as well as in potential environmental benefits. In addition, the presented analysis results could potentially provide the basis for development of a targeted simulation model including all of the five operations.

*Keywords*: GPS data analysis, operation management, machinery management, field efficiency.

## 2   Introduction

Agricultural machinery inputs are the major capital investment, which can be as high as 25% of the total cost of crop production (Adamchuk et al., 2011). Efficient use of agricultural machinery in field operations

becomes very important to reduce the cost of the operations. Therefore, knowledge about the performance of the machinery in field operations is a requirement for better operation management and planning.

The field efficiency and capacity are two important measures for estimation of machinery performance, which can be estimated by time-motion studies. Traditional methods have utilized stopwatches and meters to collect field operation data for machinery performance evaluation. For example, Renoll (1981), Sørensen and Møller (2006), Sørensen and Nielsen(2005) used stop watches and clipboard to evaluate the field machinery performance. However, these recording methods are time demanding and laborious for a technician to measure the data manually during the operation. Alternatively, in the last decade, the extensive use of Global Positioning System (GPS) equipment has provided farm managers a new promising method to monitor and evaluate the field machinery performance. GPS equipment has been used to estimate performance of various machineries in various agricultural field operations, e.g. mower, rake and baler in cotton residue collection (Ntogkoulis et al., 2014), combine harvesters in corn, soybeans, wheat harvesting (Taylor et al., 2002), slurry applicator in manure spreading (Bochtis et al., 2010), planter in corn and soybean planting (Grisso et al., 2002) and harvester of forage corn for silage (Harrigan 2003). In addition, analysis algorithms have been developed to automatically extract and analyse the GPS data. Adamchuk et al. (2011) developed an algorithm to evaluate the spatial variability of the machinery performance. The processed spatial information can be used by famers to optimize the traffic pattern. Jensen and Bochtis (2013) developed an algorithmic method for automatic recognition of machine operation modes for cooperating machines (i.e. combines and transport units in grain harvesting) based on analysing recorded GPS- trajectories.

To the authors' knowledge, all of the current studies are focused on monitoring a single machine or multiple machines that are involved in a single field operation, not on all the machines in the complete set of field operations in one crop production system. In this paper, the potato production has been chosen as the case study. There are five main sequential field operations in potato production: Bed forming, stone separation, planting, spraying, harvesting. The bed forming operation is decisive, since it determines the bed layout, the driving direction and the wheel tracks for the entire growing season. Since the machines cannot turn inside the bed area and they must follow the wheel tracks between the beds the bed forming also influences the

working width of each machine, which must be one or multiple bed widths. Consequently, investigating the performance of all machineries in potato production is a key step to make an optimal operation planning.

In addition, a large volume of GPS data is generated during the sequential field operations in one growing season, which is time consuming to analyse manually. Hence there is need to develop an automatic GPS analysis tool for decomposing GPS recordings from a complete set of field operations into time and distance elements in various activities, such as turning in the headland area, transporting, etc. Specifically, the objectives of this work are as follows:

1) To develop an analysis tool to process the recorded data in order to reveal the time contribution of different task elements of each operation.

2) To analyse the field capacity and efficiency of the different machinery involved in the related field operations.

3) To compare the measured field efficiency and capacity with computed field efficiency and capacity based on ASABE data.

# 3   Description of the operations

The five main sequential field operations involved in potato production are explained in details in the following:

1) Bed formation: Setting up perfectly formed beds is the first step towards successful establishment of a potato crop. The bed former uses shaped metal plates to lift up the soil and form it into one to more beds. This step is decisive, since the wheel tracks and bed width are determined for all subsequent field operations of the season (Fig. 1.a).

2) Stone separation: This operation is also a part of the seedbed preparation in stony and cloddy soils which can provide ideal growing conditions for fast emergence of the potatoes and reduction of the picking cost in the harvesting. A stone separator uses a digging share and separating web through which the fine soil falls into the bed while the oversize stones and clods are transferred laterally

through a cross-conveyor to an adjacent furrow between already formed beds where separation is not performed. The conveyor can be adjusted either to the right or left when the tractor is at the end of the current bed. In successive operations the machine's tires run on the rows of the processed stones and clods to bury them between alternate beds (Fig. 1.b).

3) Planting: Potato planting starts immediately after the stone separation, normally by the use of automated planters. The planter is attached behind a tractor with the seed potatoes in a container, called the hopper. Special cups lift the seed potatoes from the hopper and place them with accuracy distance into the beds. The depth of sowing is about 5-10 cm and the distance between potato tubers along the rows are about 20-40 cm. Due to capacity constraints the hopper needs to be refilled occasionally. This is done by driving to the headland area where one or more reloading units are located, refill the hopper and return to the location of the field where the hopper ran empty. The time spent for reloading is part of the non-working time (Fig. 1.c).

4) Spraying: Spraying with herbicides, pesticides, fungicides etc. are usually performed around 10 times during the entire season (Fig. 1.d).

5) Harvesting: The most common harvest method is using a potato harvester with two or three rows diggers, depending on the bed type, which can dig out the potatoes from the bed. Soil and crop are transferred onto a series of webs where the loose soil is screened out. The potatoes are conveyed to a separation unit at the back part of the harvester. The potatoes then go on to a side elevator and into a trailer or bin located somewhere in the field (Fig. 1.e).

**Fig.1 - The involved field operations in potato production: (a) bed forming; (b) stone separation; (c) planting; (d) spraying (photo source: gopixpic) (e) harvesting.**

# 4 Material and methods

## 4.1 Definition of time elements and machinery performance measures

In order to classify time elements, e.g. working, turning and stopped, etc., the following time element definitions are made as described in Table 1.

Based on these time elements the field efficiency (FE) and effect field capacity (EFC) for each operation in each field can be calculated, which is expressed as (Hunt 2008):

$$FE = \frac{T_{ef}}{T_{ef} + T_{lost}} \times 100\%$$

Where $T_{ef}$ is the effective time, $T_{lost}$ is the time lost during the operation. Delay activities that take place outside the field, such as routinely maintenance, repair, and travel to and from the field, are not included in a field efficiency measurement.

| Time elements | Symbol | Definition |
|---|---|---|
| **Table 1 - Time elements classification and definition.** | | |
| Time elements | Symbol | Definition |
| Total operation time | $T_{tot}$ | The total time spent in the field, i.e. the time span from the machine enters the field until it exits it after the completion of the operation. |
| Effective operating time | $T_{ef}$ | The time the machine has worked productively in the field to complete the operation. |
| Turning time | $T_{turn}$ | The total time of turning for changing the tracks at the headland area or crossing obstacle areas in the field. |
| Load/ unload time | $T_{ld}$ | The time spent to load the material to the machine's hopper or tank (e.g. planter, sprayer) or to unload the material to the transportable storage units (harvesting). |
| In-field transport time | $T_{trans}$ | The time spent on driving inside the field to loading or unloading areas. |
| Delay time | $T_{del}$ | The total time during which the machine is not actually processing the field (such as operator rest stops, machine repair and maintenance time, and machine travel in the interior of a field) that occurs during the execution of the in-field operations. |
| Lost time | $T_{lost} = T_{tot} - T_{ef}$ | The part of the total operating time, that is not effective. |

The effective field capacity (EFC) of a machine can be calculated with two methods (Hanna, 2002). The first one is dividing the area completed by the hours of actual field time, namely $EFC = A/T_{tot}$, where A is the

area of the field. The second method is using the estimation equation $EFC = S * W * FE / 10$, where S is the working speed (km h$^{-1}$), W is the working width (m) and $FE$ is the field efficiency.

## 4.2 Analysis tool for GPS recordings

Based on the concept introduced by Bochtis and Sorensen (2009), these five operations can be categorized into three groups: Material neutral operations (MNO) (bed formation and stone separation), material input operations (MIO) (planting and spraying), and material output operation (MOO) (harvesting) according to the flow of material into or out of the field. In order to analyse the recorded data in those operations, a dedicated tool was developed using the MATLAB ® programming software. The input parameters of the tool include the coordinates of the field boundary and obstacle boundary (if any), the inner field boundary, i.e. the border between the headland and the main cropping area, and the coordinates of the machinery motion as well as the location of the service unit(s). The output consists of decomposed distance elements (e.g. effective working, turning, transporting, etc.) and the corresponding time elements.

The consecutively recorded data can be partitioned into line segments with sequential recorded data points by the field inner boundary. Those line segments that are located inside the main cropping area are considered as the on-the-tracks working motion trajectory while the line segments that are located in the headland area are considered non-working motion trajectory, such as turning, transporting, etc.

To determine if a machine is stopped, a threshold value $v_{stop}$ is applied in each data point. Because the inherent inaccuracy in the speed measurements of GPS receivers the recorded position of a truly stopped machine may not be constant, consequently the machine is measured to have a slow movement. Therefore the value of the $v_{stop}$ parameter must be less than the usual operating speed and greater than the speed resulted by the drift error. In this analysis $v_{stop} = 0.02$ ms$^{-1}$ was used. The effective working time on each track corresponds to the total number of data points that have the speed greater than 0.02 ms$^{-1}$, so the total effective working time in the main cropping area is the summation of the effective working time on the tracks.

The non-working motion trajectory in the headland area may consist of four activities: turning, transporting, refilling and unloading. In MNO operations only the turning activity occurs, while transporting occurs in both MIO and MOO operations. Finally, refilling and unloading occurs in MIO and MOO, respectively. To distinguish the turning, transporting, refilling/unloading activities in the headland area by the use of the recorded data points, circles were drawn with the radius of a given threshold value at the centres of the locations of the service units. If a machine stays inside the circle for a given threshold period of time, $T_{service}$, then the activity of the machine is categorized as being serviced and the transport time is the time on this motion trajectory minus the $T_{service}$. Otherwise, it can be considered as turning motion. The delay time in the headland area was calculated by isolating the sets of sequential points where the speed was lower than $v_{stop}$, 0.02 ms$^{-1}$. The value of $T_{service}$ was set to 10 minutes and 1 minute for reloading in planting and unloading in harvesting, respectively. Fig. 3 presents a flow diagram of the analysis.
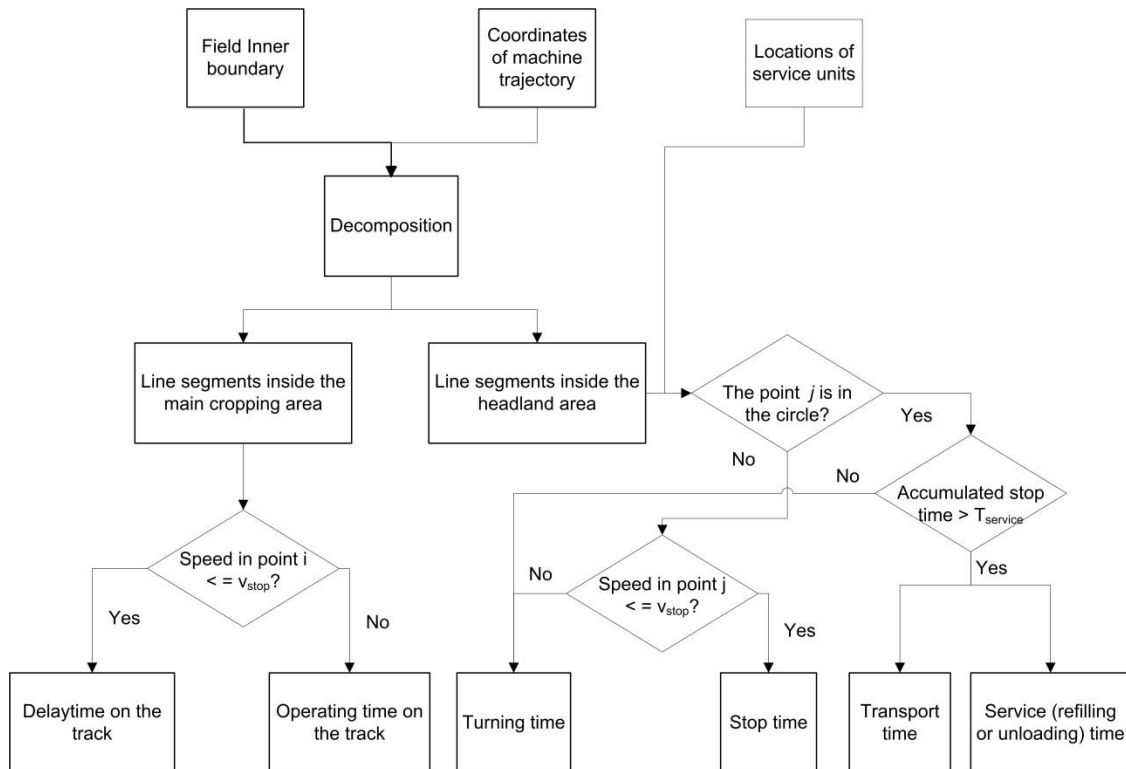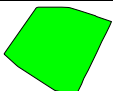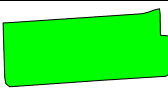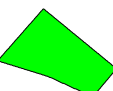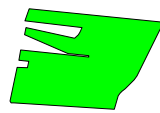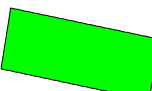


**Fig. 3 – Flow diagram of the method of analysis of the recorded GPS data.**

## 4.3 Experimental field operations

### 4.3.1 Site description

The experiment was designed to record GPS data of the activities of all the machineries involved in the sequential in-field operations of the potato production in ten fields in Lolland, Denmark, from May to December 2014. Table 2 summarizes the information about the study fields' shape, location and area.

| Table 2 – Experimental fields for case study. | | | | | | | |
|---|---|---|---|---|---|---|---|
| Field shape | Field ID | Location | Area (ha) | Field shape | Field ID | Location | Area (ha) |
| | 1 | 54º42´26.39´´N 11º19´30.20´´E | 16.41 | | 6 | 54º52´13.07´´N 11º12´31.95´´E | 7.50 |
| | 2 | 54º42´19.15´´N 11º18´46.89´´E | 22.74 | | 7 | 54º46´22.57´´N 11º25´01.07´´E | 16.59 |
| | 3 | 54º44´50.74´´N 11º12´55.79´´E | 10.85 | | 8 | 54º44´28.22´´N 11º12´38.12´´E | 22.04 |
| | 4 | 54º50´18.00´´N 11º72´54.28´´E | 19.73 | | 9 | 54º42´07.87´´N 11º18´46.22´´E | 11.45 |
| | 5 | 54º43´30.47´´N 11º16´47.47´´E | 17.45 | | 10 | 54º57´30.71´´N 11º11´03.19´´E | 13.55 |

### 4.3.2 3.3.2 Machinery and GPS Recording Equipment

The considered potato planting system consisted of 2.25 m wide beds which was the basic module width. Each bed consists of three rows. For each field crossing the bed former can produce two beds (one complete and two half beds). The stone separator, the harvester and the planter can only process one bed, while the sprayer can process 11 beds per crossing. Hence, the operating width $w$ was 4.50 m for the bed former, 2.25 m for the stone separator, the harvester and the planter, and 24.75 m for the sprayer. Two types of GPS

receivers were used for recording the positions of the vehicles involved. An AgGPS 162 Smart Antenna DGPS receiver (Trimble®, GA, 243 USA) was used for recording the trajectory of the bed former and harvester and three Aplicom A1 TRAX Data loggers (Aplicom®, Finland) were used for recording the trajectory of the stone separator, planter and sprayer (Fig. 2). The recording frequency was set to 1Hz in all experimental operations. Geo-referenced data were recorded continually including the non-working activities, e.g. turning, machine repair, operator break time. It has to be noted that only the activities of in-field machines were recorded, so the activities of transport units, e.g. the tractor for transporting seed potato from the farm to the field in planting, and for transporting harvested potato in harvesting were not monitored in the experiment. Due to the influence of the weather field 9 was not harvested at all.



**Fig. 2 – The two types of GPS receivers used in the experiment.**

# 5  Results

## 5.1  Data recording

In Fig. 4 the trajectory recordings of the bed former, stone separator, planter, sprayer and harvester in a selected field are presented. From the trajectories it is clear that the working width of the sprayer is much larger than the bed former, which is larger than the stone separator, the planter and the harvester.  Fig. 4.e gives the false impression that some of the tracks have not been harvested. The reason for this, however, is that the harvesting happens on the right-hand side of the tractor, where the GPS receiver is mounted, as shown in Fig. 1.e. Therefore, the field is always subdivided into blocks to reduce the non-working turning distance and time, and the harvester starts its harvesting from the middle bed of each block. This fieldwork pattern creates the gaps between blocks as shown in the Fig. 4.e.

(a)  Bed forming

(b)  Stone separating

(c)  Planting

(d)  Spraying

(e)  Harvesting
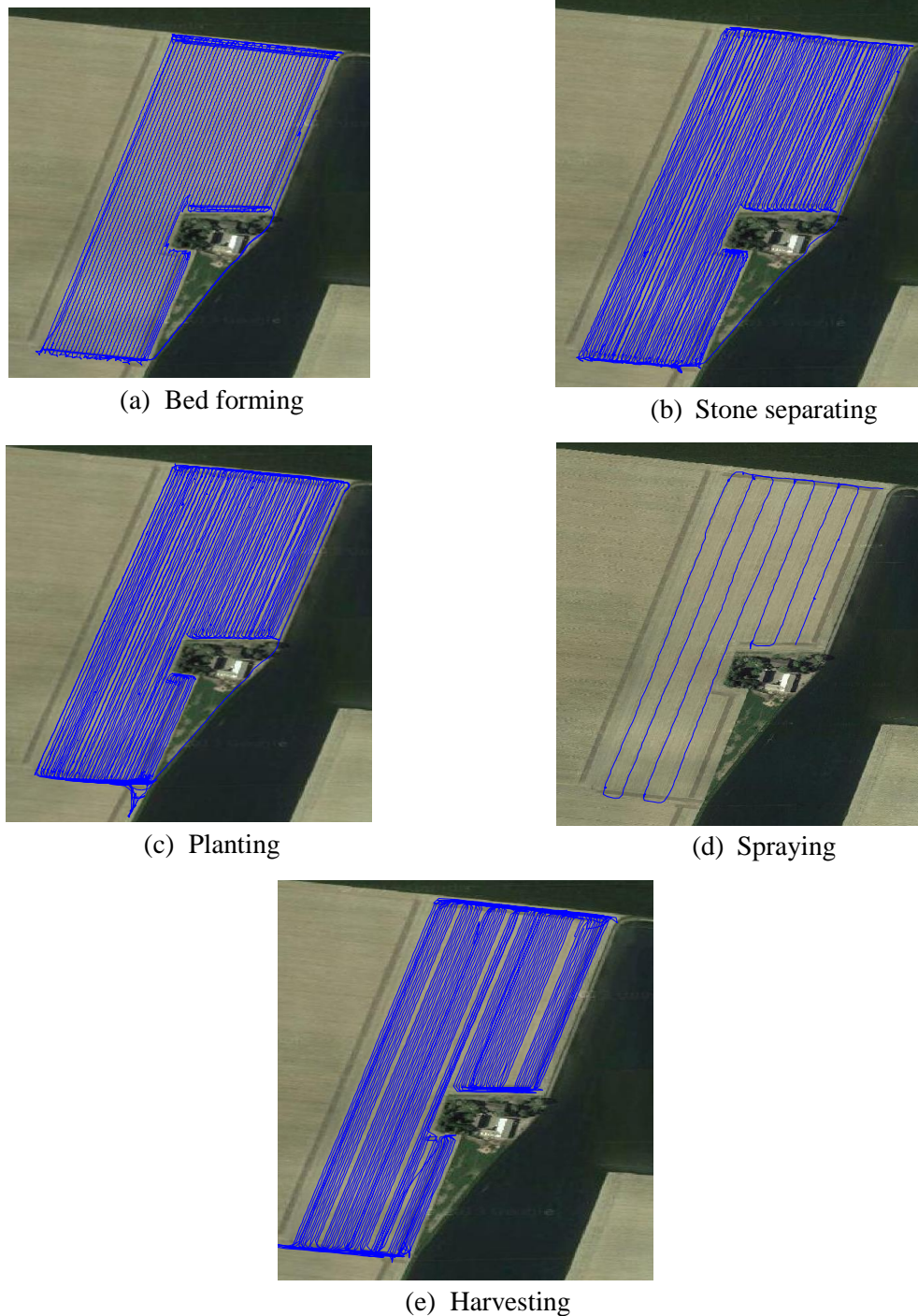
**Fig. 4 - The GPS recordings for agricultural vehicles: (a) bed former, (b) stone separator, (c) planter, (d) sprayer, and (e) harvester in potato production in Field 3.**
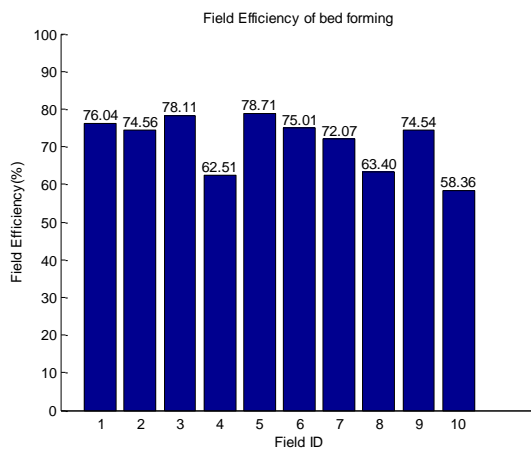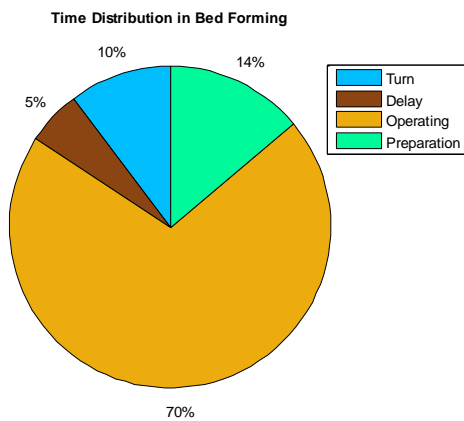
## 5.2   Classification of time elements

Figure 5.a shows the distribution of the average field operational time elements of the bed forming. The field efficiency ranged from 58.4% to 78.7% with an average of 71.3%.

Figure 5.b presents the distribution of the average field operational time elements for stone separation. The field efficiency ranged from 65.7 % to 73.4% with an average of 68.5%.

Figure 5.c is the distribution of the operation time elements for planting. The field efficiency ranged from 31.9 % to 48.3 % with an average of 40.3 %.

Figure 5.d is the distribution of the operation time elements for spraying. The field efficiency ranged from 53.2 % to 76.8 % with an average of 69.7 %.

Figure 5.e is the distribution of the operation time elements for harvesting. The field efficiency ranged from 59.0 % to 72.8 % with an average of 67.4%.



(a)



(b)

**Time Distribution in Planting**

**Field Efficiency of planting**

**Time Distribution in Spraying**

**Field Efficiency of spraying**

(c)

(d)

**Time Distribution in harvesting**

**Field Efficiency of harvesting**
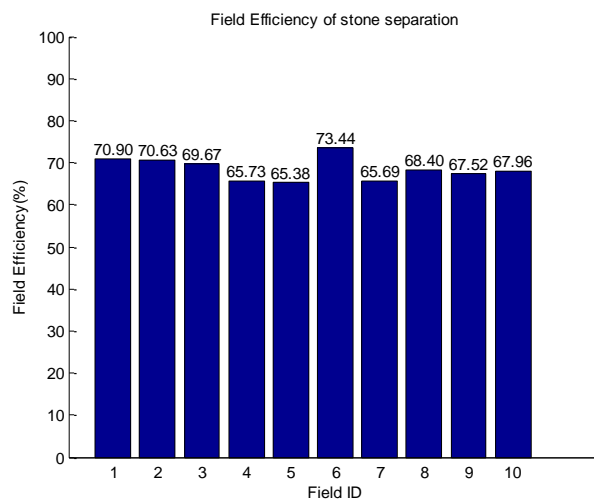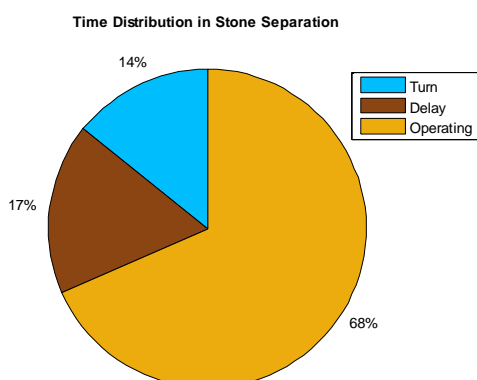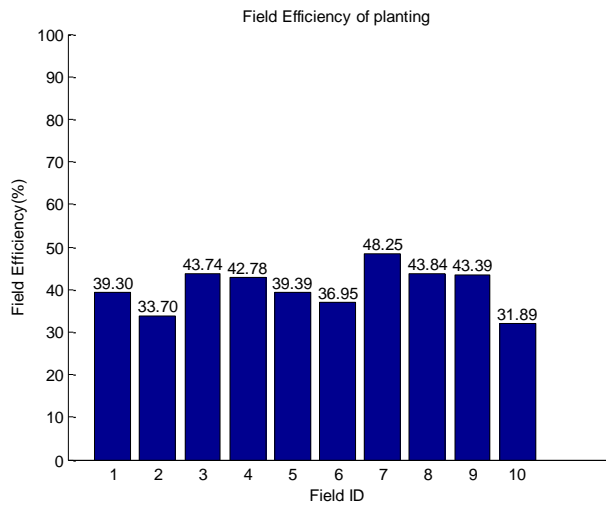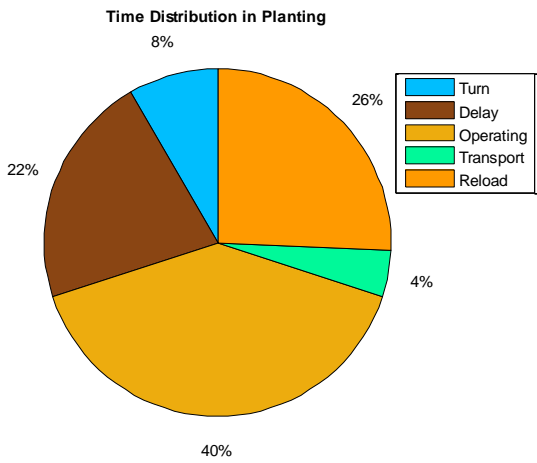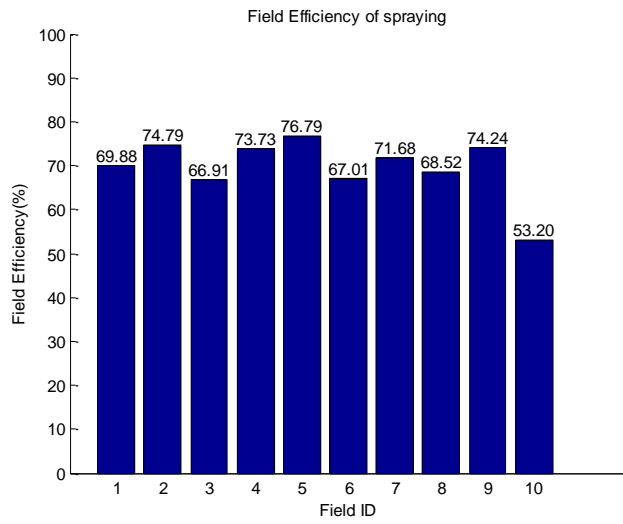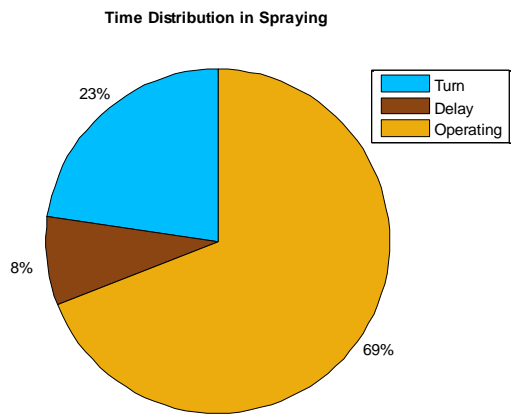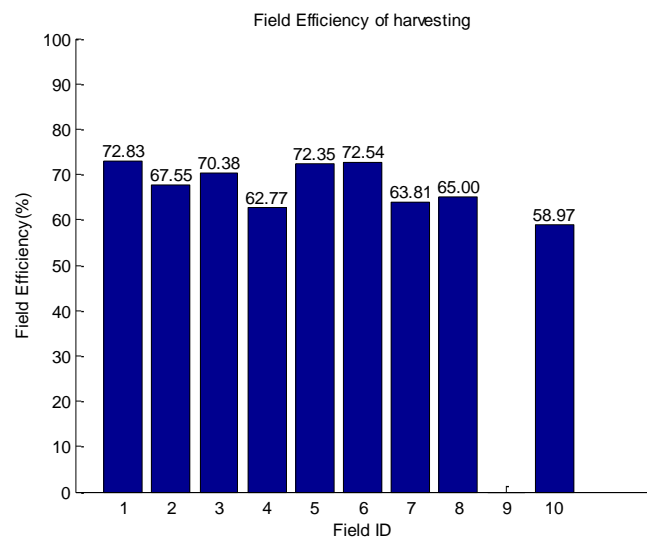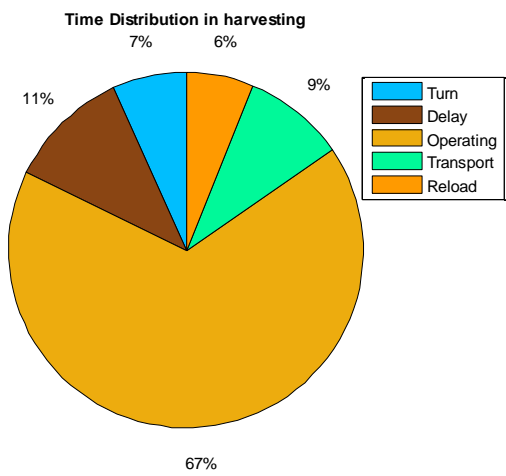
(e)

**Fig. 5 - Time distribution in bed forming, stone separation, planting, spraying, and harvesting.**

## 5.3   Field capacity distribution

Fig 6.a-e are bar charts showing the distribution of the field capacity for each machine in each of the ten fields for bed forming, stone separation, planting, spraying and harvesting. The measured field capacity for bed forming ranged from 1.12 to 1.81 ha h$^{-1}$ with an average of 1.46 ha h$^{-1}$; for stone separation, the measured field capacity was between 0.44 and 0.62 ha h$^{-1}$ with an average of 0.53 ha h$^{-1}$. For planting, the measured field capacity ranged from 0.39 to 0.56 ha h$^{-1}$ with an average of 0.47 ha h$^{-1}$. For spraying the measured field capacity ranged from 7.53 to 12.50 ha h$^{-1}$ with an average of 10.21 ha h$^{-1}$. Finally, the measured field capacity for harvesting ranged from 0.37 to 0.62 ha h$^{-1}$ with an average of 0.51 ha h$^{-1}$.

Field Capacity of harvesting
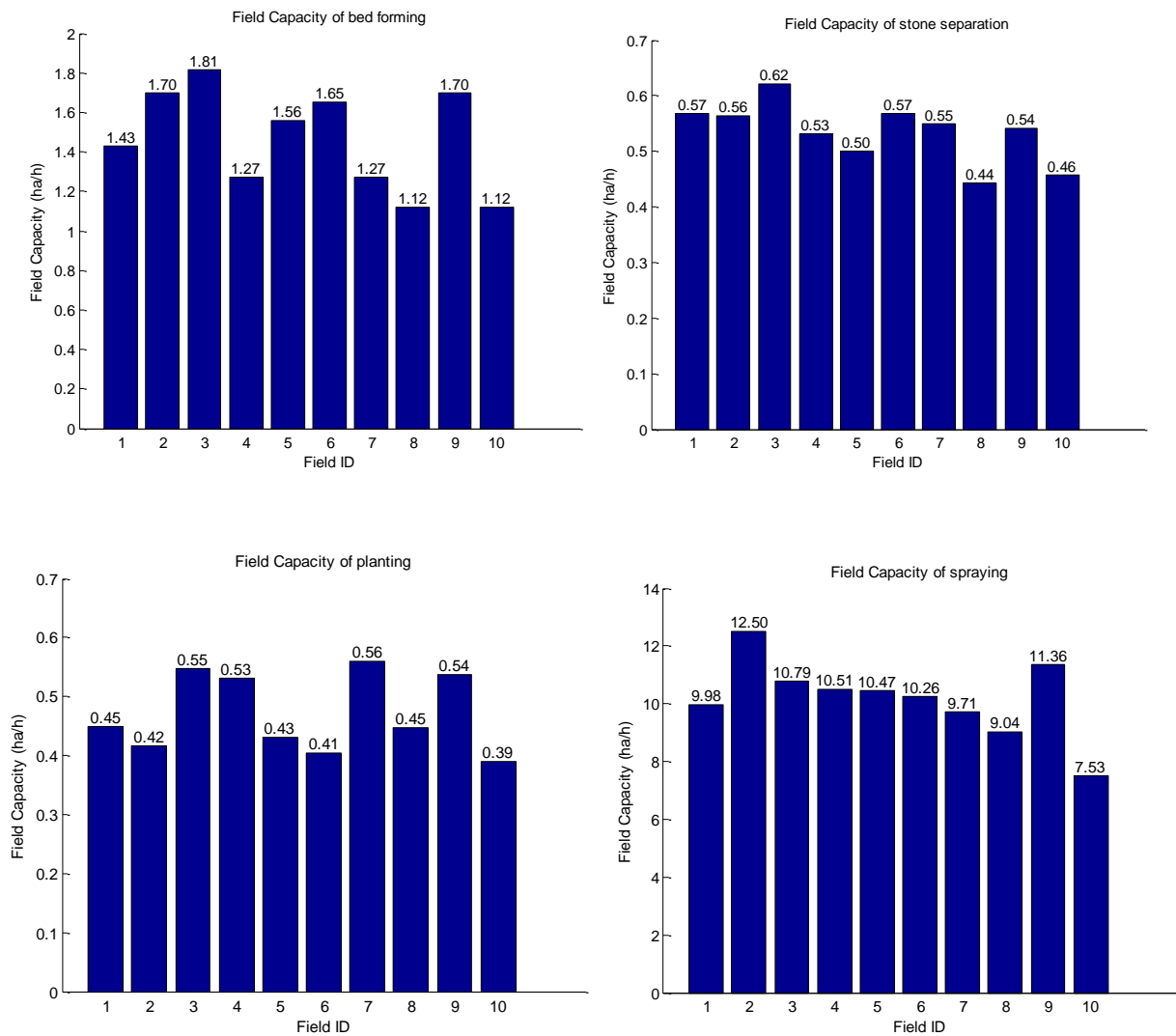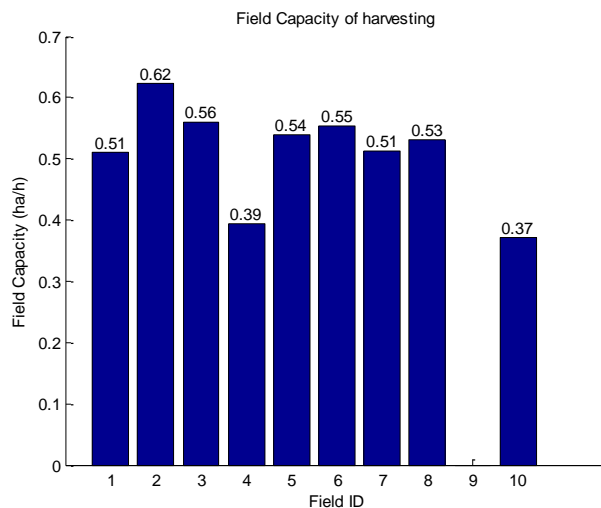
**Fig. 6 - Field capacity distribution in bed forming, stone separation, planting, spraying and harvesting.**

## 5.4 Comparison with ASABE norm data

| | Measured | | | ASABE norm | | |
|---|---|---|---|---|---|---|
| **Table 3 - Comparison of measured values and ASABE norms of field efficiency and field capacity.** | | | | | | |
| | FE(%) range (mean) | EFC (ha h$^{-1}$) range (mean) | operating speed (km h$^{-1}$) (mean) | FE(%) range (typical) | EFC (ha h$^{-1}$) range (typical) | operating speed (km h$^{-1}$) (typical) |
| Bed forming | 58.36 - 78.71 (71.33) | 1.12 - 1.81 (1.46) | 4.90 - 5.15 (5.05) | - | - | - |
| Stone separation | 65.69 - 73.44 (68.53) | 0.44 - 0.62 (0.53) | 3.42 - 3.82 (3.58) | - | - | - |
| Planting | 31.89 - 48.25 (40.32) | 0.39 - 0.56 (0.47) | 5.04 - 5.45 (5.25) | 55 - 80 (60) | 1.11 - 2.16 (1.35) | 9 - 12 (10) |
| Spraying | 53.20 - 76.79 (69.68) | 7.53-12.50 (10.21) | 5.76 - 6.12 (5.85) | 50 - 80 (65) | 6.19 - 22.77 (16.89) | 5.0 - 11.5 (10.5) |
| Harvesting | 58.97 - 72.83 (67.68) | 0.37 - 0.62 (0.51) | 4.51 - 4.68 (4.6) | 55 - 70 (60) | 0.31 - 1.02 (0.54) | 2.5 - 6.5 (4.0) |

The measured field capacities of the machinery involved in the potato production were compared with the calculated field capacity of machinery published by the Standard of the American Society of Agricultural and Biological Engineers (ASABE, 2011). The ASABE data give the field efficiency and operating speed

ranges with typical value for each machinery type. The selected values of field efficiency from ASABE and calculated field capacity are presented in the Table 3. However, there are no specific ASABE data provided for bed forming and stone separation.

# 6 Discussion

Large variations were found in the measured field efficiency and field capacity for the five main operations in the ten experimental fields. The possible factors that led to the variations include the machine manoeuvrability, the fieldwork pattern, field shape and size, soil and weather conditions. The field efficiency for irregular field shapes is expected to be less than for rectangular fields due to excessive turning time. In order to investigate the effects of field geometry on the field efficiency a shape index, MBR (Moser, Zechmeister et al. 2002), was used. MBR is defined as the ratio of the area of the field polygon and the area of the minimum bounding rectangle, and the index is used to describe the level of geometrical regularity of a field. The MBR is 1 for rectangles and approaches 0 when the shape becomes more irregular and odd. The calculated index values for the experimental fields are presented in Table 4. Furthermore, these index values were divided into two groups according the threshold value 0.77. These two groups were denoted as G1 (fields 1, 3, 5, 6 and 9) and G2 (fields 2, 4, 7, 8 and 10), respectively.

| Table 4 - Shape index values of MBR for experimental fields. ||
|---|---|
| Field no. | MBR |
| 1 | 0.84 |
| 2 | 0.74 |
| 3 | 0.82 |
| 4 | 0.63 |
| 5 | 0.85 |
| 6 | 0.92 |
| 7 | 0.71 |
| 8 | 0.72 |
| 9 | 0.90 |
| 10 | 0.56 |

It was found that the group with higher index values had higher average field efficiency. As shown in Table 5, the group of most regular fields, G1, had 10.4%, 1.8%, 0.5%, 2.6%, 8.4% higher field efficiency than G2 in bed forming, stone separation, planting, spraying, harvesting, respectively. In terms of the field capacity, the group with higher index values also had higher average field capacity, except in the case of planting where both group had the same average field capacity of 0.47 ha h$^{-1}$. The G1 fields had 0.33 ha h$^{-1}$, 0.05 hah$^{-1}$, 0.7 hah$^{-1}$, and 0.05 hah$^{-1}$ higher field capacity than G2 in bed forming, stone separation, spraying, harvesting, respectively.

| Table 5 - Comparison of field efficiency and capacity between field groups G1 and G2. | | | | |
|---|---|---|---|---|
| Operation type | Field efficiency (%) | | Field capacity (ha h$^{-1}$) | |
| | G1 | G2 | G1 | G2 |
| Bed forming | 76.50 | 66.10 | 1.63 | 1.30 |
| Stone separation | 69.40 | 67.60 | 0.56 | 0.51 |
| Planting | 40.60 | 40.10 | 0.47 | 0.47 |
| Spraying | 71.00 | 68.40 | 10.60 | 9.90 |
| Harvesting | 72.02 | 63.62 | 0.54 | 0.49 |

In addition, the fieldwork pattern that defines the traversal sequence of the tracks also affects the time lost in the field due to non-productive travel (Hunt 2008). A large portion of the non-working time takes place during the turning and/or transporting in the headland area. The turning time of a turn in the headland area depends on the distance and the turning speed. The selection of headland turning type potentially is determined by the fieldwork pattern and the width of the headland area under given working width and turning radius of the machine. The data analysis revealed that fishtail turns ($T$-turns) were commonly seen in bed forming and stone separation. The reason for this is the demand of manoeuvring space to approach an adjacent track of the T-turn. The disadvantage is that it is time demanding to make this turn, because it has to stop the machine twice and shift gears to reverse the driving direction. The GPS data analysis also revealed that a few track skip turns (loop turns: $\Omega$-turn or $\Pi$-turn) were made. Often these turns were executed at higher speed and with shorter turning distance compared to the fishtail turns. For instance, in bed forming,

the measured average speeds for $T, \Omega$ (skip 1 track), and $\Pi$ (skip 2 tracks) ( as illustrated in Fig.7) turns were 1.08 m s$^{-1}$, 1.15 m s$^{-1}$, and 1.35 m s$^{-1}$, respectively. The measured average turning distance for these three types of turns were 30.1 m, 31.2 m, and 23.3 m, respectively. For example, if the operator of the bed former use the $\Pi$ turns to cover the whole field, the field efficiency can be improved from 75.0% to 77.3% in field 6. Hence, adoption of appropriate fieldwork pattern for field coverage can improve the performance of the machinery.
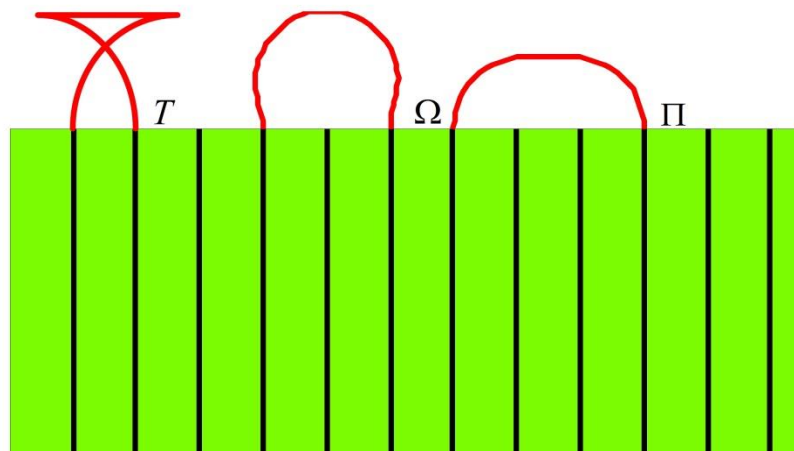


**Fig. 7 – Three common types of turns $T, \Omega$ (skip 1 track), and $\Pi$ (skip 2 tracks) used in bed forming.**

By comparing the average measured values of field efficiency and capacity with the norm values issued by ASABE (Table 3), it can be found that the measured values were lower than the norms. These deviations can partially be explained by differences of the suggested and measured working speeds. The ranges of field efficiency of spraying and harvesting were within in the ranges of ASABE norm data, while in the planning the measured highest field efficiency was even lower than the lowest field efficiency of ASABE provided. Therefore, it is obvious that the ASABE norms cannot be used directly for sufficiently predicting performance of machinery, at least in the potato production system of this study. In addition, the measured field efficiencies and capacities in bed forming and stone separation could be used as supplementary data for ASABE norms in which the specific data for these two operations are not provided.

The performance analysis of machineries involved in the potato production in one growing season is very important for farm manager to make a strategic operation plan in terms of machinery and labour demands.

Moreover, the presented analysis results provide the basis for development of a dedicated simulation model encompassing all field operations in potato production. This dedicated model can help farmers to make global plan taking into features of machinery (e.g. tank size, working width) and fields (e.g. field boundary, working directions) in all involved operations as well as quantitatively estimate and predict the operational time and cost. This is the subject of future research based on the present work.

# 7    Conclusion

GPS data of the machine motions in the five main operations in potato production (bed forming, stone separation, planting, spraying and harvesting) were gathered and analyzed from ten fields in one growing season. The performance measures field efficiency and field capacity was calculated for each operation in each field based on the extracted task time elements from the recorded data. These calculated field efficiencies and capacities differ from the corresponding norms given by ASABE. This deviation indicates that ASABE norms cannot be used directly for predicting performance of the machines used in this study. Furthermore, the development of a dedicated model including all five operations for potato production based on the statistical analysis from monitored operations is a necessary, which can help farm managers make strategic and operational plans for the entire growing season in terms of machinery and labour demands and costs under given field conditions.

# References

Adamchuk, V. I., Grisso, R., Kocher, M. F., 2011. Spatial Variability of Field Machinery Use and Efficiency. *GIS Applications in Agriculture, Volume Two: Nutrient Management for Energy Efficiency*, 135.

ASAE D497.7, 2011. Agricultural machinery management data. In ASABE STANDARD 2011. (Ed.), ASABE. St. Joseph, MI, USA: American Society of Agricultural andBiological Engineers.

Bochtis, D.D., Sorensen, C. G., 2009. The vehicle routing problem in field logistics part I. *Biosystems Engineering, 104*(4), 447-457.

Bochtis D.D., Sorensen, C. G., Green, O., Moshou, D., Olesen, J., 2010. Effect of controlled traffic on field efficiency. *Biosystems Engineering, 106*(1), 14-25.

Grisso, R. D., Jasa, P. J., Rolofson, D. E., 2002. Analysis of traffic patterns and yield monitor data for field efficiency determination. *Applied Engineering in Agriculture, 18*(2), 171-178.

Hanna, M. (2002). Estimating the field capacity of farm machines. Net, Iowa. Disponível em:< http://www. extension. iastate. edu/agdm/crops/pdf/a3-24. pdf>. Acesso em, 17.

Harrigan, T. M., 2003. Time-motion analysis of corn silage harvest systems. *Applied Engineering in Agriculture, 19*(4), 389-395.

Hunt, D., 2008. *Farm power and machinery management*: Waveland Press.

Jensen, M. A. F., Bochtis, D. D., 2013. *Automatic Recognition of Operation Modes of Combines and Transport Units based on GNSS Trajectories.* Paper presented at the Agricontrol.

Moser, D., Zechmeister, H. G., Plutzar, C., Sauberer, N., Wrbka, T., Grabherr, G., 2002. Landscape patch shape complexity as an effective measure for plant species richness in rural landscapes. *Landscape Ecology, 17*(7), 657-669.

Ntogkoulis, P. A., Bochtis, D. D., Fountas, S., Berruto, R., Gemtos, T. A., 2014. Performance of cotton residue collection machinery. *Biosystems Engineering, 119*(0), 25-34.

Renoll, E., 1981. Predicting Machine Field-Capacity for Specific Field and Operating-Conditions. *Transactions of the Asae, 24*(1), 45-47.

Sørensen, C. G.,  Møller, H. B., 2006. Operational and economic modeling and optimization of mobile slurry separation. *Applied Engineering in Agriculture*, 22(2), 185-193.

Sørensen, C. G., Nielsen, V., 2005. Operational analyses and model comparison of machinery systems for reduced tillage. *Biosystems Engineering*, 92(2), 143-155.

Taylor, R. K., Schrock., M. D., Staggenborg., S. A., 2002. Extracting Machinery Management Information from GPS Data. *ASABE,St. Joseph, Michigan.*

# Chapter 3

# Agricultural operations planning in fields with multiple obstacle areas

K. Zhou , A. Leck Jensen, C.G. Sørensen, P. Busato, D.D. Bochtis

**Abstract**

When planning an agricultural field operation there are certain conditions where human planning can lead to low field efficiency, e.g. in the case of irregular field shapes and the presence of obstacles within the field area. The objective of this paper was to develop a planning method that generates a feasible area coverage plan for agricultural machines executing non-capacitated operations in fields inhabiting multiple obstacle areas. The developed approach consists of three stages. The first two stages regard the generation of the field geometrical representation where the field is split into sub-fields (blocks) and each sub-field is covered by parallel tracks, while the third stage regards the optimization of the block sequence aiming at minimizing the travelled distance to connect the blocks. The optimization problem was formulated as a TSP problem and it was solved implementing the ant colony algorithmic approach. To validate the developed model two application experiments were designed. The results showed that the model could adequately predict the motion pattern of machinery operating in field with multiple obstacles.

*Keywords*: route planning, agricultural vehicles, ant colony algorithm, traveling salesman problem.

# 1  Introduction

When planning an agricultural field operation there are certain field conditions where experience-based planning can lead to low machinery efficiency, for example in case of irregular field shapes and in case of the presence of obstacles within the field area (Oksanen and Visala, 2007). So far, a significant amount of research has been carried out to solve the route planning problem in field operations. These advances include a number of methods for the geometrical field representation (de Bruin et al., 2009; Oksanen and Visala, 2009; Hofstee et al., 2009; Hameed et al., 2010) and a number of methods for route planning within a given field geometrical representation (Bochtis and Vougioukas, 2008; Bochtis and Sørensen, 2009; de Bruin et al., 2009; Bochtis et al., 2013; Scheuren et al., 2013).

In the case of fields with inhabited obstacles, in all developed methods the field is decomposed into sub-fields (referred to as blocks). Due to the specific nature of field operations, existing decomposition methods

of the working space from the industrial robotics discipline area (Choset, 2001; Galceran and Carreras, 2013) cannot be directly applied. Oksanen and Visala (2007) developed a field decomposition method based on the trapezoidal decomposition for agricultural machines to cover the field. After decomposition, the trapezoids are merged into blocks under the requirements that the blocks have exactly matching edges and the angles of ending edges is not too steep. Hofstee et al., (2009) developed a tool for splitting the field into single convex fields. Stoll (2003) introduced a method to divide the field into blocks based on the longest side of the field. Palmer et al. (2003) presented a method of generating pre-determined tracks in fields with obstacles. Jin and Tang (2010) developed an exhaustive search algorithm for finding the optimal field decomposition and path directions for each subfield. However, in all of the above mentioned methods the optimum order to traverse the decomposed block was not derived. A first theoretical approach that provided the traversal sequence of the resulted blocks was presented in Hameed et al., (2013). The approach was based on the implementation of genetic algorithms for the optimization of the visiting sequence of the different sub-field areas resulted by the presence of the obstacles. However, the computational requirements of the approach were exponential to the problem size (e.g. the number of obstacles in the field area) and the feasibility of the approach has not been tested in terms of their implementation on real farming conditions.

The objective of this paper was to develop a planning method that generates a feasible area coverage plan for agricultural machines executing non-capacitated operations in fields inhabiting multiple obstacle areas. The term non-capacitated refers to the operations where the capacity constraints of the machine do not allow for covering the entire field area by a single route (e.g. the presented method cannot apply to the case of harvesting). The method consists of three stages. The first two stages regard the generation of the field-work tracks and the division of the field into blocks, respectively, and the third stage regards the optimization of the sequence that the blocks are worked under the criterion of the minimization of the blocks connection distance. The problem of finding the optimal block traversal sequence was formulated as a travelling salesman problem (TSP) and it was solved by implementing the ant colony algorithmic approach.

# 2 Methodology

## 2.1 Overview

The headland pattern is one of the most common field coverage patterns for agricultural machines, in which the field is divided into two parts, the headland area and field body area. The field body is the primary cropping area and it is covered with a sequence of straight or curved field-work tracks. The distance between two adjacent tracks is equal to the effective operating width of the agricultural machine. The headland area is laid out along the field border with the main purpose to enable the machines to turn between two sequential planned tracks. The order in which the agricultural machines operate in the two types of areas depends on the type of the operation; for example, the headland area is harvested before the field body, while the field body is seeded before the headland area. When a field has obstacles headlands are also laid out around the obstacles. The field body is split into a number of sub-fields (or blocks) around the obstacles, such that all blocks are free of obstacles.

The planning method involves the following three stages:

a) In the first stage, the field area and the in-field obstacle(s) are represented as a geometrical graph. This process includes the headland generation, the obstacle handling, and an initial generation of field-work tracks (ignoring the in-field obstacles until stage 2) (section 2.2).

b) In the second stage, the field body is decomposed into block areas and the previously generated field-work tracks are divided and clustered into these block areas (section 2.3).

c) In the third stage, the problem of the optimal traversal sequence of the blocks (in terms of area coverage planning) is derived (section 2.4).

The input parameters of the planning method include:

- The boundary of the field area and the boundaries of the in-field obstacles. All boundaries are expressed as a clock-wise ordered set of vertices.

- The number of the headland passes ($h$) for the main field and around each obstacle.

54

- The driving direction ($\theta$). It determines the direction of the parallel fieldwork tracks that cover the field area.

- The operating width ($w$). This is the effective operating width of the implement and also represents the width of the field-work tracks.

- Turning radius ($c$). This is the minimal turning radius of the agricultural machines.

- The threshold parameter ($r$), for the classification of the obstacle type (explained in section 2.2.2).

A graphical description of the proposed planning system is presented in the diagram in Fig. 1.
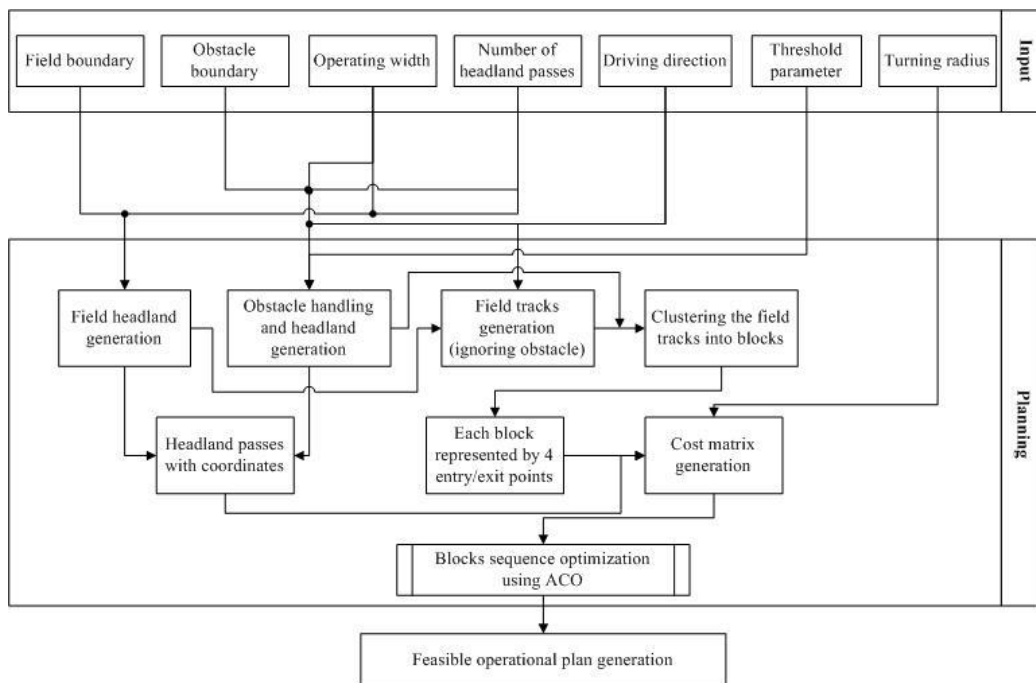


**Fig. 1. The graphical description of the proposed planning system.**

## 2.2 First stage

### 2.2.1 Generation of field headland

The field headland area is obtained by offsetting the boundary inwardly by a width equal to the multiplication of the operating width, $w$ times the number of headland passes, $h$. The distance from the field boundaries to the first headland pass is half of the operating width, $w/2$ while the distance between

subsequent headland passes equals to the operating width, $w$. An inner boundary between field headland and field body is created at distance $w/2$ from the last headland pass.

### 2.2.2    Categorizing of obstacles and generation of obstacle headlands

There are different types of obstacles in terms of their effect on the execution of a field operation. For example, certain physical obstacles due to their relatively small dimensions do not constitute an operational obstacle resulting in the generation of sub-fields (e.g. in Fig. 2a: Obstacle 5 is potentially such an obstacle). Other obstacles might exist that are close to the field boundary such that the generation of sub-fields is not required (e.g. obstacle 1 in Fig. 2). Finally, there are obstacles in close proximity that from the operational point of view should be considered as one obstacle (e.g. obstacles 2 and 3 in Fig. 2).
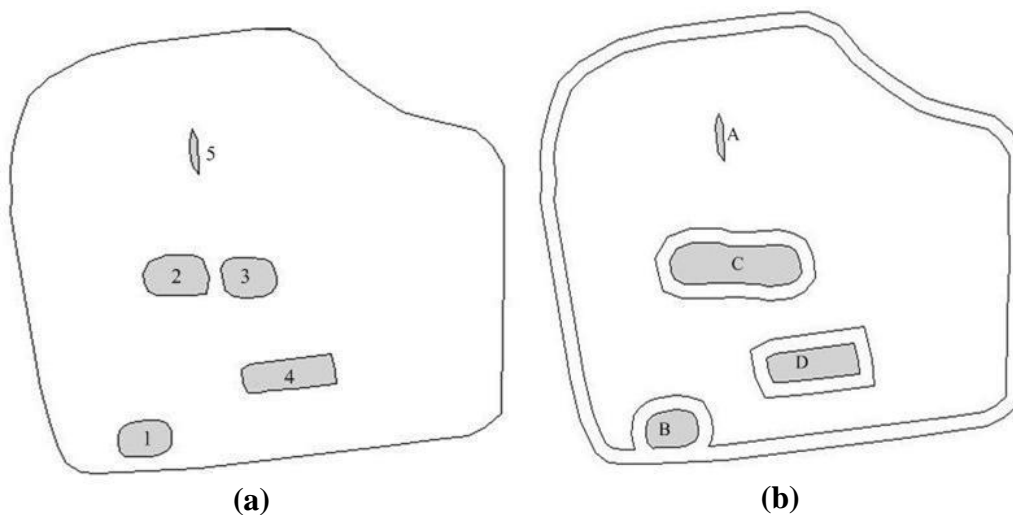


**Fig. 2. Different obstacles configurations within a field area (a) and their classification (b).**

Four types of obstacles are defined:

Type A. An obstacle that due to size and configuration in relation to the driving direction does not affect the coverage plan generation. In order to classify an obstacle as type A, the minimum boundary box of the obstacle polygon is generated with one of its edges parallel to the driving direction. If the dimension, $\Delta d$ of the minimum bounding box that is perpendicular to the driving direction is less than the threshold parameter

$r$, this obstacle is considered as a type A obstacle. Fig. 3a and Fig. 3b present how the driving direction $\theta$ determines the classification of an obstacle as type A or not.

Type B. This type includes obstacles where their boundary intersects with the inner boundary of the field. Type B obstacles are incorporated into the inner boundary of the field and the field headland is extended around this obstacle.

Type C. This type includes obstacles where the minimum distance between another obstacle is less than the operating width, $w$. In this case both obstacles are classified as of type C and a subroutine is used to find the minimal bounding polygon (MBP) to enclose these obstacles. For instance, assuming that the minimum distance between the obstacle 2 and 3 in the Fig 2.a is less than the operating width, $w$, then the minimal bounding polygon is gained by the sub-routine to represent the boundaries of these two obstacles as shown in Fig 2.b



(a)                                                                (b)
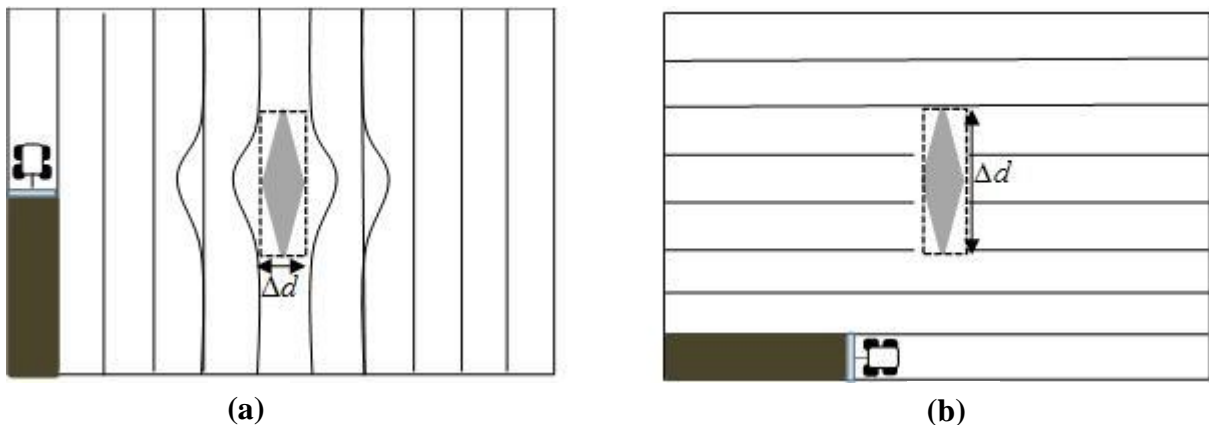
**Fig. 3. The same obstacle can be classified as of type A (a) and as of type D (b) depending on the orientation of the obstacle as compared to the driving direction, here with $r = w$.**

Type D. All remaining obstacles are considered type D. Also the resulted new obstacles derived by the connection of two or more obstacles of type C are classified as type D obstacles. Headland areas are generated only for the obstacles of type D. The method of generating obstacle headland is analogous to the method of field headland generation; however, the offset direction of the boundary is outward.

### 2.2.3    Generation of field-work tracks

Track generation concerns the process of generating parallel tracks to cover the field body. The minimum-perimeter bounding rectangle (MBR) of the inner field boundary is generated using the method of rotating calipers (Toussaint, 1983). In the first step, depicted in Fig. 4, the MBR is generated around the inner field boundary, and a reference line $l$ parallel to $\theta$ is created intersecting one vertex on the MBR while all other vertices of MBR are located on the same half-plane determined by the line $l$. Let $v$ be the vertex of the MBR with the longest perpendicular distance from $l$, and let $v'$ be the projection of $v$ on $l$. Then the number of the field-work tracks for a complete covering of the filed polygon area is given by $n = \lceil |vv'|/w \rceil$ (where $\lceil \rceil$ is the ceil function). The line segments to cover the entire MBR are generated sequentially from the reference line $l$. The distance from $l$ to the first line segment along the $vv'$ line equals to $w/2$, while the distance between the subsequent line segments along $vv'$ equals to $w$.
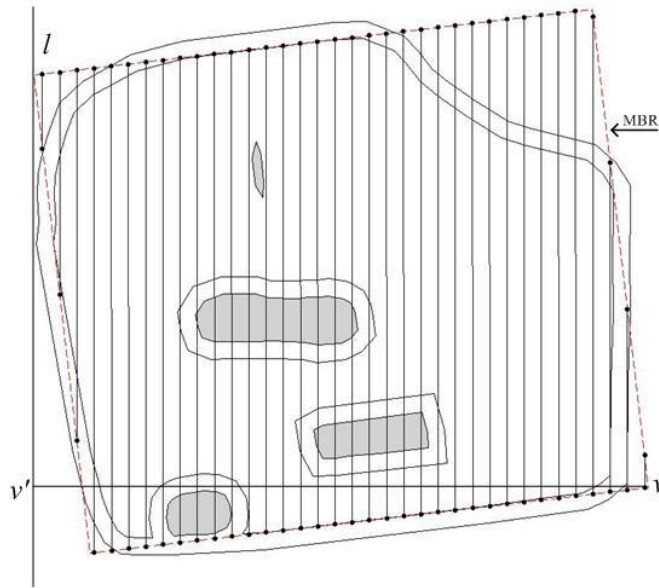


**Fig. 4. The MBR of the field is covered by a set of straight lines that are parallel to the reference line *l*.**

Let $T_0 = \{1,2,3...n\}$ denote the set of indices of these line segments, each of which intersects with the MBR in the form of two ending points on the MBR border. For each line segment $i \in T_0$, if it has $m_i$ intersections with the inner field boundary it is subdivided into $m_i + 1$ new line segments. Each new line segment is

58

checked if it is inside or outside the field body (disregarding the obstacles). If it is inside (the solid line segments in Fig. 5), the line segment is saved as a field-work track, otherwise it is discarded (the dashed line segments in Fig. 5). In order to give each field-work track an index value, one of the two outmost tracks is arbitrary selected as the first track associating it with the index of value 1. Let $T = \{1,2,3...n'\}$ be the ordered set of tracks.
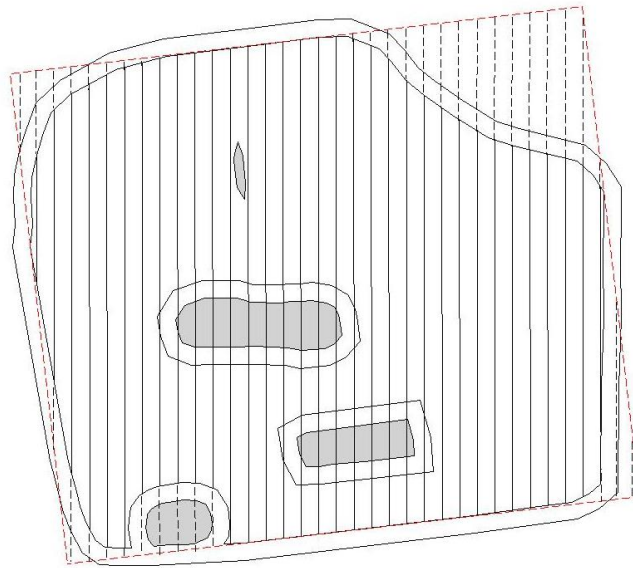


**Fig. 5. The field body is covered by field-work tracks (the solid lines)**

## 2.3    Second stage

### 2.3.1    Decomposition of field body into blocks

In this step, the field body is decomposed into blocks, following the boustrophedon cellular decomposition method (Choset and Pignon, 1997). Specifically, a line, termed as a *slice,* parallel to the driving direction $\theta$, sweeps through the inner field boundary from left to the right. Whenever the slice either meets a new obstacle (*in* event) or leaves an obstacle (*out* event) one or more preliminary blocks are formed behind the slice with block boundaries along the slice (see Fig. 6). When the decomposition is completed, an adjacency non-complete graph is built where each node of the graph represents a preliminary block and two nodes of the graph are connected if there are common sections between the edges of the corresponding preliminary blocks (Fig. 7). The next step is to merge the generated preliminary block areas according to the adjacency

graph. The merging requirement is that two connected blocks in the graph have a common edge. After the merging process, the generated block areas are indexed.



**Fig. 6. The sequential stages of the generation of preliminary blocks**.



**Fig. 7. The adjacency graph of the preliminary blocks (a) and the final generated blocks (b).**

### 2.3.2    Clustering tracks into blocks

In section 2.2.3 the set T of field-work tracks, disregarding the obstacles, was generated. In the following, a method of dividing the tracks of T into segments defined by the obstacles and clustering the divided tracks into block areas is introduced. Let $B = \{1,2,...,k\}$ be the generated block areas as described in s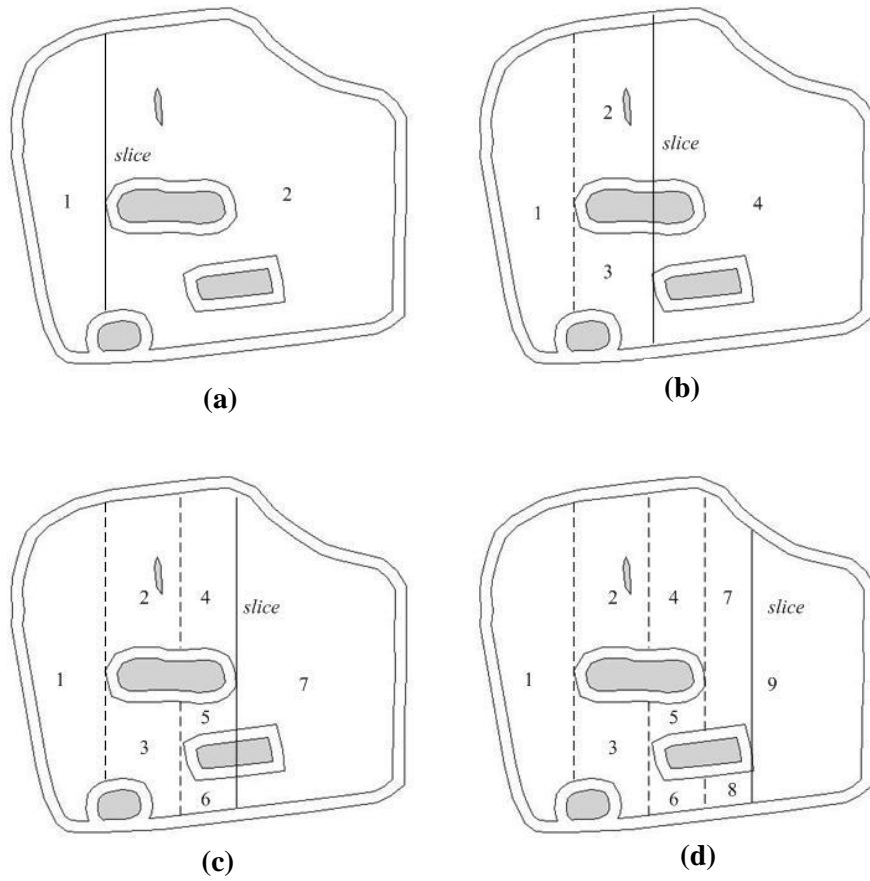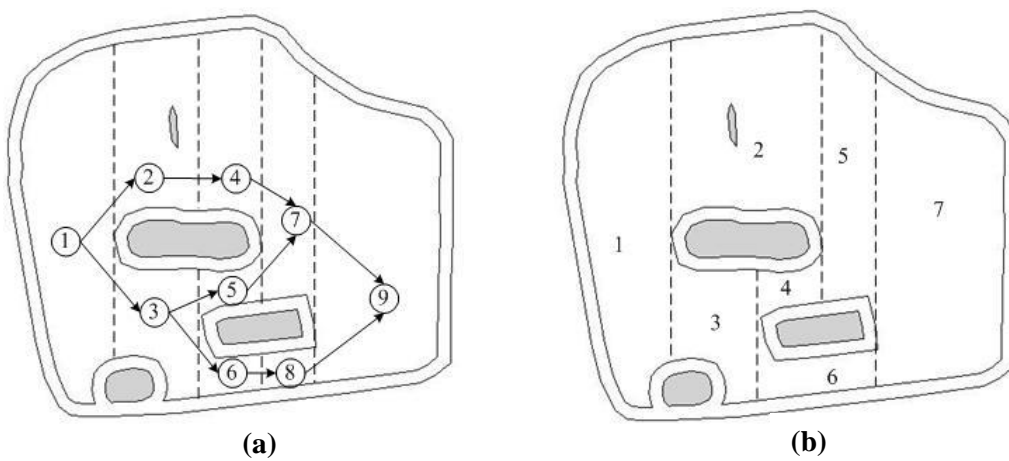ection 2.3.1. The whole processing of clustering includes $\|T\|$ iterations. In each iteration, if a track $i \in T$ intersects with the boundary of a block area $j \in B$, it is subdivided into segments. The resulted segments are checked if they are located inside or outside the area of block $j$. The segments located inside the block area are given the same index value as the index of the block. The set of the tracks in block $i \in B$ is denoted as $T_i, i \in B$. An example of division and clustering of the initial tracks is presented in Fig. 8.

## 2.4    Third stage

### 2.4.1    Construction of traversal graph

After the second stage the field has been divided into blocks and field-work tracks have been assigned to each block. Each block is a sub-field without obstacles, so the coverage of the corresponding area could be planned either using an optimized track sequence (e.g. *B-pattern*), or a conventional way of the continuous track sequence can be used. On the presented work the latter case has been adopted and also the assumption that the work inside a block is always commenced in one of its two outmost tracks (the first or the last track of the block) has been considered. By making this assumption, each block can be represented by 4 entry/exit points: $N = \{n_{ij}, i \in B, j \in \{1,2,3,4\}\}$, where the nodes $n_{i1}$ and $n_{i2}$ are end points of the first track and $n_{i3}$, $n_{i4}$ are end points of the last track of block $i$. For a given block the exit point is determined by the entry point and the parity of the number of the tracks of the block. For example, considering block 1 in Fig. 8 which has an odd number of tracks, for the case of the continuous pattern if the operation commences at the end of the track corresponding to node $n_{12}$, then the operation will be completed at the end of the last track corresponding to node $n_{14}$.
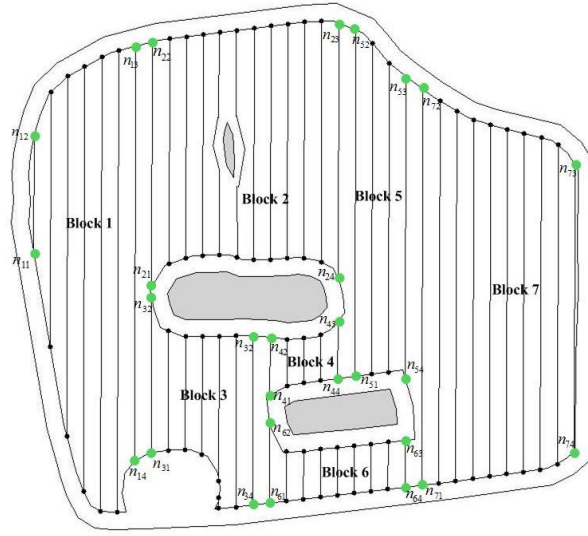
**Fig. 8. Division and clustering of the initial tracks into the generated block areas and the corresponding four entry/exit points for each block.**

The problem of the block sequencing is equivalent with the problem of traversing the undirected, weighted graph $G = \{N, E\}$, where $N$ is the set of graph nodes consisting of the entry/exit points, as defined previously, and $E$ is the set of edges, consisting of paths between any entry/exit points. Each edge $E_{n_{ix}n_{jy}}$, $n_{ix} \neq n_{jy}$ is associated with a weight $c_{n_{ix}n_{jy}}$, $n_{ix} \neq n_{jy}$ which corresponds to the transit cost from node $n_{ix}$ to node $n_{jy}$. Although $G$ can be considered as a complete graph, some potential connections between nodes within a block are not allowed while others have to be enforced. For each block the function $e_i = (-1)^{\mathrm{mod}(|T_i|, 2)}$ is defined and its value (1 or -1) depends on the parity of the number of the tracks in the block. By using this function the cost for the connection between nodes belonging to the same block is given by: $c_{n_{i1}n_{i2}} = c_{n_{i3}n_{i4}} = 0$, $c_{n_{i2},n_{i3}} = c_{n_{i1}n_{i4}} = L^{-e_i}$, and $c_{n_{i2}n_{i4}} = c_{n_{i1}n_{i3}} = L^{e_i}$, where $L$ is a (relatively) very large positive number (as shown in Fig. 9).
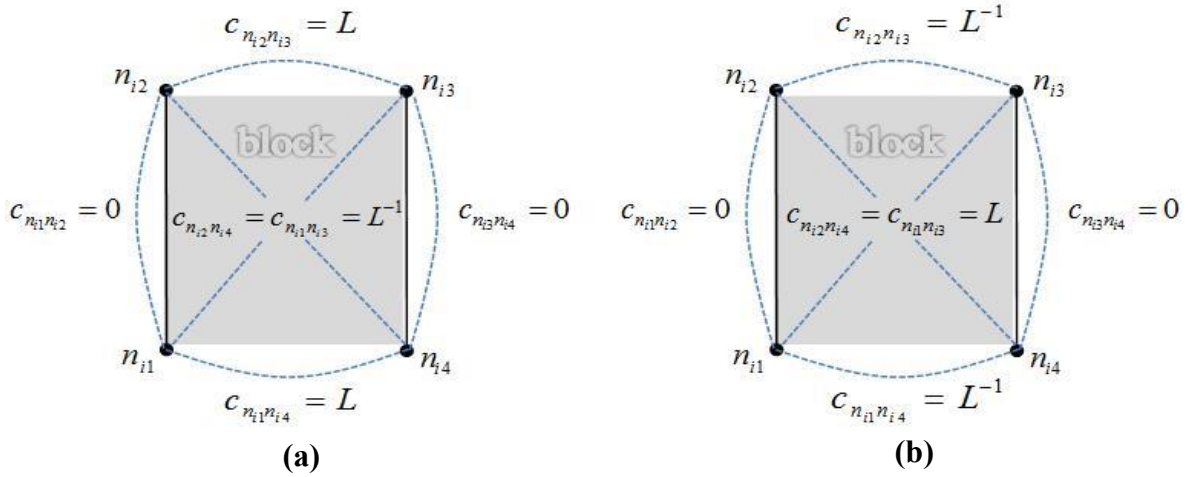
**Fig. 9. Internal cost assignment for blocks with odd (a) or even number of tracks (b).**

In order to avoid connections between blocks that in the physical operation will result in the situation where the machine travels on a part of the field main area in order to move from one block to the other, both of the blocks must have nodes that are located either on the inner boundary of the field or in the outer boundary of the same obstacle in order to allow a connection between two blocks.

For each pair of nodes of graph $G$ a binary function $s(n_{ix}, n_{jy})$ is defined which returns the value 1 if $n_{ix}$ and $n_{jy}$ are both located either on the inner boundary of the field or on the outer boundary of an obstacle, and value 0 otherwise. If $s(n_{ix}, n_{jy}) = 1$ the cost for the connection of $n_{ix}$ and $n_{jy}$ is the actual shortest turning connection distance along the headland pass of the field or the obstacle. In contrast, a relatively large number, $L$, is assigned to the cost $c_{n_{ix}n_{jy}}$ when $s(n_{ix}, n_{jy}) = 0$.

### 2.4.2 Optimization of block traversal sequence

Since the problem graph has been considered as a complete graph, the problem of finding the shortest path for visiting all blocks is equivalent to finding the Hamiltonian path through the constructed graph $G$, which is equivalent to the travelling salesman problem (TSP) (Hahsler and Hornik, 2007). Furthermore, since the cost of the connection between two nodes is independent of the direction, the specific case regards the symmetric TSP. The TSP is a well-known combinatorial optimization problem, which is a non-

deterministic Polynomial-time hard (NP-hard) problem (Garey and Johnson, 1979). Various algorithmic approaches have been developed based on exact solution approaches (e.g. branch-and-bound, and branch-and-cut, etc.) and approximate approaches (e.g. tabu search, genetic algorithm and ant colony algorithm, etc.) (Glover and Kochenberger, 2002). For the particular problem presented here, any of the developed TSP solving methods can be implemented, in principle, since the size of the computational problem is relatively small. This is due the fact that the number of obstacles in an agricultural field is limited because of operational considerations.

Among the different solving methods the ant colony (ACO) algorithm has been selected. ACO is a mathematical model based on ants' behavior in finding the shortest route between ant colonies and food sources. The principle is based on the fact that every ant deposits pheromone on the traveled path. For a detailed description of the method refer to Dorigo and Gambardella (1997). In the presented problem, the cost of the connection of two nodes, $c_{n_{ix}n_{jy}}, i, j \in B, x, y \in \{1,2,3,4\}$, is connected with the so-called heuristic value for moving between the two nodes in the ACO notion. Beyond the cost matrix, the parameters that have to be quantified in the ACO are parameter $\rho$, which represents the evaporation rate of the pheromone, and parameters $\alpha$ and $\beta$, which are adjustable parameters to weight the importance of the pheromone. For the above mentioned parameters $\rho$, $\alpha$ and $\beta$, the values that were experimentally found to provide the best solutions (Colorni et al., 1992) are 0.5, 1, and 5, respectively, while for the number of ants the suggested value equals to $n$, where $n$ is the number of graph nodes. The above mentioned values have been implemented in the presented work. Since ACO is a heuristic algorithm, as the number of iterations increases, the convergence of the found solution to the optimal one is improved. However, in the way that the algorithmic approach has been devised, e.g. the internal cost assignment in the generated blocks, all the traversal constraints imposed in covering an agricultural field area has been taken into account and consequently, only workable solutions are considered. This means that even in one iteration of the ACO process a sub-optimal workable solution can be provided.

The complexity of the problem depends on the number of obstacles within the field that are classified as type D obstacles (after the process of classification). For $O_D$ obstacles the number of the generated blocks is $3O_D + 1$. Given that in a symmetric TSP with $n$ nodes the number of potential permutations equals to $(n-1)!/2$, and that each block generates four nodes in the graph, the number of permutations as a function of the obstacles is given by: $(12O_D + 3)!/2$.

## 3 Results and discussion

### 3.1 Feasibility of the method

To evaluate the feasibility of the plan generated by the method, the simulated output for two field operations were compared with the actual planned and performed operations by the farmer in two fields. The first field has one type D obstacle and an area of 16.16 ha (Fig. 10a). The second field has two type D obstacles and an area of 24.25 ha (Fig. 10b). The specific operations involved potato seedbed forming and harrowing. The trajectory of the tractor was recorded using an AgGPS 162 Smart Antenna DGPS receiver (Trimble, GA, USA). Its accuracy is ± 20.3-30.5 cm pass-to-pass. In order to provide the model with the accurate data on field geometry, the vertices along the field edges were measured by tracking the field boundaries with the same GPS receiver. The Douglas-Peucker line simplification algorithm (Douglas and Peucker, 1973) was applied to process the GPS coordinates of the field geometry.
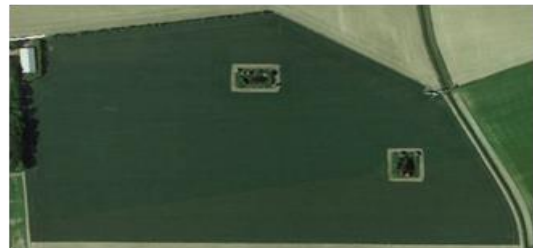


(a)  (b)

Fig. 10. The selected experimental fields: field A (a) and field B (b).

### 3.1.1 Field A

- *Experimental operation*

For the operation in field A, an AB line was set and set for the navigation system by driving the tractor along the longest edge of the field from one headland to the opposite headland. The operating width was 4.95 m while the turning radius of the tractor was 6 m. During the whole operation, two drivers were involved. It has to be noted that potato is a high-profit crop; hence the farmer minimizes the headland area for turning. Furthermore, since the turning radius is greater than half of the operating width, there is not enough space for the vehicle to make smooth turns such as omega and pi turns, with the guidance system, and forward-reverse (fishtail) turns were used (as shown in Fig. 11). During the bed preparing operation, the tractor was steered automatically by a steering system mounted on the tractor, while for the turning operation, the drivers steered manually and headed towards the next track according to the on-screen information of the guidance system. The coverage of the field was performed following the continuous fieldwork pattern.

Based on the analysis of the GPS recordings (Fig. 11), the measured effective working distance was 32,823 m, the measured non-working headland turn distance was 1,720.2 m and the connection distance of blocks was 112.3 m. The average effective operating speed was 1.2 m/s, while the average turning speed was 0.85 m/s.



**Fig. 11. The GPS recordings of operation in field A.**

- *Simulated operation*

The operating width, the turning radius and the driving direction for the simulated operation were set to the same as in the experimental one (4.95 m, 6 m and 143.5°, respectively), resulting in 49 tracks and 4 blocks (Fig. 12). The headland passes number was also selected to be 2 as in the actual operation.

For finding the shortest connection distance of blocks, the total number of ants, $m$, was set to 16, while $\rho$, $\alpha$ and $\beta$ were set to 0.5, 1, and 5, respectively. The number of iterations was set to 100. Ten runs were performed with an average computational time of 2.92 s.

The optimal sequence of the blocks and the corresponding entry and exit nodes was: $\{[n_{11} \ n_{12} \ n_{14} \ n_{13}] \rightarrow [n_{31} \ n_{32} \ n_{34} \ n_{33}] \rightarrow [n_{23} \ n_{24} \ n_{22} \ n_{21}] \rightarrow [n_{41} \ n_{42} \ n_{43} \ n_{44}]\}$. The estimated total effective distance, including the infield working distance and the working distance in the headlands, during the whole operation was 32,791 m. The estimated non-working headland turn distance was 1,682.5 m. The connection distance of the blocks was 106.9 m.



**Fig. 12. The generated plan for field A.**

### 3.1.2 Field B

- *Experimental operation*

In the operation in field B the operating width was 12 m and the turning radius of the tractor was 6.5 m. The driving direction was along the longest edge of the field boundary. During the whole operation only one driver was involved. Due to the turning radius is nearly equal to half of the operating width, there is enough headland area space for the vehicle to make omega turns, with the guidance system (as shown in Fig. 13). During the operation, the tractor was steered automatically by the steering system, while for the turning operation, the driver steered manually and headed towards the next track according to the on-screen information of the guidance system.

Based on the analysis of the GPS recording (Fig. 13), the measured effective working distance was 19,643 m, the measured non-working headland turn distance was 1,370 m and the connection distance of blocks was 450.4 m. The average effective operating speed was 1.5 m/s, while the average turning speed was 0.9 m/s.
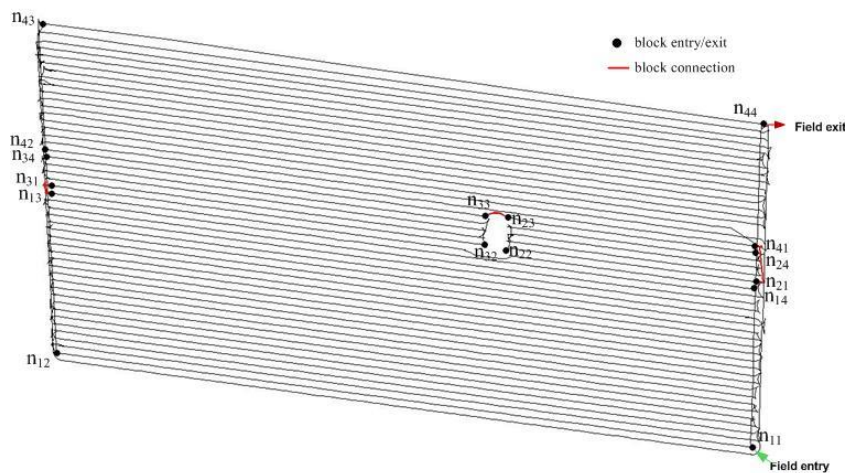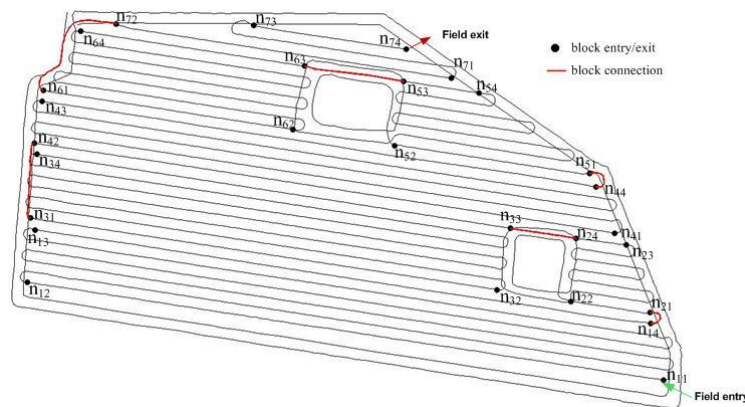


**Fig. 13. The GPS recordings of operation in field B.**

- *Simulated operation*

The operating width, the turning radius and the driving direction for the operation were the same as in the actual operation (12 m, 6.5 m and 172.5° respectively), resulting in 44 tracks and 7 blocks (Fig. 14). The number of headland passes was set to 2 as in the actual operation.

For finding the shortest connection distance of blocks, parameters of the ACO algorithm were set to $\rho = 0.5$, $\alpha = 1$ and $\beta = 5$, and the number of iterations was 100. The number of the ants used was 28 which equals

to the number of the nodes presenting the entry and exit points of blocks. Ten runs were performed with an average computational time of 11.51 s.

The optimal sequence of the blocks and the corresponding entry and exit nodes was:

$\{[n_{11}\ n_{12}\ n_{13}\ n_{14}] \rightarrow [n_{21}\ n_{22}\ n_{23}\ n_{24}] \rightarrow [n_{33}\ n_{34}\ n_{32}\ n_{31}] \rightarrow [n_{42}\ n_{41}\ n_{43}\ n_{44}] \rightarrow [n_{51}\ n_{52}\ n_{54}\ n_{53}] \rightarrow [n_{63}\ n_{64}\ n_{62}\ n_{61}] \rightarrow [n_{72}\ n_{71}\ n_{73}\ n_{74}]\}$. The estimated total effective distance, including the infield working distance and the working distance in the headlands, during the whole operation was 19,634 m. The estimated non-working headland turnings distance was 1,350.5 m. The connection distance of the blocks was 445.3 m.
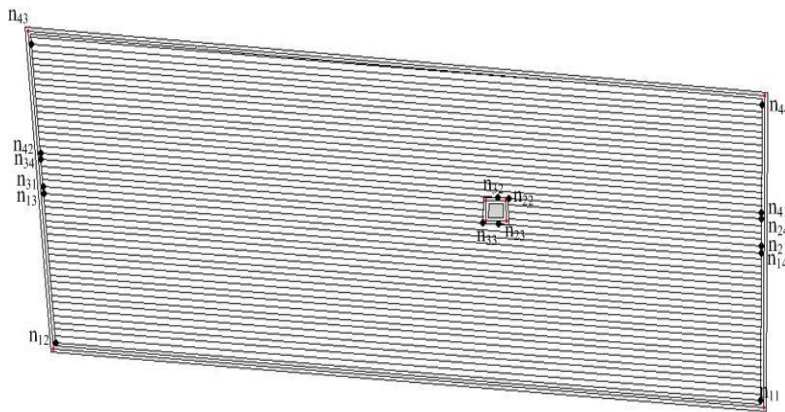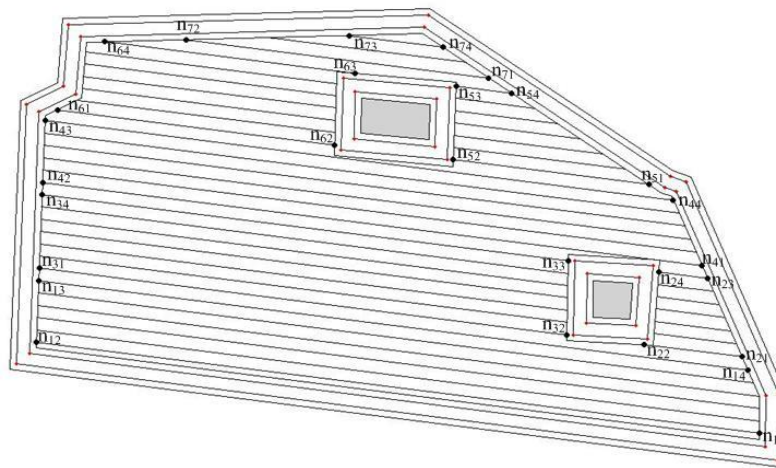


**Fig. 14 - The generated plan for field B.**

## 3.2 Comparison between simulated and experimental results

The comparison between the experimentally performed and planned operation and the simulated operation shows that the developed method can simulate the field operation with sufficient accuracy. As shown in Table 1, the prediction error in terms of total travelled distance was 0.21% for field operation A and 0.15% for field operation B. The relatively small errors between the measured and the predicted values of the operational time elements are mainly arisen from two reasons. First, due to the actual conditions of the field surface and the positioning error, the vehicle cannot exactly follow the planned parallel tracks. In addition, the GPS guidance system only navigates on the in-field parallel tracks while the turnings in the headland areas of the field and the obstacles were manually executed and was depended on the driver's abilities.

**Table 1. Comparison between the data from the experimental and the simulated operations**

| | Operation A | | | Operation B | | |
|---|---|---|---|---|---|---|
| | Simulated (m) | Measured (m) | Error (%) | Simulated (m) | Measured (m) | Error (%) |
| Total effective distance | 32,791 | 32,823 | 0.10 | 19,634 | 19,643 | 0.045 |
| Non-working distance | 1,682.5 | 1,720.2 | 2.23 | 1,350.5 | 1,370 | 1.4 |
| Connection distance of blocks | 106.9 | 112.3 | 5.05 | 445.3 | 450.4 | 1.14 |
| Total travelled distance | 34,580.4 | 34,655.5 | 0.21 | 21,429.8 | 21,463.4 | 0.15 |

To test the performance of the ACO algorithm for the solution of the optimization part of the method, an exhaustive algorithm was used to obtain the optimal block sequence examining all the combinations of the block connections in both cases of field A and field B. The exhaustive algorithm provided the same solutions as the ACO for both cases. For the field A, the exhaustive algorithm provided the optimal block sequence in 0.58 s while the ACO algorithm provided the same solution in 2.92 s. However, as the number of in-field obstacles increased to two in the case of field B, the computational time of the exhaustive algorithm increased to 560.8 s while the computational time for the ACO algorithm was 9.98 s. This was expected since the computational steps and consequently the computational time of the exhaustive enumeration algorithm increases exponentially with the size of the problem making it unfeasible for medium to large scale problems (e.g. up to 3-4 blocks).

## 3.3 Simulated test cases

In order to demonstrate how the developed method can handle more complicated cases, three fields, including 3, 4, and 5 obstacles, respectively, were selected. The parameters regarding the input and output

are shown in Table 2, while the solutions are presented in Fig. 15. As expected, the computational time increases with increasing number of obstacles. However, it has to be noted that, regarding the number of iterations, as the number of obstacle increases, more iterations are needed to guarantee that the best solution can be obtained. However, due to the nature of the implemented algorithm, the system could be considered either as an on-line or as an offline system. As it can be seen in Table 2, even in the most complicated of the examined cases, the algorithm can provide feasible sub-optimal solutions in less than one minute making its use feasible for an online system.



**(a)**
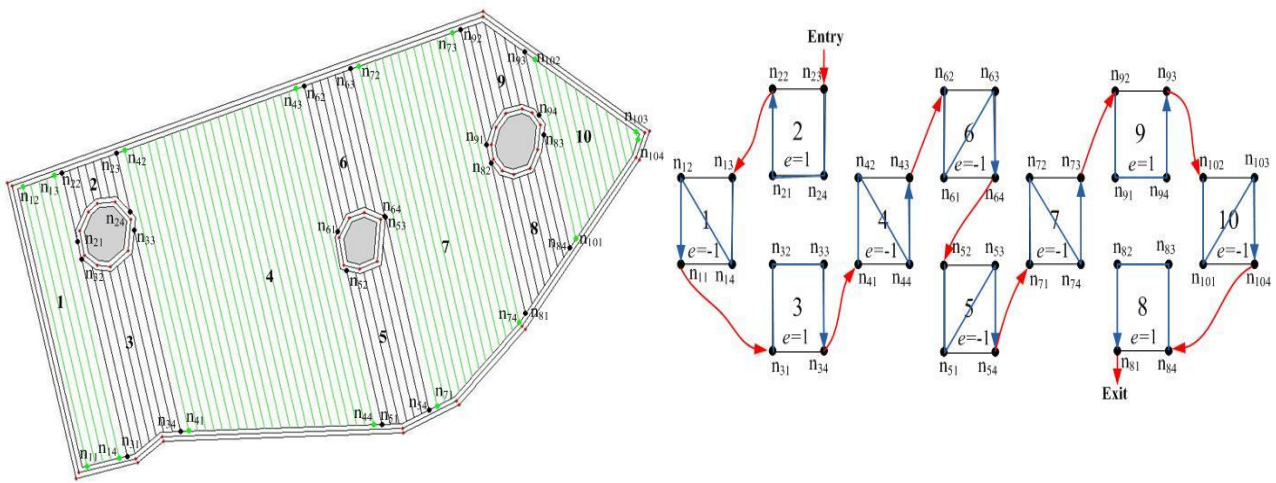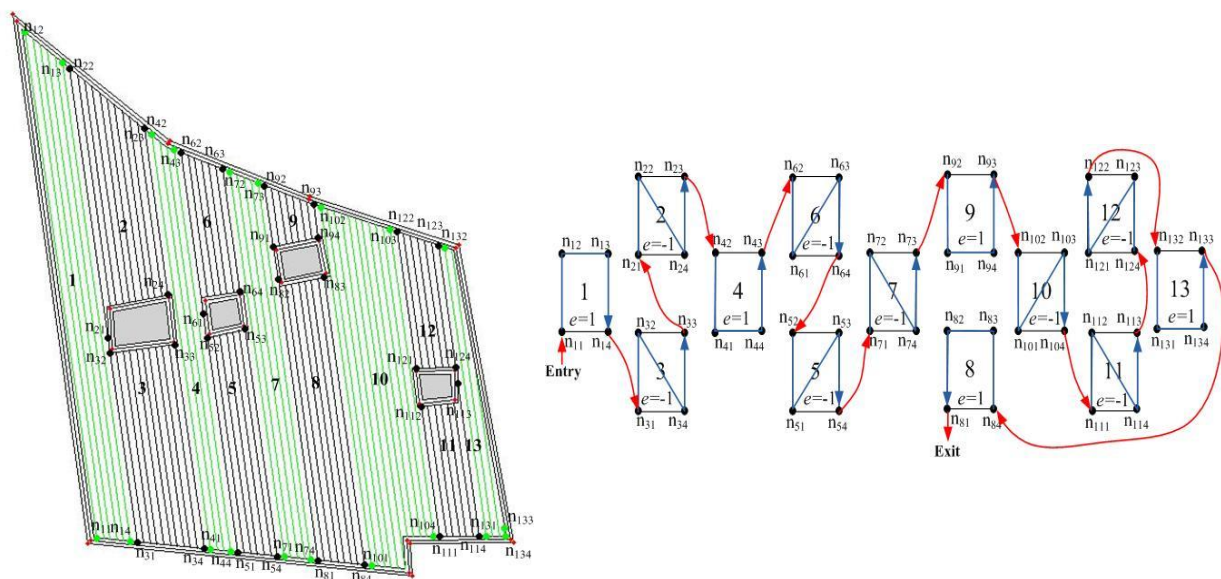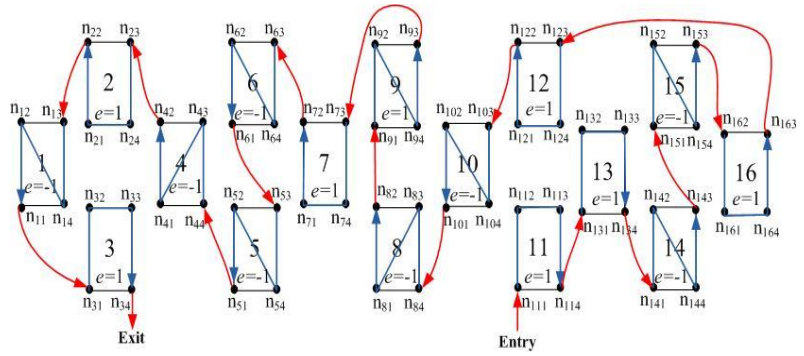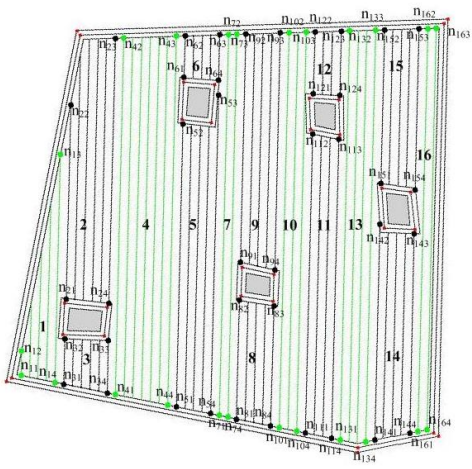
**(c)**

Fig.15. The resulted solution of the method for the test cases regarding fields with (a) 3 obstacles, (b) 4 obstacles, and (c) 5 obstacles.

**Table 2. Parameters and results from the three simulated test cases.**

| Field | (a) | | | | (b) | | | | (c) | | | |
|---|---|---|---|---|---|---|---|---|---|---|---|---|
| Area(ha) | 20.21 | | | | 56.54 | | | | 4.81 | | | |
| Number of obstacles | 3 | | | | 4 | | | | 5 | | | |
| Driving angle(°) | 105 | | | | 108.2 | | | | 31.8 | | | |
| Operating width (m) | 9 | | | | 12 | | | | 15 | | | |
| Minimum turning radius (m) | 6 | | | | 6 | | | | 6 | | | |
| Number of headland passes | 1 | | | | 1 | | | | 1 | | | |
| $\rho$ | 0.5 | | | | 0.5 | | | | 0.5 | | | |
| $\alpha$ | 1 | | | | 1 | | | | 1 | | | |
| $\beta$ | 5 | | | | 5 | | | | 5 | | | |
| Iterations | 20 | 100 | 200 | 400 | 40 | 100 | 200 | 400 | 50 | 100 | 200 | 400 |
| Average processing time (s) | 3.7 | 27.5 | 55.1 | 109.3 | 22.3 | 69.4 | 118.3 | 233.7 | 57.1 | 123.3 | 235.5 | 465.8 |
| Blocks connection distance (m) | 386.5 | 371.5 | 371.5 | 371.5 | 788.4 | 765.1 | 765.1 | 765.1 | 864.6 | 856.4 | 856.4 | 856.4 |
| Total effective working distance (m) | 21,823 | | | | 46,020 | | | | 31,680 | | | |
| Non-working distance (m) | 2,973.9 | | | | 1,790.7 | | | | 1,573.2 | | | |

# 4  Conclusions

In this paper, a planning method for simulating field operations in fields with multiple obstacle areas was presented. The method implies that the field is divided into blocks around the in-field obstacle(s), such that

the blocks contain no obstacles, and the optimal block traversal sequence was formulated as a TSP problem which is solved by applying the ACO algorithmic approach.

The validation of the method showed that it can simulate field operations with sufficient accuracy. Based on two experimental set-ups, the errors in the prediction of total travelled distance were 0.15% and 0.21%, respectively. Furthermore, the optimization part of the method was validated by comparing the ACO algorithm solutions with an exhaustive enumeration algorithm for the small-sized problems included in the two previously mentioned cases.

It was also demonstrated that the method can provide feasible solutions for more complicated field operational environments in terms of the number of obstacles included in the field area. Even in the cases of conditions seldomly experienced in practice, e.g. involving 5 obstacles, the derivation of an improved solution was exhausted within 100 iterations corresponding to 123 s computational time.

The developed method can be used as part of a decision support system providing feasible field operation solutions in testing different driving directions, operating widths, machine turning radius etc. Furthermore, the method can be incorporated in navigation-aiding systems for agricultural machinery, since currently such systems cannot provide a complete route for covering fields that include obstacles.

## References

Bochtis, D.D., Sørensen, C.G., 2009. The Vehicle Routing Problem in Field Logistics Part I. *Biosystems Engineering* 104(4), 447-457.

Bochtis, D.D., Vougioukas, S.G., 2008. Minimizing the non-working distance travelled by machines operating in a headland field pattern. *Biosystems Engineering*, 101(1), 1-12.

Bochtis, D.D., Sørensen, C.G., Busato, P., Berruto, R., 2013. Benefits from optimal route planning based on B-patterns. *Biosystems Engineering* 115 (4), 389-395.

Choset, H., 2001. Coverage for robotics - a survey of recent results. *Annals of Mathematics and Artificial Intelligence* 31, 113-126.

Choset, H., Pignon, P., 1997. Coverage Path Planning: The Boustrophedon Decomposition. International Conference on Field and Service Robotics, Canberra 1997.

Colorni, A., Dorigo, M., & Maniezzo, V., 1992. An Investigation of some Properties of an "Ant Algorithm". PPSN 92, 509-520.

de Bruin, S., Lerink, P., Klompe, A., Van der Wal, D., Heijting, S., 2009. Spatial optimisation of cropped swaths and field margins using GIS. *Computers and Electronics in Agriculture* 68(2), 185-190.

Dorigo, M., Gambardella, L. M., 1997. Ant colony system: A cooperative learning approach to the traveling salesman problem. *IEEE Transactions on Evolutionary Computation*, 1(1), 53-66.

Douglas, D., Peucker, T., 1973. Algorithms for the reduction of the number of points required to represent a digitized line or its caricature, *The Canadian Cartographer* 10(2), 112-122.

Galceran, E., Carreras, M., 2013. A survey on coverage path planning for roborics. *Robotics and Autonomous Systems* 61(12), 1258-1276.

Garey, M., Johnson, D., 1979. Computers and Intractability: a Guide to the Theory of NP-Completeness. Freeman, San Francisco, CA, USA.

Glover, F., Kochenberger, G., 2002. Handbook of Metaheuristics. Kluwer Academic Publishers, Norwell, MA, USA.

Hahsler, M., Hornik, K., 2007. TSP - Infrastructure for the Traveling Salesperson Problem. *Journal of Statistical Software* 23(2), 1-21.

Hameed, I.A., Bochtis, D.D., Sørensen, C.G, Nørremark, M.A., 2010. Automated generation of guidance lines for operational field planning. *Biosystems Engineering* 107 (4), 294-306.

Hameed, I.A., Bochtis, D.D., Sørensen, C.G., 2013. An optimized field coverage planning approach for navigation of agricultural robots in fields involving obstacle areas. *International Journal of Advanced Robotic Systems* 10, 1-9.

Hofstee, J.W., Spätjens L.E.E.M., IJken.H., 2009. Optimal path planning for field operations. Proceedings of the 7th European Conference on Precision Agriculture. Wageningen Academic Publishers, The Netherlands, 511-519.

Jin, J., Tang, L., 2010. Optimal coverage path planning for arable farming on 2D surfaces. *Transactions of the ASABE*, 53 (1), 283-295.

Oksanen, T., Visala, A., 2007. Path planning algorithms for agricultural machines. *Agricultural Engineering International*, The CIGR Journal, Volume IX.

Oksanen, T., Visala, A., 2009. Coverage path planning algorithms for agricultural field machines. *Journal of Field Robotics* 26 (8), 651-668.

Palmer, R. J., Wild, D., Runtz, K., 2003. Improving the efficiency of field operations. *Biosystems Engineering* 84(3) 283-288.

Scheuren, S., Stiene, S., Hartanto, R., Hertzberg, J., Reinecke, M., 2013. Spatio-Temporally Constrained Planning for Cooperative Vehicles in a Harvesting Scenario. Künstl Intell 27:341-346.

Stoll, A., 2003. Automatic operation planning for GPS-guided machinery. In: J Stafford and A Werner (Eds.), Proceedings of the 4th European Conference on Precision agriculture. Wageningen Academic Publishers, The Netherlands. 657-644.

Toussaint, G.T., 1983. Solving geometric problems with the rotating calipers. In: Proc.2nd IEEE Mediterranean Electrotechnical Conference (MELECON 1983), pp. 1-4.

# Chapter 4

# A Web–based Tool for Comparing Filed Area Coverage Practices

K.Zhou, A.L.jensen, D.D.Bochtis, C.G.Sørensen

## Abstract

In recent years, field coverage planning has been a topic of considerable interest among researchers and famers. Farmers may gain benefit and help by using tools that allows them to optimize the operation plans for field coverage. The aim of this paper was to develop a web-based field coverage planning system in terms of maximizing overall field operation efficiency. The farmers can define field-specific data (e.g. field boundary, driving direction, and headland numbers) field's boundary, driving direction and set the implementation parameters (e.g. minimum turning radius, working width) via a web interface. The output parameter includes driving direction, total working distance and overlapped area, which provides the farmer with a reference coverage plan ahead of the execution of field operations.

**Keywords:** Web-based, Field coverage, Path planning, Agricultural vehicles

## 1  Introduction

Currently, the agricultural sector has been undergoing a significant development towards 'informatisation', which requires innovative technology and knowledge to be integrated as part of arable farming. In addition, farmers and agricultural advisers are facing the pressures from environmental, social, energy and safety regulations. These requirements force farmers and agricultural advisers to reduce the production costs and maximize the farming profit while maintaining the highest agriculture product quality, the maximization of agricultural machinery productivity is a key element in the continued efforts of improving source utilization and field operation efficiency (Sørensen and Bochtis, 2010).

A number of aiding systems for agricultural machines have been developed ranging from navigation-aiding systems to automated auto-steering systems and fully autonomous vehicles. All these systems are aimed to increase farming efficiency, productivity and free the operators who make steering continuously. However, the disadvantage of these systems is that they are dependent on the experience of the machine operator' coverage strategy, whereas there is no evidence that these experience-based strategies are optimal or even near optimal (Oksanen, 2007). Moreover, there is a certain need required by farmers and machine contractors

that agriculture field machine operations need to be performed precisely by utilizing optimized route, such as fertilizing, spraying, seeding and harvesting, in a way that field operations can be executed in a manner that minimizes consuming time, cost and environmental impact.

In an effort to provide a solution to the problem mentioned above, many algorithms and computer simulation models and decision support tools for optimizing coverage planning have been reported in literature. All of these approaches are to solve two distinct problems: geometrical field representation and route planning within the representation .The first problem regards to the generation of discrete geometric primitives, such as points, lines and polygons. So far, a number of methods have been developed to deal with this problem (Bruin *et al.*, 2009; Hameed *et al.*, 2010; Jin and Tang, 2010; Oksanen and Visala, 2009). The second problem is to find the optimal route of the agricultural vehicles within the geometrical representation. In relation to this problem, advanced methods based on combinatorial optimization have recently been introduced (Bochtis and Sørensen, 2009).

Nevertheless, only few research results on web-based coverage path planning have been reported.  A web-based tool for the operational planning of liquid organic fertilizer application using the umbilical system was developed by (Busato *et al.*, 2013). The developed web-based tool can be used as an integral part of a decision system for suggesting the user on decision making regarding the implementation and operation of the umbilical system. Bruin *et al.* (2010) developed a web-based tool, named: Geo Arable field Optimization Service (GAOS), for spatial optimisation of straight cropped swaths and field margins using geographical interaction technology. However, the developed tool has some drawbacks when dealing with complex field shapes with curved edges, or obstacles inside. Here, a web-based tool field coverage path planning is proposed. The user can interactively change the input parameters with the system via webpage interface and select between a ranges of objective functions. Also, it can generate the specific output parameters, such as driving direction, total working distance, overlapped area, etc., and the visualization of the coverage plan on Google Maps.

# 2 System design and development

## 2.1 Architecture

The web-based system has been developed as a three-layer architecture, consisting of the presentation, application, and data layers. Fig. 1 shows the schematic overview of the system. The *presentation layer* is the user interface. It allows users to input the parameter, including the field-specific data, operational data and machinery data, processed by the *application layer,* and then it presents the processed results to the user.

1. The *application layer* processes the data sent by the user, generates and stores the results into the database.

2. The *data layer* consists of the database. Its function is to store the data in an organised and structured way and to enable users to retrieve the specified data.

3. The further details of these three layers are described in the following three sub-sections.
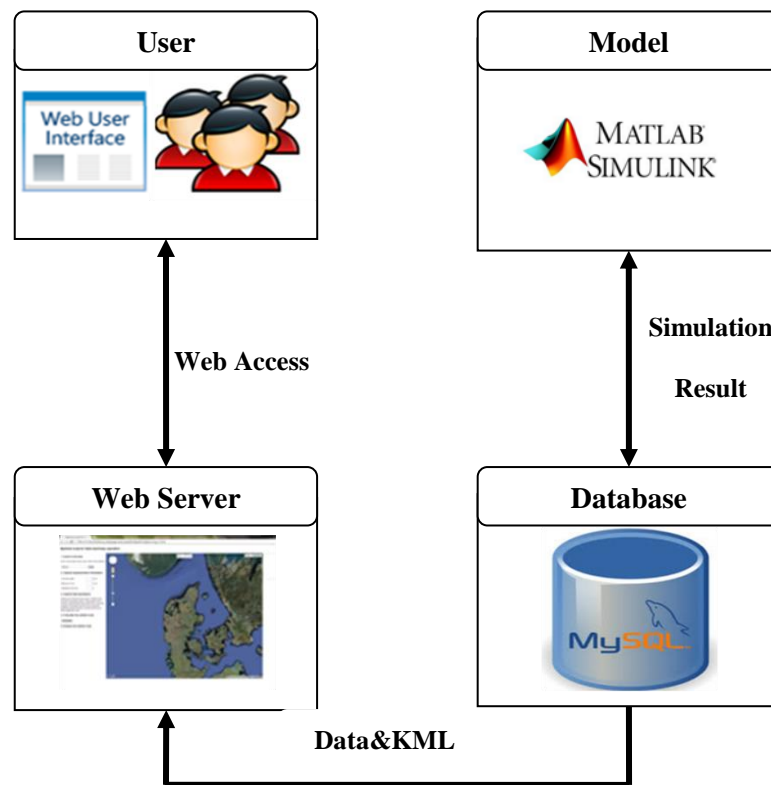


**Fig.1 - System architechture.**

## 2.2    Presentation layer

The task of the presentation tier is to ensure that the system is both interactive and user-friendly while enabling users with different technical skills and knowledge to access it easily. With the provision of a friendly user interface and easy way to access the information in mind, the design of the presentation layer was based on the Google Maps API interface, a free web mapping technology, developed by Google and currently widely used in different kinds of systems and applications (Chow, 2008). JavaScript and HTML (Hypertext Markup Language) were used in this layer.
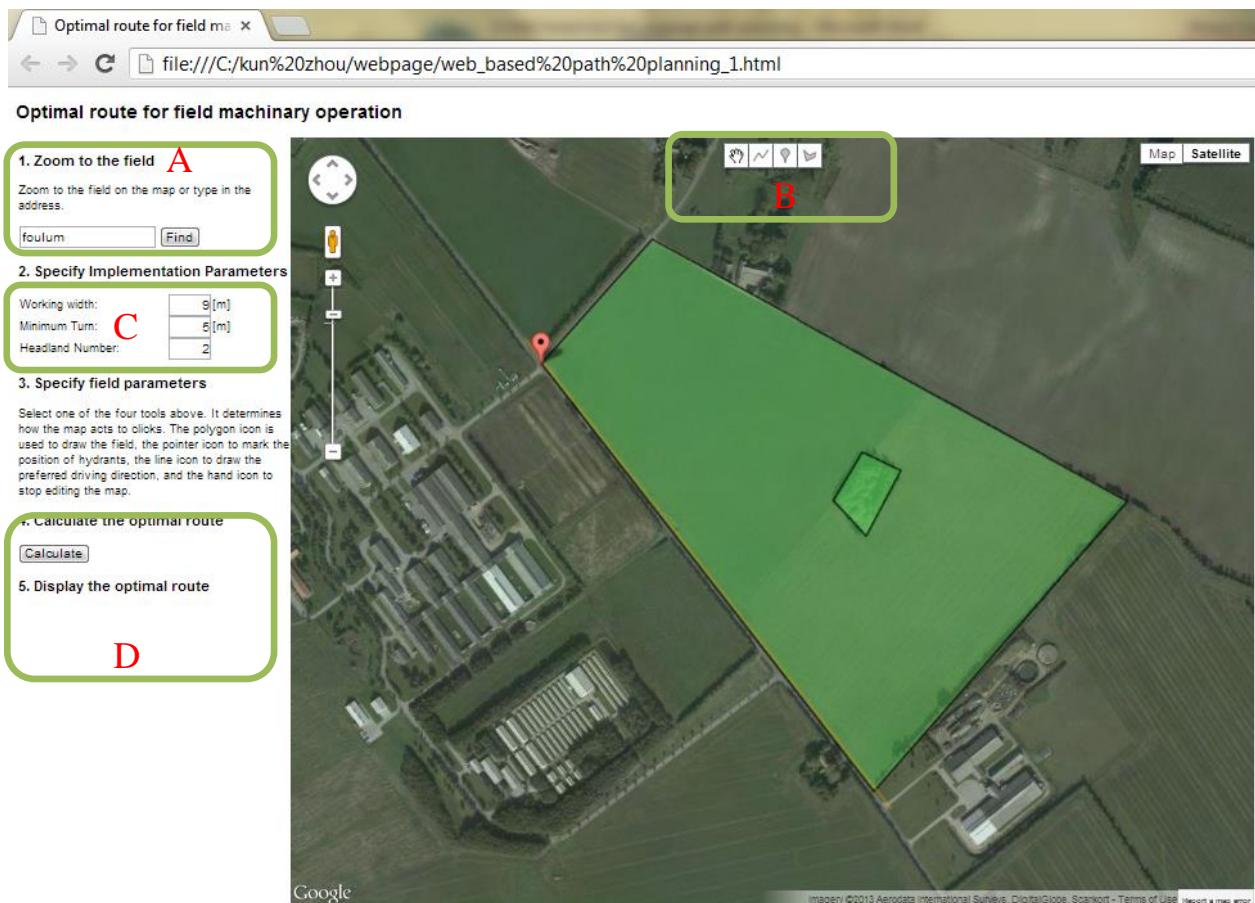


**Fig.2 - The main webpage.**

The system, when loaded, shows a webpage that is divided into 4 different sections (Fig. 2). On section A, the users can easily find the field area by typing in the specific field location, when a specific field is

81

selected, the map in the section B is moved to the corresponding location. The main components of the system are found in section B and C, which are used for users to input the parameters. There are three sets of input parameter to the application layer, namely the field-specific data, operational data and machinery data. The field-specific data consists of field boundary, obstacle area and the vehicle driving direction. In section B, the field and obstacle boundary can be defined using the "Polygon" function of Google Maps JavaScript API, which are presented by a series of coordinates in an ordered sequence. The vehicle driving direction, which regards the direction of the parallel field-work tracks, is specified by two points using the "Polyline" function of Google Maps JavaScript API. Operational data includes the working width that is the width of the implements and also the width of the field-work tracks, and average speeds (effective working speed, turning speed). All the input parameters values are integrated into a string. Then the string transmission between client and server is executed through Hypertext Text Transfer Protocol (HTTP).

The system outputs in section D estimate the total working distance, headland turning distance, number of tracks , time spent (according to the a user specified working speed). The coverage path plan is generated as a KML (Keyhole Markup Language) file for visualization in Google maps, as well as coordinates for uploading to a GPS device mounted on the agricultural vehicle.

## 2.3    Application Layer

### 2.3.1    Script for dynamic web pages

The application layer consists of a set of scripts on the web server, which is the medium between the data layer and the presentation layer. The coverage path planning model was implemented using the MATLAB technical programming language (the MathWorks, Inc., Natwick, MA, USA).

During the processing of the request from the user, as mentioned in the section 2.2, all the user input parameters were combined as a query string to the application layer, upon the server received the query string from the users; the Active Server Pages (ASP) script named "Caculate.asp" was activated. Then this ASP script opens a Microsoft object called XMLHTTP that can call a web server. The coverage path planning model extracted the input variables from the query string, the output of the execution of the model

are coordinates of the route and the other outcomes (e.g., total covered distance, turning distance and overlapped area). The coordinates of the calculated route was stored in a KML file that can be used to display geometrical data on Google Maps or other graphic systems.

### 2.3.2    The coverage path planning model

As we mentioned above, coverage path planning includes two problems: geometrical field representation and route planning within the representation. In the first stage the coordinates of the tracks to be followed by the agricultural vehicles are automatically generated. Given the field boundary, the number of headland passes, the driving direction and the vehicle implement width. Each track is presented by the starting and the ending points located the internal field boundary that is the offset of the field boundary equalling with the vehicle implement width. The headland area that is dedicated for machinery turnings comprises a number of sequential passes. In the second stage, the sequential track routing patter was applied to traverse the tracks generated in the first stage.

## 2.4   Data layer

The MySql, an open source relational database management system, was adopted to store user inputs and model outputs, which has the ability to efficiently search, store and retrieve data in databases. The results of simulation to be presented to users were stored in the database. The coordinates of the polygon and waypoints of the paths were saved as KML file that can be showed on the Google Map in specific folders on the server.

## 3   Results and discussion

The system was tested by applying it in two fields, namely a convex field and a convex field with an obstacle inside. The polygons of the two fields were specified using the user interface of the tool mentioned in section 2.2. Both fields are located at Foulum Research Center, Demark. The convex field [Fig.3a, 9.5711, 56.4950] has an area of app. 5.4 ha, while the other one [Fig.3b, 9.5980, 56.4859] has an area of app. 25.85ha.
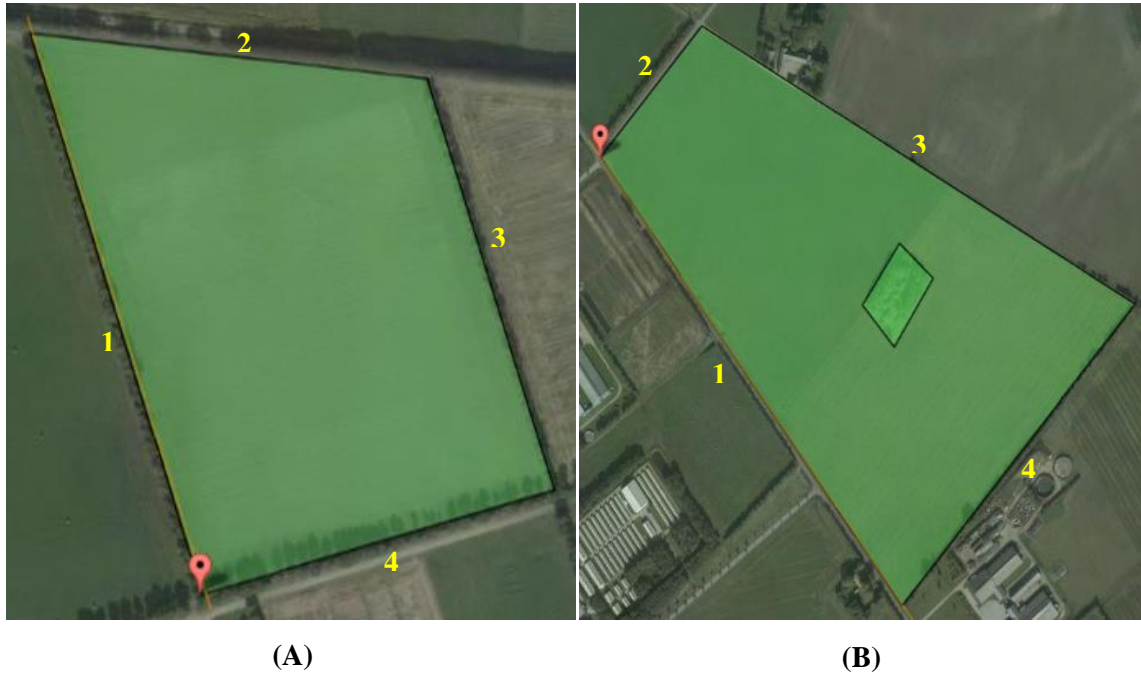
**Fig.3 - The two test fields (A) convex and (B) convex field with obstacle.**

The number of the headland passes for both fields was selected to be 2. The operating width was assumed to be equal to 9 m while the vehicle minimum turning radius was assumed to be equal to 6 m. The total effective time of a field operation was calculated, assuming an average operating speed of 8 km /h. Similarly, the total non-working time was calculated based on the total non-working distance in the headland area. Here omega-turning was used considered as the sole type of turnings assuming an average turning speed of 3 m/s. In order to test the impact of the driving angle, all driving angles (defined as the angle between the driving direction and the UTM Easting axis) along each edge of the field boundary were selected. The resulted driving angle were for field A 107.34 °, 196.23°,287.79 °, 353.74 °,and for the field B were 128.31° , 50.40° ,331.40 °, 228.74°, respectively.

The output operational parameters are listed in Table 1. For field A, the best driving angle based on the covered distance within these four driving angles is 107.34 °, resulting to tracks parallel to the longest edge. Fig. 4 presents the geometrical representation of the fields providing the field-work tracks when the driving angle is 107.34 ° and the visualization of the coverage plan as a KML file is presented on Google Maps. In

the case of field B, the best angle is 128.31 °, the geometrical representation of the field-work tracks and visualization of the coverage plan of field B are presented in Fig. 5.

**Table1. Output operational parameters of field A and field B.**

| Scenario | Field A | | | | Field B | | | |
|---|---|---|---|---|---|---|---|---|
| Driving Angle(°) | 107.34 | 196.23 | 287.79 | 353.74 | 50.40 | 128.31 | 228.74 | 331.40 |
| Number of tracks | 18 | 31 | 18 | 28 | 91 | 69 | 90 | 70 |
| Tracks length (m) | 4306 | 4312 | 4305 | 4299 | 24459 | 24700 | 24240 | 24222 |
| Non-working distance (m) | 1040 | 1877 | 1040 | 1626 | 3186 | 2406 | 2846 | 2431 |
| Headland pass length(m) | 1777 | 1777 | 1777 | 1777 | 4308 | 4308 | 4308 | 4308 |
| Overlapped area($m^2$) | 314 | 733 | 329 | 1435 | 3545 | 3347 | 1630 | 4438 |
| Estimated operation time (h) | 1.11 | 1.39 | 1.11 | 1.30 | 4.66 | 4.43 | 4.52 | 4.38 |
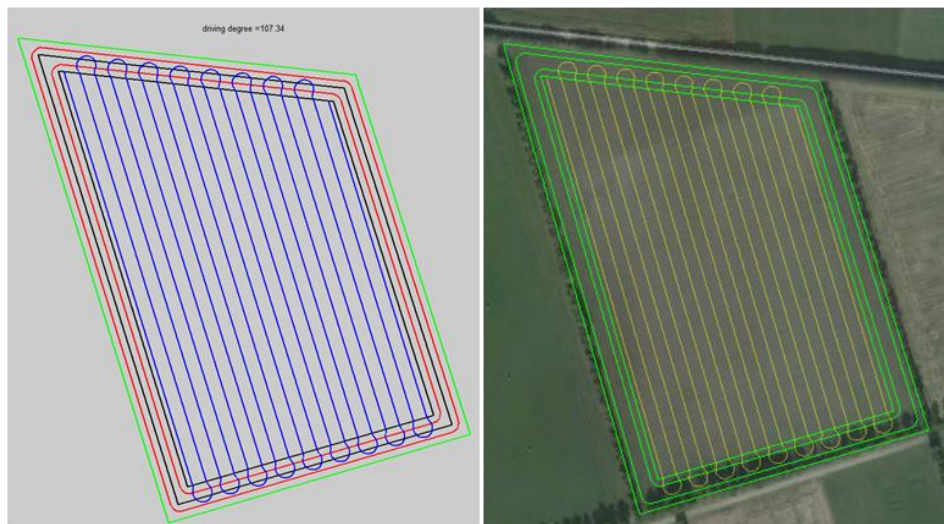


**Fig.5 - The geometrical representation and visualization of coverage plan for field A.**

**Fig.5 -The geometrical representation and visualization of coverage plan for field B.**

# 4   Conclusion

A web-based tool for field coverage path planning was developed and tested on two types of fields. The tool

enables users with different technical skills and knowledge to access it easily. The specific output parameters

generated by the tool, such as total working distance, turning distance and overlapped area, provide the

farmer a reference coverage plan ahead of the execution of field operations.

# References

Bochtis, D.D., Sorensen, C. G., 2009. The vehicle routing problem in field logistics part I. *Biosystems Engineering, 104*(4), 447-457.

Bruin, S. d., Janssen, H., Klompe, A., Klompe, L., Lerink, P., & Vanmeulebrouk, B., 2010. *GAOS: spatial optimisation of crop and nature within agricultural fields.* Paper presented at the International Conference on Agricultural Engineering-AgEng 2010: towards environmental technologies, Clermont-Ferrand, France, 6-8 September 2010.

Bruin, S. d., Lerink, P., Klompe, A., van der Wal, T., & Heijting, S., 2009. Spatial optimisation of cropped swaths and field margins using GIS. *Computers and Electronics in Agriculture, 68*(2), 185-190.

Busato, P., Sørensen, C. G., Pavlou, D., Bochtis, D. D., Berruto, R., & Orfanou, A., 2013. DSS tool for the implementation and operation of an umbilical system applying organic fertiliser. *Biosystems Engineering, 114*(1), 9-20.

Chow, T. E., 2008. The Potential of Maps APIs for Internet GIS Applications. *Transactions in GIS, 12*(2), 179-191.

Hameed, I. A., Bochtis, D. D., Sorensen, C. G., Noremark, M., 2010. Automated generation of guidance lines for operational field planning. *Biosystems Engineering, 107*(4), 294-306.

Jin, J., Tang, L., 2010. Optimal Coverage Path Planning for Arable Farming on 2d Surfaces. *Transactions of the ASABE, 53*(1), 283-295.

Oksanen, T., 2007. *Path planning algorithms for agricultural field machines*: Helsinki University of Technology.

Oksanen, T., Visala, A., 2009. Coverage path planning algorithms for agricultural field machines. *Journal of Field Robotics, 26*(8), 651-668.

Sørensen, C. G., Bochtis, D. D., 2010. Conceptual model of fleet management in agriculture. *Biosystems Engineering, 105*(1), 41-50.

# Chapter 5

# Simulation model for the sequential in-field machinery operations in the potato production system

K. Zhou, A. Leck Jensen, D.D. Bochtis, C.G. Sørensen

# Abstract

In potato production multiple sequential operations have to be carried out during the yearly production, and each operation may have its own set of operational features, given by the used machinery, e.g. operating width and turning radius. An optimal planning for one operation may lead to restrictions and reduced efficiency to later operations. For example, the optimal driving direction of the seedbed former may not be the optimal for the planter, sprayer and harvester, but once the beds are formed the same driving direction is set for the subsequent operations of the growing season. Therefore, there is a need to develop an approach for predicting and optimizing the overall performance of all operations, given a selected field and the required machines. With this purpose, a targeted model for simulating all the field operations in potato production is presented in this paper.

To quantify the set of input parameters and to validate the model, all the relevant operations in potato cultivation (bed forming, stone separation, planting, spraying and harvesting) were carried out and monitored in four experimental fields. The simulation model predicted the field efficiency and the field capacity with satisfactory precision for all operations in all fields. The errors in prediction of the field efficiency and the field capacity ranged from 0.46 % to 4.84 % and from 0.72 % to 6.06%, respectively. In addition, the capability of using the developed model as a management planning tool for decision support on operational decisions (e.g. driving direction, reloading position) and machinery dimensioning (e.g. tank/hopper size) was demonstrated.

**Keywords:** Agricultural operation modelling and simulation; Machinery management; Machinery performance

# 1   Introduction

Most arable crops are annual and the cultivation requires the successful and well-timed execution of a sequence of field operations, beginning with the soil preparation and sowing in the autumn or spring and ending with the harvest in the summer or early autumn. Each field operation requires specific machines, and

often the machines are even specific for the crop. It is in the interest of the farm manager to optimize the efficiency of the machines, such that the field operation is executed with sufficient quality at the lowest possible cost. The cost of execution of a field operation may include several factors, such as the operators' salaries, the depreciation of the machines, the consumption of fuel and input material (seed, fertilizer etc.), the damage to the soil (soil compaction) and the crop (damaged plants, spilled harvested material etc.). The efficiency of each field operation is determined by a range of selected operational feature (e.g. driving direction, working width, working speed, track sequence, turn type, etc.).

Farmers strive to optimize the execution of the field operations by applying their acquired knowledge and experience. However, this may lead to sub-optimal planning, due to the complexity of the decisions with many influencing factors, particularly in the case where some factors are competitive, that affect the overall performance of the machinery and operation. Instead of acquiring experience in practice, simulation models have proven to be valuable tools for farm managers providing a basis for making managerial or technical decisions by being able to simulate the consequences of a great number of alternative scenarios in a more time and cost effective manner. In the last few decades, a considerable number of field operation simulation models have been developed and applied to analyze and optimize the production process and reduce the cost in agricultural field operations. These simulation models include models of grain harvesting (Benson *et al.*, 2002; Busato, 2015; de Toro *et al.*, 2012), plantation in greenhouse (Bechar *et al.*, 2007; van 't Ooster *et al.*, 2012, 2014), manure handling (Bochtis *et al.*, 2009; Busato *et al.*, 2013; Hameed *et al.*, 2012) and tillage (Sørensen and Nielsen, 2005). However, a common characteristic of the above-mentioned models is that they are only able to simulate a single field operation.

There is a need for models that can simulate all the required operations of an entire growing season of crop production systems. The reason for this is that the operations are not independent, so the optimal plan for one operation is likely lead to restrictions and reduced efficiency for the subsequent operations. Thus, the combination of optimal plans for each operation is not necessarily an optimal plan, not even a feasible plan, when the entire sequence of operations of the growing season is considered. For example, the optimal driving direction may not be the same for all field operations, but for fields with crops cultivated in rows or

beds or for fields with Controlled Traffic Farming (CTF) the driving direction cannot be changed from operation to operation. Likewise, for operations using machines with different working widths there is a strong inter-dependency that must be taken into account. The decision-making process in multiple operations planning is very critical in the case where an operational feature should be identical in all operations.

This paper considers the potato production system as a study case. Potatoes are cultivated in beds, so once the beds are formed the driving direction is determined for the remaining operations of the season. The working widths of the machines vary from the width of a single bed (e.g. planting) to multiple beds (e.g. spraying), which also has influence on the optimal bed layout design of a given field. Potato production includes complex field operations, where multiple cooperating machine units have to be coordinated in order to achieve optimization of the performance of the overall system. For instance in planting, coordination may encompass the determination of locations of the refilling units (small mobile containers with seed potatoes) and of the appropriate refilling quantity for the planter in order to apply the next round of planting based on the application rate. However, these decisions and coordination are quite complex for the farm manager and machine operators to be made appropriately.

In this paper, a simulation model for the sequential in-field operations in the potato production system is developed and applied. The detailed description of these operations is presented in Section 2.1, the work process in each operation is analyzed and modelled in Section 2.2 and the model is implemented in Section 2.3. Section 3 explains how experimental operations in four fields were conducted to quantify input parameters and validate the simulation model. Next, in Section 4 it is demonstrated that the validated model is feasible to provide support of field operational decisions such as driving direction, fieldwork pattern, etc. Finally, conclusions are made in Section 5.

# 2 Development of the simulation model

## 2.1 Description of the potato production system

In potato production, five sequential field operations are executed each growing season: Bed formation, stone separation, planting, spraying and harvesting.

1) Bed formation: This is a crucial step which determines the potato bed layout and wheel tracks for all subsequent field operations of the entire season (Fig. 1.a). The bed former uses shaped metal plates to lift up the soil and form it into one or more beds.

2) Stone separation: This operation is also a part of the seedbed preparation to ensure that the seedbed is free of oversize stones and clods in order to provide ideal growing conditions for the potatoes, as well as to reduce the need for picking up stones and clods and sorting them from the potatoes during harvest. Usually, the operation is completed by using a stone separator which enables the fine soil to fall through sieves into the bed, while the oversize stones and clods are transferred by a conveyor to an adjacent furrow between previously formed beds. The conveyor can be adjusted either to the right or left side when the stone separator is at the end of each bed. In successive operations the machine's tires run on the ridge of the processed stones and clods to bury them between alternate tracks (Fig. 1.b).

3) Planting: Potato planting starts immediately after the stone separation, normally by the use of automated planters. The planter is attached behind a tractor with the seed potatoes stored in a small tank, called the hopper. Special cups lift the seed potatoes from the hopper and place them with accuracy distance into the tracks. The depth of sowing is about 5-10 cm and the distance between potato tubers along the rows are about 20-40 cm (Fig. 1.c). Due to capacity constraints the hopper needs to be refilled from the reloading station (Fig. 1.d) occasionally. This is done by driving to the headland area where one or more reloading units are located.

4) Spraying: Spraying with herbicides, pesticides or fungicides are usually performed around 10 times during the growing season (Fig. 1.e).

5) Harvesting: The most common harvest method is using a potato harvester with diggers, depending on the bed type, which can dig out the potatoes from the bed. Soil and crop are transferred onto a series of sieves where the loose soil is sieved out. The potatoes are conveyed to a separation unit at the back part of the harvester. The potatoes then either go on to a side elevator or into transportable storage units that are located in the field or along the field boundary (Fig. 1.f).



|  (a)  |  (b)  |
|  (c)  |  (d)  |
|  (e)  |  (f)  |

**Fig. 1 - The involved field operations and machines/units in potato production: (a) bed forming; (b) stone separation; (c) planting; (d) reloading unit; (e) spraying (Photo source: gopixpic); (f) harvesting.**

The above described operations can be categorized into three groups, according to whether material flows into or out of the field: Material neutral operations (MNO) (bed formation, stone separation), material input operations (MIO) (planting, spraying), and material output operation (MOO) (harvesting). The operations of
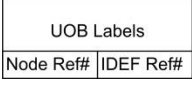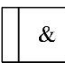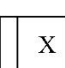
each category have similar work processes, so they are modelled generically in the next section. Furthermore, agricultural machines involved in those operations are classified as primary units (PUs) that perform the main field task (e.g. tractors with implements or self-propelled machines) and service units (SUs) (e.g. a tractor with trailer) that load or unload the PUs during the operation (Bochtis and Sørensen, 2009; Bochtis and Sørensen, 2010).

## 2.2  Modelling of the work process

The IDEF3 modelling method (Mayer *et al.*, 1995) was chosen to model the work process of tasks and decisions involved in the potato production system. IDEF3 diagrams describe workflows as an ordered sequence of events or activities in a situation or process (Kusiak and Zakarian, 1996). The IDEF family of functional modelling languages has been extensively used in the industrial area for design and manufacturing processes, business systems modeling and project management (Kusiak *et al.*, 1994; Shen *et al.*, 2004). In the past decade IDEF has been applied to describe the work process of various operations in the agricultural context, e.g. in food chain traceability systems (Hu *et al.*, 2013; Thakur and Hurburgh, 2009; Zhang *et al.*, 2011), in harvesting of roses (van 't Ooster *et al.*, 2014), in rice harvesting (Busato, 2015), in biomass supply chain (Zhang *et al.*, 2012) and in information management systems in viticulture (Peres *et al.*, 2011).

An IDEF3 process flow description is made up of units of behaviors (UOBs), links and junction boxes. A UOB represents a process, activity, action or decision occurring in the process. Links represent the relationships between these UOBs, consisting of three types of links: precedence, relational, and object flow links. In this paper, only the precedence links indicating a simple temporal precedence between UOBs were used. Junctions show the logic branching within a process, which include the logical *AND* (*&*), *OR* (*O*) and *XOR* (*X*). The process paths converge (*fan-in*) or diverge (*fan-out*) at a junction. The explanations of these symbols are presented in Table 1.

| Table 1 - Symbols of IDEF3 schema and their descriptions. | | |
|---|---|---|
| Symbols | Name | Description |
| UOB Labels<br>Node Ref# \| IDEF Ref# | Unit of behavior (UOB) | Activity occurring in the process. The UOB label is a 'verb-phrase' identifying the activity. The Node Ref # is a unique number, the IDEF Ref # is an optional reference (not used). |
| → | Simple precedence link | This link expresses temporal constraints between UOBs. |
| & | Synchronous AND | Fan-in: All preceding activities must be completed before this activity starts.<br>Fan-out: All of the following activities must be started. |
| O | Synchronous OR | Fan-in: This activity starts only when at least one of the preceding activities have completed.<br>Fan-out: One or more of the following activities must be started. |
| X | XOR (Exclusive OR) | Fan-in: This activity starts when exactly one preceding activity has completed.<br>Fan-out: Exactly one of the following activities must be started. |

In the following sections the processes with corresponding sequential decisions that must be made during an operation are analyzed and modelled using IDEF3. The process of analyzing and modelling was based on onsite observations of farmer's practices and on interviews with a group of experts in Denmark.

## 2.2.1 Modelling of material neutral operations

The work and decision processes (Fig. 2) in the MNO operations are simpler in comparison to those in MIO and MOO operations. Basically, as Fig. 2 illustrates, there are two overall types of activities in MNO: First, the tracks in the main cropping area are processed and then the headland passes are processed. Specifically, the activity 'Operation commences' (UOB1) initializes the operation, then the PU moves to the field and starts processing the first track (UOB2) until it reaches at the end of the track (UOB3). Then a decision is made (in junction J2): If there are any unprocessed tracks the PU enters such a track (UOB4), otherwise it turns to the headland (UOB5) to process the headland passes (UOB6 and UOB7). Whenever the PU finishes

processing a headland pass it is evaluated (junction J4) whether there are still unprocessed headland passes, otherwise the operation terminates (UOB9). The detailed description of actions involved in MNO is presented Table 2.

| Table 2 - Description of UOBs and junctions of the IDEF3 process diagram for the MNO. | | |
|---|---|---|
| ID | Activity | Description |
| UOB1 | Operation commences | The parameter settings are initialized as follows:<br>– The PU object is created and the relevant parameters, including the effective working width etc. are set. The accumulated effective working distance/time and turning distance/time are initialized to zero.<br>– The field object is created, where all fieldwork tracks and headland passes are generated and reordered according to the predetermined fieldwork pattern. |
| J1 | | J1 is a fan-in junction that sends the PU to UOB2. |
| UOB2 | PU operates on a track | The first fieldwork track to be processed is selected. The working speed of the PU is looked up from a database and the length of the current track is computed. |
| UOB3 | PU is at the end of current track | The time duration on the current track is computed by track length divided by working speed, and the total effective distance and time are updated. |
| J2 | | A decision process is triggered based on whether there are unprocessed fieldwork tracks. If there are unprocessed fieldwork tracks then the PU turns to enter a new track (UOB4) according to the fieldwork pattern, otherwise it moves to the headland area (UOB5). |
| UOB4 | PU turns to enter a new track | The turn distance and time is acquired from the database and the accumulated turn distance and time are updated. Then the activities in UOB2, 3 and 4 are repeated iteratively until all fieldwork tracks have been processed. |
| UOB5 | PU moves to the headland area | The decision to activate this activity is made in J2 after all the fieldwork tracks have been processed. In this activity the selection of the first headland pass to be processed is made. |
| J3 | | J3 is a fan-in junction that sends the PU to UOB6. |
| UOB6 | PU operates on a headland pass | The working speed of the PU is obtained and the length of the current headland track is computed. |
| UOB7 | PU is at the end of current headland | The time duration on the current headland track is computed by |

| | | the track length divided by the working speed, and the accumulated effective distance and time are updated. |
|---|---|---|
| J4 | | The decision is made to turn the PU to enter a new headland pass (UOB8) if there are still headland passes to be processed or to terminate the simulation (UOB9). |
| UOB8 | PU turns to enter a new headland pass | The turn distance and time is acquired from a database lookup, and the accumulated turn distance and time are updated. Then the activities in UOB6, 7 and 8 are repeated iteratively until all headland passes have been processed. |
| UOB9 | Operation terminates | The accumulated simulation results for the PU are saved. The results include the total time spent in the field, the total effective time and the total turning time. Time-based field efficiency and field capacity are calculated. The simulation of the operation is shut down. |
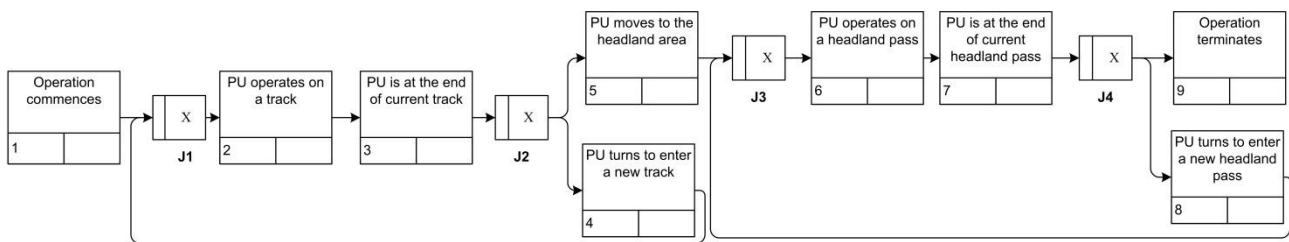


**Fig. 2 – IDEF3 process diagram for the MNO.**

### 2.2.2 Modelling of material input operations

In material input operations the PU receives material from one or more SUs, which are normally located in the headlands or outside the field near the field boundary. Due to the limited load capacity of a PU, the PU has to execute a number of tours for a complete coverage of the field. A tour consists of the following four parts (as shown in Fig. 3): (1) reloading material from the SU (reload), (2) driving back to the position where the PU stopped the application on the previous tour (full transport), (3) applying the material to the field (applying) (4) driving back to the SU's location to get a new refill (empty transport).

The MIO operations consist of activities by both the PU and the SU; the PU iteratively performs tours from the SU to the tracks and back to the SU for reload. First the tours processes the tracks in the field body,

afterwards the headland passes are processed. Meanwhile, the SU is also performing tours, from the field and back to the farm for reload, when the tank capacity of the SU is insufficient for the next reload of the PU. These processes are modelled in the IDEF3 process diagram in Fig. 4 and explained detailed in Table 3.
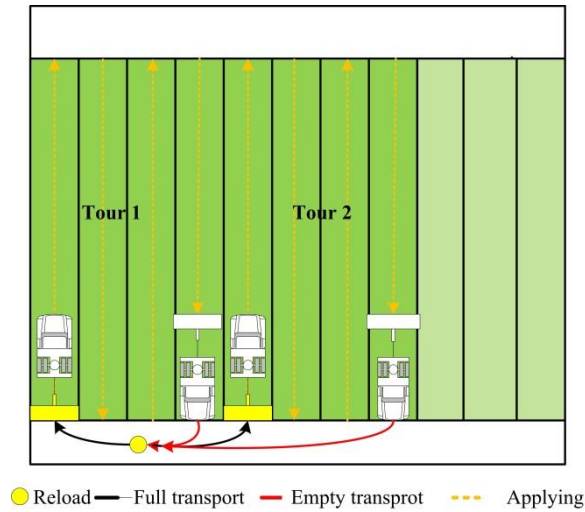


**Fig. 3 - Illustration of a typical route: The machine is reloaded at the SU (yellow circle), follows the black path with full load, resumes application in the field tracks (yellow paths), and when the hopper is empty or almost empty follows the red path to the SU.**
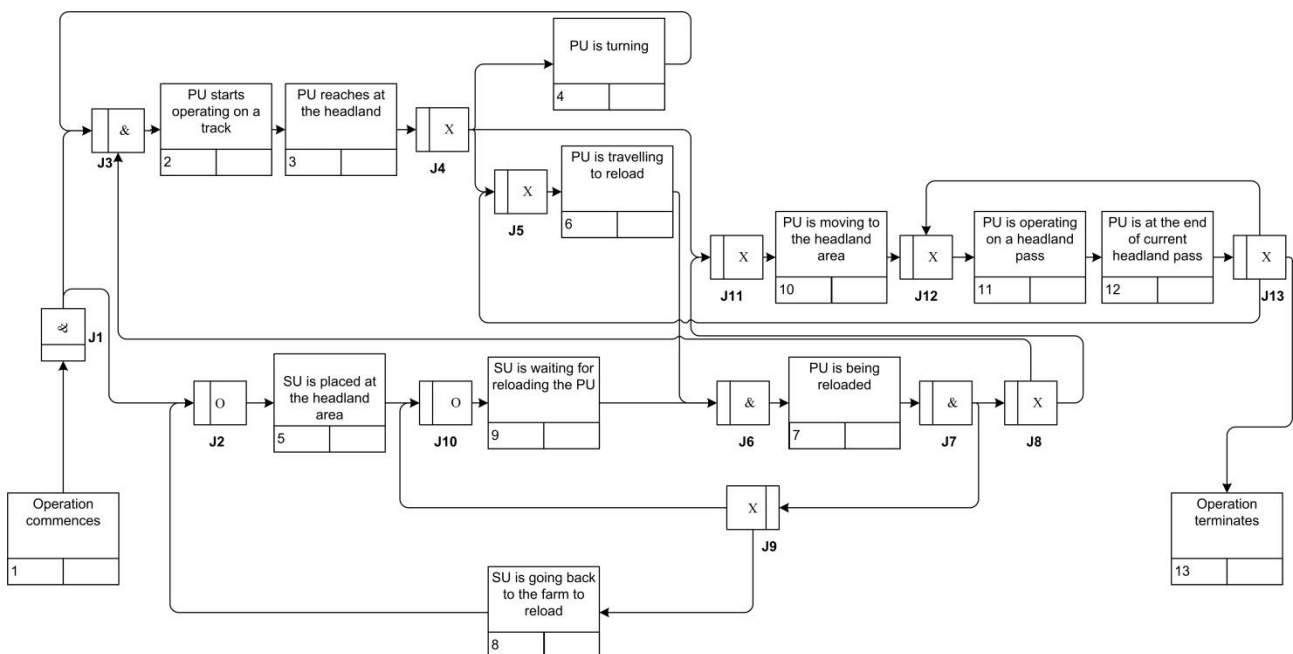


**Fig. 4 – IDEF3 process diagram for the MIO.**

| | Table 3 - Description of UOBs and junctions of the IDEF3 process diagram for the MIO. | |
|---|---|---|
| ID | Activity | Description |
| UOB1 | Operation commences | The initialization of parameters for the PU, SU and field are done as follows:<br>− Field object: Fieldwork tracks and headland passes with coordinates are generated and reordered according to the predetermined fieldwork pattern.<br>− PU object: Effective working width is set, accumulated effective distance/time, accumulated turning and transport distance/time are initialized to zero. Tank capacity is set to full.<br>− SU object(s): Location is set, capacity is set to full. |
| J1 | | The PU object is sent to J3 and the SU object(s) to J2. |
| J2 | | J2 is a fan-in junction that sends the SU(s) to UOB5. The type of the junctions J2 and J10 are synchronous OR (O) to handle multiple SUs, but for simplicity the description is for one SU. |
| J3 | | J3 is a fan-in junction that sends the PU to UOB2. |
| UOB2 | PU starts operating on a track | The PU's working speed is obtained from the database and the length of the current track is computed. The PU is send to UOB3. |
| UOB3 | PU reaches at the headland | The time duration on the current track is computed using the working speed and length of the track, and the accumulated effective distance and time of the operation are updated. The current quantity of material in the tank is updated by subtracting the quantity of applied material on this track. The PU is send to J4. |
| J4 | | A decision-making process is triggered with the following four possible outcomes: (1) If the PU is at the opposite headland with respect to the headland where the SU is located, then the PU makes a turn (UOB4) to enter a new track; (2) If the PU is at the same headland as the SU and it has sufficient material for applying the two successive tracks, then the PU makes a turn (UOB4) to enter a new track, otherwise (3) it is sent to UOB6 through J5 to get reloaded; (4) If all fieldwork tracks have been applied the PU moves to UOB10 through J11. |
| UOB4 | PU is turning | The turn distance and time are acquired from the database and the accumulated turn distance and time of the PU are updated. Then the activities in UOB2, 3 and 4 are repeated until the PU |

| | | has to be reloaded in activity UOB6. |
|---|---|---|
| J5 | | J5 is a fan-in junction that sends the PU to UOB6. |
| UOB6 | PU is travelling to reload | The speed for travelling to reload is taken from the database. The shortest feasible path from the PU to the SU and its distance and corresponding travel time is computed. As long as the SU is available then both PU and SU are sent to J6. |
| J6 | | The PU reload involves both the PU and the SU objects. J6 sends the two objects to UOB7 when both are ready. |
| UOB7 | PU is being reloaded | The accumulated reloading time for the PU is updated. The PU's capacity is set to full and the SU's capacity is reduced by the quantity reloaded to the PU. After reloading, both of them are sent to J7. |
| J7 | | The resuming distance and corresponding time are computed based on the current position of the PU and the resuming point. The PU is sent to J8, while the SU is sent to J9. |
| J8 | | A decision is made to send the PU to process a new track if there are unprocessed tracks left (UOB2 via J3), otherwise to send the PU to process the headland area (UOB10 via J11). |
| J9 | | If the remaining quantity of material in the SU is not sufficient for another reload, then it is sent back to the farm to reload (UOB8), otherwise it is sent to UOB9 through J10. |
| J10 | | J10 is a fan-in junction that sends the SU to UOB9. |
| UOB9 | | The SU is waiting for the next reload of the PU. |
| UOB8 | SU is going back to the farm to reload | The SU is travelling back to the farm to get reloaded. After reload it reenters the field via J2. |
| UOB5 | SU is placed at the headland area | The SU is placed at the headland area and the positon of the SU is updated. |
| J11 | | J11 is a fan-in junction that sends the PU to UOB10. |
| UOB10 | PU is moving to the headland area | The PU is moving to the headland area and starts operation, and the first headland pass to process is selected. |
| J12 | | J12 is a fan-in junction that sends the PU to UOB11. |
| UOB11 | PU is operating on a headland pass | The PU's working speed is obtained from the database and the length of the current pass is computed. The PU is send to UOB12. |
| UOB12 | PU is at the end of current headland pass | The time duration on the current pass is computed using its length and the working speed, and the accumulated effective distance and time are updated. The current quantity of material in the tank is updated by subtracting the quantity of applied |

| | | material on this pass. The PU is send to J13. |
|---|---|---|
| J13 | | A decision-making process is triggered with the following four possible outcomes: (1) If the entire field is processed the simulation terminates (UOB13); (2) Else, if the PU has sufficient material in the tank to apply the next headland pass, then the PU moves to this pass (UOB11 via J12); (3) If the field is not completed, but the quantity of material in the tank is insufficient for a headland pass, then the PU goes to reload (UOB6 via J5). |
| UOB13 | Operation terminates | All of the accumulated results of simulations are saved. The results include the total effective working distance/time, non-working distance/time and reloading time, time-based field efficiency and field capacity are calculated. The operation process is shut down. |

### 2.2.3 Modelling of material output operations

The MOO category only consists of a single operation, namely harvesting. In the potato harvesting operation, it is common for farmers to allocate temporary transportable SUs (e.g. field bins, wagons) in the field since the distance to the farm is often long. This enables the operator to harvest efficiently without delays caused by the SUs transporting the harvested potatoes from the field to the farm. In addition, fewer transport drivers are required. The temporary transportable SUs are always located in the headland area to avoid soil compaction in the cropping area. The MOO is similar to the MIO in the sense that it involves simultaneous activities by both the PU and the SU. Unlike the other operations categories, the PU begins by processing the headland area. The reason for this is to make room for turning without damaging the crop, when the field body area is processed afterwards. The processes of the PU and the SUs in the MOO are modelled in the IDEF3 process diagram in Fig. 5, and the main nodes are explained detailed in Table 4.

**Fig. 5 – IDEF3 process diagram for the MOO.**
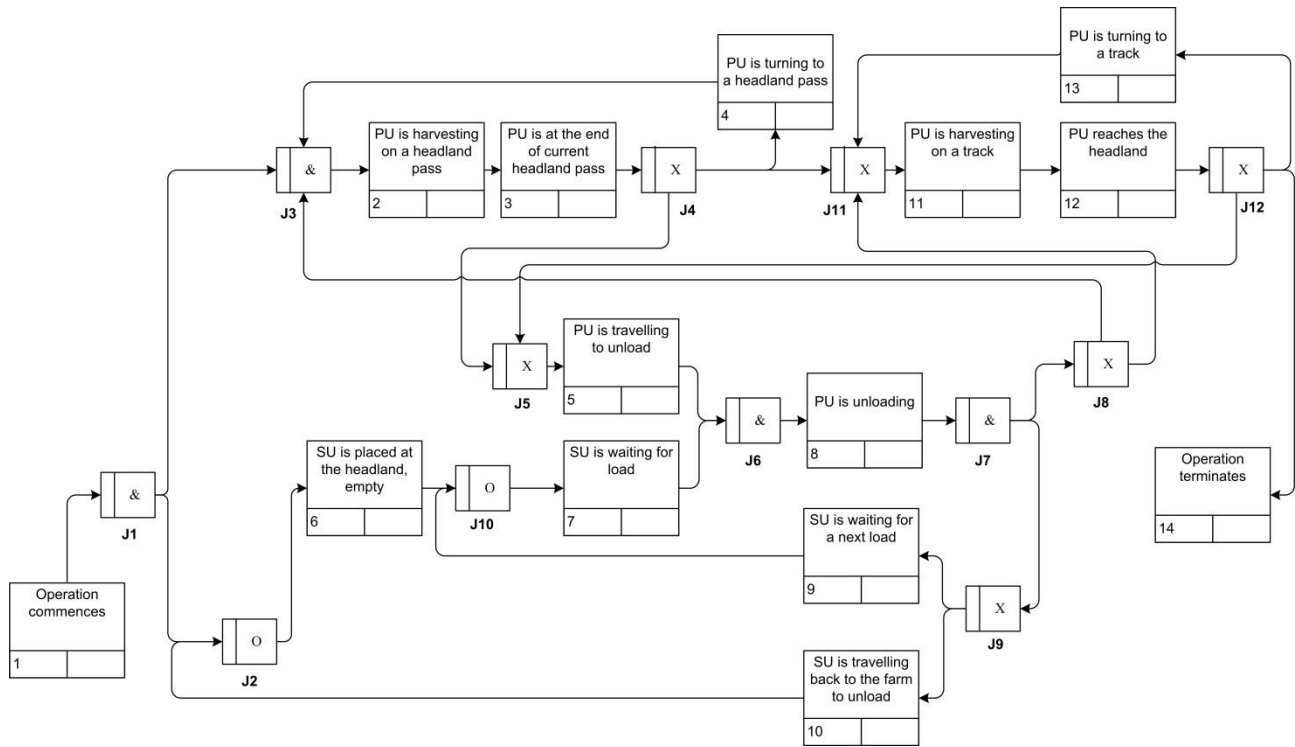
| ID | Activity | Description |
|---|---|---|
| **Table 4 - Description of UOBs and junctions of the IDEF3 process diagram for the MOO.** | | |
| UOB1 | Operation commences | The initialization of parameters for the PU, SU and field are done as follows:<br>– Field object: Fieldwork tracks and headland passes with coordinates are generated and reordered according to the predetermined fieldwork pattern.<br>– PU object: Effective working width, total effective distance/time, total turning distance/time and transport distance/time are set. Tank load is set to empty.<br>– SU object: Location is set; tank load level is set to zero.<br>The PU and SU are sent to UOB2 and UOB6 through J1 and J3 and through J1 and J2, respectively. |
| UOB2 | PU is harvesting on a headland pass | The PU is travelling to the headland area and selects a headland pass to be harvested. The working speed of the PU is obtained from the database and the length of the current pass is computed. The PU is send to UOB3. |
| UOB3 | PU is at the end of current headland pass | The time duration on the current pass is computed using the working speed and the length of the current pass, and the |

103

| | | |
|---|---|---|
| | | accumulated effective distance and time are updated. The remaining tank capacity is computed. The PU is sent to J4. |
| J4 | | A decision-making process is triggered with the following three outcomes: (1) If there is remaining space in the tank for harvesting another headland pass, then the PU makes a turn to enter a new pass (UOB4); (2) Otherwise the PU is sent to UOB5 via J5 to unload; (3) If all the headland area has been harvested the PU is sent to UOB11 via J11 to harvest the main field area. |
| UOB4 | PU is turning to a headland pass | The turn distance and time is acquired from the database, and the accumulated turn distance and time of the PU are updated. Then the activities in UOB2, 3 and 4 are repeated until the PU has to be unloaded in UOB5. |
| UOB5 | PU is travelling to unload | The travelling speed with full load is acquired from the database. The distance to be travelled from the current position to the unload position and the corresponding time are computed. As soon as the SU is available at UOB7, both the PU and the SU are sent to J6. |
| J6 | | The unloading involves both the PU and the SU. J6 combines them and sends them to UOB8. |
| UOB8 | PU is unloading | The time of unloading the PU to the SU is updated. The load level of the SU is incremented with the unloaded quantity, and the load level of the PU is set to 0. Both units are sent to J7. |
| J7 | | The PU is sent to J8, while the SU is sent to J9. |
| J8 | | The decision is made to send the PU either to harvest a headland pass if there are any unharvested beds, (UOB2) otherwise to harvest the fieldwork tracks in the main field area (UOB11). The travelling speed with empty load is acquired from the database. The distance to be travelled from the current position to the resuming position and the corresponding time are computed and updated. |
| UOB11 | PU is harvesting on a track | The PU is travelling to the main field area and selects a fieldwork track to be harvested. The working speed of the PU is obtained from the database and the length of the current track is computed. The PU is send to UOB12. |
| UOB12 | PU reaches the headland | The time duration on current track is computed using working speed and length of current track, and the total effective distance and time are updated. The remaining space in the hopper of the PU is computed. The PU is sent to J12. |

| | | |
|---|---|---|
| J12 | | Based on data for the remaining tank load capacity of the PU, the location of the nearest SU (in this or the opposite headland) and the expected harvested quantity to go to the nearest SU the decision is made whether to harvest another track (UOB13) or to unload (UOB5). If all fieldwork tracks have been harvested the PU is sent to UOB14. |
| UOB13 | PU is turning to a track | The turn distance and time is acquired from the database and the accumulated turn distance and time of the PU are updated. Then the activities in UOB11, 12 and 13 are repeated until the PU has to be unloaded in UOB5. |
| J9 | | If the remaining capacity of the SU is not sufficient for another unload it is sent to UOB10; otherwise it sent to UOB9. |
| UOB9 | SU is waiting for a next load | The SU waits for the next load from the PU. |
| UOB10 | SU is travelling back to the farm to unload | The SU is labeled unavailable for unload. On return from the farm the SU is sent to UOB6 via J2. |
| UOB6 | SU is placed at the headland, empty | The SU is placed in the headland area and the location of the SU is updated. |
| UOB14 | Operation terminates | All of the accumulated results of the simulation are saved. The results include the total effective working distance/time, non-working distance/time and unloading time, time-based field efficiency and field capacity are calculated. The operation process is shut down. |

## 2.3   Implementation of the simulation model

The simulation model was developed using the MATLAB® technical programming language (The MathWorks, Inc., Natick, USA). An overview of the model is presented in Fig. 6. In the simulation model, the field, in geometrical sense, is represented as a series of line segments. For the geometrical representation of a field with obstacle areas, a tool developed by Zhou *et al.* (2014) was used. The inputs consist of the boundary of field and obstacle(s) (if any), the working width of the machine, the number of headland passes and the driving direction. The output of this tool is a set of coordinates of points representing the parallel fieldwork tracks for the field area coverage and the headland passes, where each track is represented by two points in the case of straight tracks or a series of ordered points in the case of curved tracks, while each headland pass is represented by a series of sequentially ordered points (Fig. 7). Each fieldwork track and

headland pass is assigned several properties, e.g. width, length, driving direction for machines. In addition, values of the following input parameters of the simulation model are set: The maximum tour distance (i.e. the distance that a PU can cover before reloading (for MIOs) or unloading (for MOOs), the fieldwork pattern (i.e. the layout of the tracks sequence for the PU to cover the field), travelling speed elements (effective operating, turning and transport speeds) and location(s) of SU(s). As an output, the simulation gives the segmentation of the task time and travelled distance for each element (e.g. effective operating, turning, transporting) of the operation. Additionally, two indices for estimation of the machinery performance are given as output: field efficiency and field capacity (Hunt, 2008).
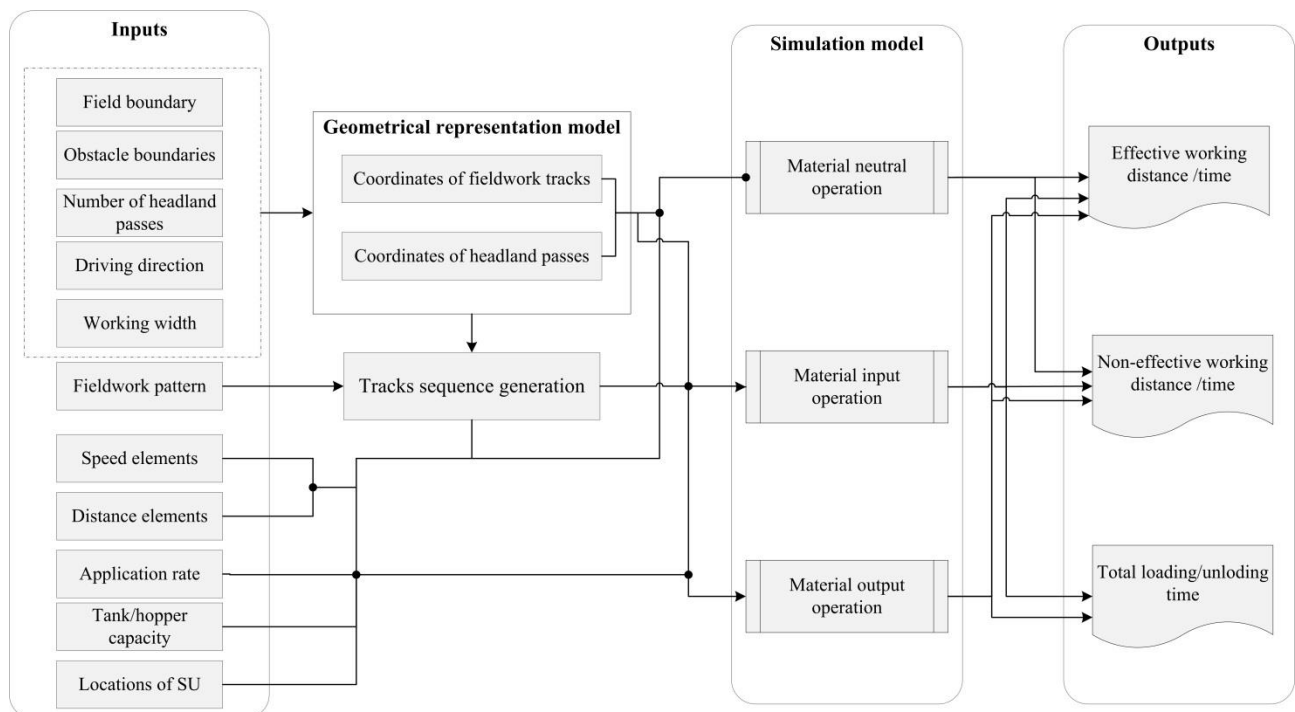


**Fig. 6 – Overview of the simulation model.**
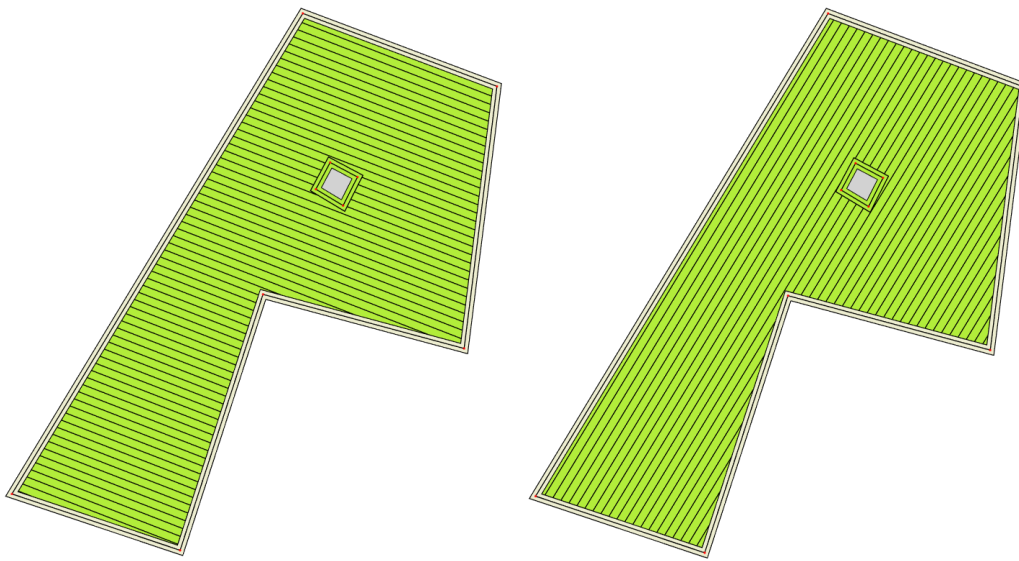
**Fig. 7 – Two alternative geometrical representations of a field with a single obstacle where different driving directions have been selected.**

# 3    Materials and methods

Data acquisition in fours fields is described in Section 3.1. GPS decomposition tool for collected data analysis is introduced in Section 3.2. Methods for input data of the model and model validation are described in Section 3.3 and 3.4, respectively. The simulated scenarios to demonstrate the model as decision support system (DSS) is given in Section 3.5.

## 3.1    Data acquisition

In order to evaluate and validate the model field experiments were designed and conducted to record all field operations during the period of May to November 2014 in four fields (referred to as F1, F2, F3, and F4). The area and location of these fields are summarized in Table 5. The trajectories of the tractors used in the operations were recorded using two types of GPS receiver: AgGPS 162 Smart Antenna DGPS receivers (Trimble®, GA, USA) for the bed former and harvester, three Aplicom A1 TRAX Data loggers (Aplicom®, Finland) for the stone separator, planter and sprayer. The coordinates of the locations of the service units were extracted from the recorded GPS data. Moreover, in order to provide the model with accurate data on field geometry, the vertices along the field edges were measured by tracking the field boundaries using the

tractor with the AgGPS DGPS receiver. The features of machineries that were used in the experimental field operations are presented in the Table 6.

| Table 5 - Characteristics of the experimental fields. | | | | | | | |
|---|---|---|---|---|---|---|---|
| Field shape | Field ID | Location | Area (ha) | Field shape | Field ID | Location | Area (ha) |
| | F1 | 54º44´50.74´´N 11º12´55.79´´E | 10.85 | | F2 | 54º42´22.75´´N 11º18´41.00´´E | 14.35 |
| | F3 | 54º42´14.19´´N 11º18´59.16´´E | 2.56 | | F4 | 54º42´25.00´´N 11º19´31.62´´E | 5.38 |

| Table 6 - Specifications of machineries involved in the potato production system. | | |
|---|---|---|
| Operation type | Operating width (m) | Load capacity |
| Bed former | 4.5 | - |
| Stone separator | 2.25 | - |
| Planter | 2.25 | 3500kg |
| Boom-type sprayer | 24.75 | 3000 L |
| Harvester | 2.25 | 7000 kg |
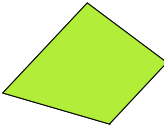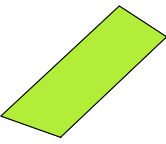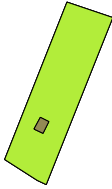
## 3.2 Decomposition of recorded GPS data

The recorded GPS data were analyzed and decomposed into sequences of productive and non-productive activities of the vehicles. This was done for each operation and field with a dedicated auxiliary tool developed using the MATLAB® programming software. The input parameters of the tool include the coordinates of the field boundary, the inner field boundary, the location of the reloading unit(s) and the coordinates of the machinery trajectories.

For the bed formation and the stone separation operations the motion sequences were categorized in two types: Effective working in the field body and (non-effective) turning in the headland. A turn was defined to begin with the first and end with the last sequential data point inside the headland, determined by the recorded coordinates of the inner field boundary, and the remaining recorded data points inside the inner field boundary are considered as the effective on-the-tracks working. The MIO and the MOO operations have a third type of motion activity, also counting as non-effective, namely reloading and unloading at SUs in the headland area. To distinguish the recorded points of turning and reloading or unloading motion in the headland area, circles were drawn with the radius of a given threshold value at the centers of the locations of the SUs. If a machine stays inside the circle for a given period of time, the machine is considered to be in reloading/unloading process and the transport distance is the length of the current path minus the length of the path in the circle, likewise, the transport time is the total time spent on this motion path minus the service time in the circle. Otherwise, the activity is considered to be turning.

## 3.3   Quantification of input parameters

To quantify the input parameters of the simulation model, the following parameters were extracted and calculated from the collected data of the operations in the fields F1 and F2 as well as measured directly during the operations in the fields:

- The average effective working speed of the machine in each operation.
- The average turning length of each turn type ($\Omega$, $\Pi$, $T$) (Bochtis and Vougioukas, 2008) with different skip track numbers, and the corresponding turning time (to estimate the turning speed of the machine).
- The average transport speeds with full/empty load was estimated by the transport distance and the corresponding time.
- The average service time (loading/unloading time) for the machines in material input/output operations.

## 3.4 Model validation

The quantified input data were used as the values of the simulation parameters for model validation. To estimate the accuracy of the model, the actual outputs from the operations that were carried out in fields F3 and F4 were compared with the outputs from the simulation model.

## 3.5 Simulated scenarios

The potential use of this simulation model as a decision support system (DSS) in terms of field operational decisions (e.g. driving direction, location of the service unit, fieldwork pattern, etc.) and machinery dimensions (e.g. working width, tank size, hopper size, etc.) was investigated. The same operational features of the machine regarding the task time elements, speed elements and distance elements were used. Field F2 was selected for the scenarios study. The operational scenarios are evaluated based on combinations of the following variables:

- Two driving directions: 61° (dr1) and 156.5° (dr2) as presented in Fig. 8.
- Two potato hopper capacities: 3500 kg and 4500 kg.
- Two potato harvester capacities: 7000 kg and 8000 kg.
- Five locations of the SU: In the corners and on the middle points of the field edges, as illustrated in Fig. 8.
- Three fieldwork patterns (as defined in iTEC PRO, 2007):

  1. Continuous Pattern (CP), in which the number of skipped passes is $0$ (resulting in the track sequence $\rho = [1,2,3,4,...]$);

  2. First turn Skip Pattern (FSP), in which the vehicle skips a set number of tracks, $s > 0$, in one headland and $s - 1$ in the opposite headland, then repeating in the adjacent block of tracks (e.g. $\rho = [(1,4,2,5,3),(6,9,7,10,8),...]$ with skip number $s = 2$).

  3. From back Furrow Pattern (FFP), in which the field is split into blocks, evenly sized on number of tracks. In each block the operations start from the center track, moves outwards until the block

is covered, then changes to the next block (e.g. $\rho=[(3,4,2,5,1),(8,9,7,10,6),...]$ when the blocks contain 5 tracks).

In order to investigate these variables' effect on the field operations, six scenarios were composed using the variable combinations shown in the Table 7.

| Table 7 – Setups for simulated scenarios. | | | | | | | |
|---|---|---|---|---|---|---|---|
| Scenario | | 1 | 2 | 3 | 4 | 5 | 6 |
| Driving direction (º) | | dr1 | dr1 | dr1 | dr2 | dr2 | dr2 |
| Fieldwork pattern | Bed former | CP | CP | CP | CP | CP | CP |
| | Stone separator | CP | CP | CP | CP | CP | CP |
| | planter | FSP(6)[a] | FSP(6) | FSP(6) | FSP(6) | FSP(6) | FSP(7) |
| | sprayer | CP | CP | CP | CP | CP | CP |
| | harvester | FFP(6)[b] | FFP(6) | FFP(6) | FFP(6) | FFP(6) | FFP(9) |
| Location of SUs | planter | S2 | S2 | S1:1-6[c] S2:7-12 S3:13-19 | S5 | S1:1-6 S5:7-12 S4:13-19 | S5 |
| | Harvester | S2 | S2 | S1: 1 – 24 S2: 25 – 48 S3: 49 – 71 | S5 | S1:1-32 S5:33-64 S4:65-59 | S5 |
| Machine capacity | planter | 3500 | 4500 | 4500 | 4500 | 4500 | 4500 |
| | Harvester | 7000 | 8000 | 8000 | 8000 | 8000 | 8000 |
| [a] FSP(6) indicates that the skipped number of tracks is 6 in each headland turning. [b] FFP(6) means that the tracks of the field are divided evenly into 6 blocks. [c] S1:1-6 means that the 1st to the 6th reloading occurred with the SU in location S1. | | | | | | | |
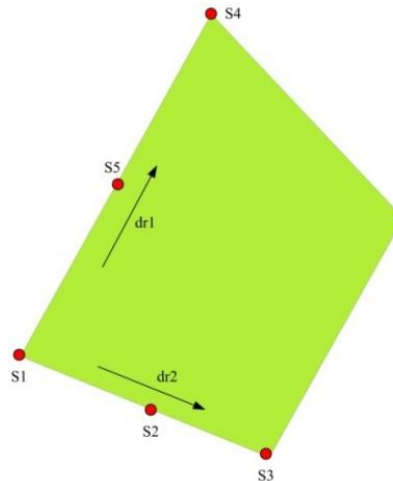
**Fig. 8 – Selected driving directions and locations of SUs in field F2 for the scenario analyses.**

# 4  Results and discussion

## 4.1  Quantification of input parameters

The recorded data in fields F1 and F2 were decomposed into segmentations of time and distance elements using the dedicated auxiliary tool (section 3.2). These decomposed data were used for quantifying the input parameters, as shown in Table 8. Regarding the quantification of turning lengths and speeds it should be noted that in bed forming, stone separation and spraying the continuous fieldwork pattern was always used in the fields, so no data with skipped tracks ($s = 0$) were available. The bed former and the stone separator used T-turns, while the sprayer could take the easier Π-turns. For planting and harvesting different turn types and skip numbers were used. It is possible to have skipped track numbers larger than the quantified 7. In this case the turning speed is assumed to be same as the turning speed for $s = 7$, while the turning distance is calculated as: $d(s) = d(7) + w * (s - 7)$, where $w$ is the working width.

| Table 8 – Values of measured parameters for the machine in each operation. | | | | |
|---|---|---|---|---|
| Parameter | | Number of samples | Mean | Standard deviation |
| **Bed forming** | | | | |
| Working speed on tracks (m s$^{-1}$) | | 260 | 1.43 | 0.05 |
| Turning length (m) / speed (m s$^{-1}$) | T-turn (s =0) $_a$ | 110 | 31.1 /1.09 | 2.78/0.04 |
| **Stone separation** | | | | |
| Working speed on tracks (m s-1) | | 235 | 0.96 | 0.08 |
| Turning length (m) / speed (m s$^{-1}$) | T-turn (s=0) | 210 | 40.8/0.63 | 2.94/0.08 |
| **Planting** | | | | |
| Working speed on tracks (m s$^{-1}$) | | 340 | 1.48 | 0.14 |
| Turning length (m) / speed (m s$^{-1}$) | T-turn (s=0) | 70 | 40.3/0.65 | 3.54/0.09 |
| | T-turn (s=1) | 40 | 37.3/0.64 | 3.08/0.07 |
| | T-turn (s=2) | 40 | 35.5/0.64 | 2.15/0.09 |
| | T-turn (s=3) | 40 | 33.4/0.65 | 3.04/0.07 |
| | Ω-turn (s=4) | 40 | 29.1/0.86 | 2.38/0.09 |
| | Ω-turn (s=5) | 60 | 28.5/0.85 | 2.67/0.12 |
| | Π-turn (s=6) | 64 | 26.3/1.18 | 2.33/0.13 |
| | Π-turn (s=7) | 78 | 28.6/1.19 | 2.49/0.07 |
| Transport speed with full load (m s$^{-1}$) | | 45 | 1.32 | 0.13 |
| Transport speed with empty load (m s$^{-1}$) | | 45 | 1.38 | 0.10 |
| Reloading time (min) | | 45 | 17 | 3.50 |
| **Spraying** | | | | |
| Working speed on tracks (m s$^{-1}$) | | 90 | 1.63 | 0.11 |
| Turning length (m) / speed (m s$^{-1}$) | Π-turn (s=0) | 80 | 31.5/ 1.37 | 2.58/0.13 |
| **Harvesting** | | | | |
| Working speed on tracks (m s$^{-1}$) | | 260 | 1.26 | 0.07 |
| Turning length (m) / speed (m s$^{-1}$) | T-turn (s=0) | 33 | 39.4/0.63 | 2.95/0.05 |
| | T-turn (s=1) | 32 | 37.3/0.64 | 3.24/0.04 |
| | T-turn (s=2) | 33 | 35.5/0.68 | 2.19/0.09 |
| | T-turn (s=3) | 33 | 33.6/0.65 | 2.81/0.10 |
| | Ω-turn (s=4) | 34 | 30.2/0.78 | 2.43/0.09 |
| | Ω-turn (s=5) | 32 | 32.5/0.77 | 2.58/0.03 |
| | Π-turn (s=6) | 31 | 28.6/1.01 | 2.73/0.04 |
| | Π-turn (s=7) | 32 | 30.8/1.02 | 2.12/0.08 |
| Transport speed with full load (m s$^{-1}$) | | 60 | 1.02 | 0.06 |
| Transport speed with empty load (m s$^{-1}$) | | 60 | 1.03 | 0.08 |
| Unload time (min) | | 60 | 1.20 | 0.4 |

$^a$ Skipped track number *s*, for instance if a tractor turns from track 1 to track 3, the skipped track number *s* is 1.

## 4.2 Model validation

The model validation was based on 30 runs of the simulation model. In each run the input parameters of the model were drawn randomly from the samples in Table 8. Other parameters (i.e. driving direction, machine load capacity (transformed into meters of driving until empty or full), fieldwork pattern and location of the

SUs) used in the simulation were extracted from the GPS recordings for each operation. In addition, through the analysis of the GPS recordings from the two experimental fields F3 and F4, it was observed that during the reloading/unloading transport phase in planting and harvesting, operators executed three types of maneuverers to reach a SU in the headland area, depending on the location of the SU, relative to the current track (exit) and the next track (entry) to be entered. These three types of maneuverers are illustrated in Fig. 9 and described as follows: (a) When the SU is located between the exit and entry tracks, then a Π-turn is executed if there is enough space and distance for it, otherwise a T-turn is made (Fig. 9.a); (b) when the SU is located outside the exit and entry tracks but closest to the exit track, a turn to reach the SU along the headland border is performed, then after unloading the machine is driven backwards passing the entry track in order to be able to make a forward turn into the entry track (Fig. 9.b); (c) when the SU is located outside of the exit and entry tracks but closest to the entry track, a forward turn is made, the exit track is passed to reach the SU, and after unloading the machine is driven in reverse to enter the entry track (Fig. 9.c). The turn radius was set to 8.30 m for executing a turn in the simulation of the transportation phase, which was extracted from the GPS recordings. In order to simulate the operations as closely as possible to the experimental conditions, these three types of maneuverers were performed in the simulations.



|        (a)        |        (b)        |        (c)        |
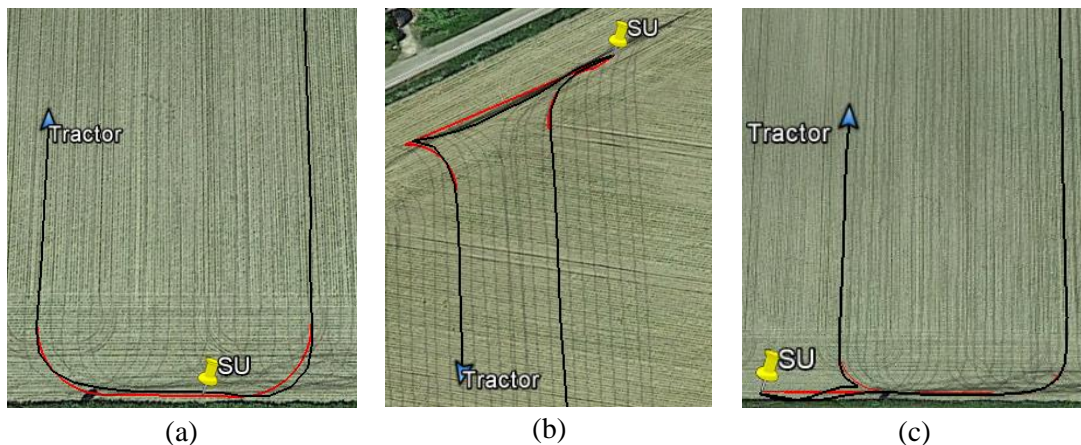
**Fig. 9 - An example of extracted three types of maneuverers in the unloading transport phase of potato harvesting from GPS recordings (black line)as well as the simulated maneuverers (red line).**

The distance that one full hopper of the planter can cover was measured to 3100 m and 3500 m for F3 and F4, respectively. The reason for the capacity not being equal is that the potato varieties planted in the two fields had different tuber size. For the harvester the distance that one full hopper can cover was measured to 860 m

and 840 m, respectively, due to yield differences. Finally, even though spraying is a MIO, no refilling was necessary in either field, because the tank capacity of the sprayer was sufficiently large to cover each of the fields. The driving direction was 78º and 85º, resulting in 42 and 68 beds in F3 and F4, respectively. These numbers were set as the values of input parameters for the simulations. The comparisons between the simulated and measured results are summarized in Table 9 and 10 for operations in F3 and F4, respectively. The errors for the machinery performance indicators field efficiency and field capacity range from 0.46 % to 4.84 % and from 0.72% to 6.06%, respectively (Table 11). Based on the relatively small values of errors we conclude that the simulation model is sufficiently validated for our purpose. It can be seen from Table 11 that the planting and harvesting had larger values of errors, which was mainly caused by the time variation in the service (reloading and unloading) phase.

| Table 9 – Comparison between measured and simulated results in F3. | | | | | | |
|---|---|---|---|---|---|---|
| | | **Bed forming** | **Stone separation** | **Planting** | **Spraying** | **Harvesting** |
| Effective distance (m) | Meas. | 5436 | 10896 | 10903 | 983 | 10939 |
| | Sim. | 5497 | 10978 | 10978 | 975 | 10978 |
| Effective time (s) | Meas. | 3926 | 11190 | 7525 | 567 | 8613 |
| | Sim. | 3844 | 11435 | 7417 | 598 | 8712 |
| Turning distance (m) | Meas. | 638 | 1756 | 1239.5 | 98 | 1316 |
| | Sim. | 622 | 1674 | 1190.6 | 95 | 1243 |
| Turning time(s) | Meas. | 696 | 2772 | 1121 | 78 | 1450 |
| | Sim. | 661 | 2657 | 1073 | 69 | 1346 |
| Transport distance (m) | Meas. | - | - | 866 | - | 1201 |
| | Sim. | - | - | 841 | | 1156 |
| Transport time (s) | Meas. | - | - | 723 | | 1031 |
| | Sim. | - | - | 701 | | 963 |
| Service time (min) | Meas. | - | - | 75.4 | | 19.2 |
| | Sim. | - | - | 65 | | 15.6 |
| Total distance (m) | Meas. | 46272 | | | | |
| | Sim. | 46228 | | | | |
| Total time (min) | Meas. | 756.1 | | | | |
| | Sim. | 738.5 | | | | |

| Table 10 - Comparison between measured and simulated results in F4. | | | | | | |
|---|---|---|---|---|---|---|
| | | **Bed forming** | **Stone separation** | **Planting** | **Spraying** | **Harvesting** |
| Effective distance (m) | Meas. | 11278 | 22542 | 22531 | 2055 | 22495 |
| | Sim. | 11323 | 22656 | 22656 | 2076 | 22656 |
| Effective time (s) | Meas. | 7492 | 23239 | 15327 | 1255 | 17787 |
| | Sim. | 8002 | 23525 | 15425 | 1289 | 17879 |
| Turning distance (m) | Meas. | 1088 | 2611 | 1871 | 134 | 1676 |
| | Sim. | 1056 | 2658 | 1818 | 128 | 1592 |
| Turning time (s) | Meas. | 1065 | 4320 | 1771 | 139 | 1832 |
| | Sim. | 982 | 4163 | 1627 | 115 | 1892 |
| Transport distance (m) | Meas. | - | - | 1526 | | 2704 |
| | Sim. | - | - | 1468 | | 2640 |
| Transport time (s) | Meas. | - | - | 1422 | | 2458 |
| | Sim. | - | - | 1328 | | 2340 |
| Service time (min) | Meas. | - | - | 148 | | 49.6 |
| | Sim. | - | - | 132 | | 38.4 |
| Total distance (m) | Meas. | 92511 | | | | |
| | Sim. | 92727 | | | | |
| Total time (min) | Meas. | 1499.4 | | | | |
| | Sim. | 1479.8 | | | | |

| Table 11 - Comparison of time-based field efficiency and field capacity between measured and simulated in F3 and F4. | | | | | | | |
|---|---|---|---|---|---|---|---|
| Parameters | | F3 | | | F4 | | |
| | | Meas. | Sim. | Error (%) | Meas. | Sim. | Error (%) |
| Field efficiency (%) | Bed forming | 84.94 | 85.33 | 0.46 | 87.55 | 89.07 | 1.74 |
| | Stone separation | 80.15 | 81.15 | 1.25 | 84.32 | 84.96 | 0.76 |
| | Planting | 54.16 | 56.66 | 4.62 | 55.94 | 58.65 | 4.84 |
| | Spraying | 87.91 | 89.66 | 1.99 | 90.03 | 91.81 | 1.98 |
| | Harvesting | 70.33 | 72.86 | 3.60 | 71.00 | 73.23 | 3.14 |
| Field capacity (ha h$^{-1}$) | Bed forming | 1.99 | 2.04 | 2.51 | 2.26 | 2.16 | 4.42 |
| | Stone separation | 0.66 | 0.65 | 1.52 | 0.70 | 0.69 | 1.43 |
| | Planting | 0.66 | 0.70 | 6.06 | 0.71 | 0.73 | 2.82 |
| | Spraying | 14.29 | 13.82 | 3.29 | 13.89 | 13.79 | 0.72 |
| | Harvesting | 0.77 | 0.75 | 2.60 | 0.77 | 0.79 | 2.60 |

## 4.3  Simulated scenarios

The simulated results of the six scenarios, as specified in Table 7, for field F2 are presented in Table 12. In each scenario, 10 times of spraying is executed for a growing season, while the other operations are only executed once.

### 4.3.1  Effect of driving direction

It can be found that the driving direction is an important factor when comparing scenario 2 and scenario 4, in which the total bed length, the total effective operating distance and the total effective operating time in the two scenarios are approximately the same, but scenario 4 has 66 more beds than scenario 2. Thus, more turns are required to cover the same bed length, which will lead to reduced field efficiency. Taking the bed forming operation as an example, the turning distance was 46.1% and the turning time 46.9% higher in scenario 4 than in scenario 2, resulting in a 6.4 % reduction of field efficiency in scenario 4 relative to scenario 2.

### 4.3.2  Effect of fieldwork pattern

Scenario 4 and 6 differ in the fieldwork patterns of the planting and harvesting operations. The simulations demonstrate a 17.3% reduction in the combined turning time of the planter and the harvester in scenario 6, relative to scenario 4, indicating a substantial potential for improving the machinery performance by selection of a suitable fieldwork pattern for the particular field.

### 4.3.3  Effect of machinery capacity

Scenario 1 and 2 differ in the capacity of the hopper for planting and the storage tank for harvesting. As expected, by increasing the machinery capacity, the non-working time can subsequently be reduced, specifically, scenario 2 showed an 8.8% reduction in the combined non-working time of the planter and the harvester, relative to scenario 1. Notably, 14.3% less service time is needed in scenario 2 than in scenario 1 due to less service visits required to cover the entire field.

### 4.3.4    Effect of SU location

The difference between scenario 2 (4) and 3 (5) is that in scenario 2 (4) the SU is located in the middle of one headland, while in scenario 3 (5) the SU is moved between 3 positions in the same headland in order to be near the planter or harvester. The simulations show that the location of the SU has effect on the operational time and field efficiency where the non-working time reduced with 13.2% in scenario 3, relative to scenario 2. With respect to SU location scenarios 4 and 5 have a setup similar to scenarios 2 and 3, respectively, so comparing these two scenarios shows an 8.3% reduction of non-working time in the both planting and harvesting in scenario 5, relative to scenario 4. Hence positioning SUs at an appropriate location can improve the system and operational efficiency, but an assistant tool is required to predict the total transport distance by the PU corresponding to the allocated position of the SU.

From the above analysis of the effect of each test variable on operational time and field efficiency, it can be concluded that the developed simulation model can be used as a decision support system (DSS) to provide decision makers with necessary operational information to evaluate alternative scenarios. In general, the developed model can quantify and predict the operational cost, time for various operational scenarios prior to field working.

| Scenario | | 1 | 2 | 3 | 4 | 5 | 6 |
|---|---|---|---|---|---|---|---|
| **Table 12 – Outputs of the simulation for the different scenarios.** | | | | | | | |
| Number of beds | | 144 | 144 | 144 | 210 | 210 | 210 |
| Effective operating dist. (m) | Bed former | 29315 | 29315 | 29315 | 29273 | 29273 | 29273 |
| | Stone separator | 58664 | 58664 | 58664 | 58575 | 58575 | 58575 |
| | Planter | 58664 | 58664 | 58664 | 58575 | 58575 | 58575 |
| | Sprayer | 56790 | 56790 | 56790 | 54430 | 54430 | 54430 |
| | Harvester | 58664 | 58664 | 58664 | 58575 | 58575 | 58575 |
| **Total effective operating dist.(m)** | | **262097** | **262097** | **262097** | **259428** | **259428** | **259428** |
| Effective operating time (h) | Bed former | 5.69 | 5.69 | 5.69 | 5.69 | 5.69 | 5.69 |
| | Stone separator | 16.97 | 16.97 | 16.97 | 16.95 | 16.95 | 16.95 |
| | Planter | 11.01 | 11.01 | 11.01 | 10.99 | 10.99 | 10.99 |
| | Sprayer | 9.7 | 9.7 | 9.7 | 9.3 | 9.3 | 9.3 |
| | Harvester | 12.93 | 12.93 | 12.93 | 12.91 | 12.91 | 12.91 |
| **Total effective operating time (h)** | | **56.30** | **56.30** | **55.84** | **55.84** | **55.84** | **55.84** |
| Turning dist.(m) | Bed former | 4447 | 4447 | 4447 | 6499 | 6499 | 6499 |
| | Stone separator | 5834 | 5834 | 5834 | 8527 | 8527 | 8527 |
| | Planter | 3033 | 3441 | 3441 | 5297 | 5297 | 5308 |
| | Sprayer | 4095 | 4095 | 4095 | 5670 | 5670 | 5670 |
| | Harvester | 3144 | 3144 | 3144 | 6753 | 6753 | 5325 |
| **Total turning dist. (m)** | | **20553** | **20961** | **20961** | **32746** | **32746** | **31329** |
| Turning time (h) | Bed former | 1.13 | 1.13 | 1.13 | 1.66 | 1.66 | 1.66 |
| | Stone separator | 2.57 | 2.57 | 2.57 | 3.76 | 3.76 | 3.76 |
| | Planter | 0.91 | 0.95 | 0.95 | 1.47 | 1.47 | 1.23 |
| | Sprayer | 0.8 | 0.8 | 0.8 | 1.2 | 1.2 | 1.2 |
| | Harvester | 0.95 | 0.95 | 0.95 | 1.95 | 1.95 | 1.60 |
| **Total turning time (h)** | | **6.36** | **6.40** | **6.40** | **10.40** | **10.40** | **9.45** |
| Transport dist. (m) | Planter | 3826 | 3143 | 1791 | 3921 | 3142 | 3932 |
| | Harvester | 12932 | 12932 | 7692.1 | 20015 | 14813 | 19991 |
| **Total transport distance (m)** | | **16758** | **16075** | **9483** | **23936** | **17955** | **23923** |
| Transport time (h) | Planter | 0.83 | 0.69 | 0.37 | 0.87 | 0.65 | 0.88 |
| | Harvester | 3.30 | 3.30 | 1.95 | 5.10 | 3.75 | 5.10 |
| **Total transport time (h)** | | **4.13** | **3.99** | **2.32** | **5.97** | **4.40** | **5.98** |
| Service time (h) | Planter | 6.52 | 5.38 | 5.38 | 5.38 | 5.38 | 5.38 |
| | Harvester | 1.42 | 1.42 | 1.42 | 1.78 | 1.78 | 1.78 |
| **Total Service time(h)** | | **7.93** | **6.80** | **6.80** | **7.16** | **7.16** | **7.16** |

# 5   Conclusion

In this paper, a targeted model for simulating all the field operations involved in potato production was developed. The model was validated based on the recorded data from the experimental, sequential operations, which showed that the model can sufficiently well predict and evaluate the operational time and distance carried out by agricultural machines involved in potato production. The errors ranged from 0.46 % to 4.84 % and 0.72% to 6.06% in the predictions of field efficiency and field capacity, respectively. Furthermore, the capabilities of the simulation model as a decision support system (DSS) have been demonstrated. It was shown that it is feasible to evaluate different user scenarios in terms of field operational decisions (e.g. driving direction, fieldwork pattern, location of the service unit, etc.) and machinery dimensions (e.g. tank and hopper size).

# References

Bechar, A., Yosef, S., Netanyahu, S., Edan, Y., 2007. Improvement of work methods in tomato greenhouses using simulation. *Transactions of the ASABE, 50*(2), 331-338.

Benson, E. R., Hansen, A. C., Reid, J. F., Warman, B. L., Brand, M. A., 2002. Development of an in-field grain handling simulation in ARENA. *ASAE Paper*, 02-3104.

Bochtis, D. D., Sorensen, C. G., 2009. The vehicle routing problem in field logistics part I. *Biosystems Engineering, 104*(4), 447-457.

Bochtis, D. D., Sorensen, C. G., 2010. The vehicle routing problem in field logistics: Part II. *Biosystems Engineering, 105*(2), 180-188.

Bochtis, D. D., Sørensen, C. G., Jørgensen, R. N., Green, O., 2009. Modelling of material handling operations using controlled traffic. *Biosystems Engineering, 103*(4), 397-408.

Bochtis, D. D., Vougioukas, S. G., 2008. Minimising the non-working distance travelled by machines operating in a headland field pattern. *Biosystems Engineering, 101*(1), 1-12.

Busato, P., Sørensen, C. G., Pavlou, D., Bochtis, D. D., Berruto, R., Orfanou, A., 2013. DSS tool for the implementation and operation of an umbilical system applying organic fertiliser. *Biosystems Engineering, 114*(1), 9-20.

Busato, P. (2015). A simulation model for a rice-harvesting chain. *Biosystems Engineering, 129*, 149-159.

de Toro, A., Gunnarsson, C., Lundin, G., Jonsson, N., 2012. Cereal harvesting – strategies and costs under variable weather conditions. *Biosystems Engineering, 111*(4), 429-439.

Hameed, I. A., Bochtis, D. D., Sorensen, C. G., Vougioukas, S., 2012. An object-oriented model for simulating agricultural in-field machinery activities. *Computers and Electronics in Agriculture, 81*, 24-32.

Hu, J. Y., Zhang, X., Moga, L. M., Neculita, M., 2013. Modeling and implementation of the vegetable supply chain traceability system. *Food Control, 30*(1), 341-353.

Hunt, D. (2008). *Farm power and machinery management*: Waveland Press.

iTEC PRO operators manual. (2007). Moline, Illinois: A John Deere Illustrationª Manual, Deere & Company. OMPC21038 Issue J7.

Kusiak, A., Larson, T. N., Wang, J. R., 1994. Reengineering of Design and Manufacturing Processes. *Computers & Industrial Engineering, 26*(3), 521-536.

Mayer, R. J., Menzel, C. P., Painter, M. K., Dewitte, P. S., Blinn, T., Perakath, B., 1995. Information integration for concurrent engineering (IICE) IDEF3 process description capture method report: DTIC Document.

Peres, E., Fernandes, M. A., Morais, R., Cunha, C. R., Lopez, J. A., Matos, S. R., Reis, M. J. C. S., 2011. An autonomous intelligent gateway infrastructure for in-field processing in precision viticulture. *Computers and Electronics in Agriculture, 78*(2), 176-187.

Shen, H., Wall, B., Zaremba, M., Chen, Y. L., Browne, J., 2004. Integration of business modelling methods for enterprise information system analysis and user requirements gathering. *Computers in Industry, 54*(3), 307-323.

Sørensen, C. G., Nielsen, V., 2005. Operational Analyses and Model Comparison of Machinery Systems for Reduced Tillage. *Biosystems Engineering, 92*(2), 143-155.

Thakur, M., Hurburgh, C. R., 2009. Framework for implementing traceability system in the bulk grain supply chain. *Journal of Food Engineering, 95*(4), 617-626.

van 't Ooster, A., Bontsema, J., van Henten, E. J., Hemming, S., 2012. GWorkS – A discrete event simulation model on crop handling processes in a mobile rose cultivation system. *Biosystems Engineering, 112*(2), 108-120.

van 't Ooster, A., Bontsema, J., van Henten, E. J., Hemming, S., 2014. Simulation of harvest operations in a static rose cultivation system. *Biosystems Engineering, 120*, 34-46.

Zhang, F. L., Johnson, D. M., Johnson, M. A., 2012. Development of a simulation model of biomass supply chain for biofuel production. *Renewable Energy, 44*, 380-391.

Zhang, X., Feng, J., Xu, M., Hu, J., 2011. Modeling traceability information and functionality requirement in export-oriented tilapia chain. *J Sci Food Agric, 91*(7), 1316-1325.

Zhou, K., Leck Jensen, A., Sørensen, C. G., Busato, P., Bochtis, D. D., 2014. Agricultural operations planning in fields with multiple obstacle areas. *Computers and Electronics in Agriculture, 109*, 12-22.

# Chapter 6

# Quantifying the benefits of alternative fieldwork patterns in potato cultivation system

K. Zhou, A. Leck Jensen, D.D. Bochtis, C.G. Sørensen

(Submitted)

# Abstract

A sub-optimal fieldwork pattern is a main reason for lost time in fieldwork operations due to excessive non-working distance and time. Even though algorithms exist that can calculate an optimal route plan of a specific operation that covers the field with minimum non-working distance and time, so far no commercial navigation-aiding system for agricultural vehicles exist that can implement this type of patterns. Yet, the implementation of applicable standard fieldwork pattern in real life operations can provide near-optimal solutions compared to the simple fieldwork patterns generally selected by operators.

In this paper, a novel approach for the assessment of the savings, in terms of non-working distance and time, derived from the implementation of five selected common fieldwork patterns against the operators' used fieldwork patterns is presented. The assessment method simulates the non-working distance and time corresponding to the selected fieldwork patterns. In order to do this, turn models are fitted to actual turns recorded in field experiments, and the turn models together with model of in-field transport and material reloading are evaluated. Three operations: bed forming, stone separation and planting in potato cultivation were chosen as the case study, which were recorded and analyzed in three different fields. The simulation results based on the five selected fieldwork patterns showed that the savings for bed forming were up to 18.4% in (non-working) turning distance and 32.7% in turning time; for stone separation the savings in terms of turning distance and time were 35.0% and 60.9%; for the planting the savings were 22.6% in distance and 24.8% in time when compared with the actual operation in the three case study fields. The increase in time-based field efficiency is up to 2.7%, 7.2% and 7.1% for bed forming, stone separation and planting, respectively.

*Keywords*: Operations management; Fieldwork pattern; Machinery management

# 1   Introduction

In agricultural field operations (such as ploughing, seeding and harvesting) the vehicle (typically a tractor with an implement, depending on the operation) covers the entire field, normally by following straight or

curved tracks along one side of the field. This creates an area in each end of the tracks, called the headland area, where the vehicle must make a turn in order to enter the next track. The remaining area, called the field body, consists of the tracks where the primary cropping is done. The order of which the tracks are traversed, i.e. the fieldwork pattern, determines how efficiently the turnings can be made in the headland. The most common fieldwork pattern is the continuous headland pattern where the tracks are traversed sequentially from one side of the field to the next. This fieldwork pattern is popular because it is simple for the driver to follow, but the narrow turnings from one track to the neighboring makes it inefficient.

Field efficiency, defined as the time a vehicle is working effectively divided by the total time it is committed to the operation (Hunt, 2008), is an important measure of machine performance. Obviously, the field efficiency can be improved by reducing the non-working distance and time. Part of the total non-working time is unpredictable (e.g. machine breakdown), but other parts can be reduced by planning, notably the time spent for turnings and for reloading/unloading material tanks (e.g. reloading the seeding tank for seeding and unloading the crop tank for harvest). Fig.1 shows a geometrical representation of a field.



**Fig. 1 - Geometrical representation of a field with outer field border (yellow), field tracks (green) in the field body, turnings (red) in the headland areas and refilling path (black) / resuming path (blue) to/from a service unit (SU).**

The field efficiency is not a constant value for a given operation. Rather, it is affected by the vehicle maneuverability, fieldwork pattern, field shape, field size, crop yield (for harvesting operation), soil conditions, system capabilities (e.g. the tank size of the seeding machine) and the driver's experience.

Particularly, the fieldwork pattern is an important factor, since it is variable for a particular operation where the field, machinery and crop are given. The fieldwork pattern affects the amount of wasted time due to excessive non-working distance and time during the operation. This has been tested experimentally in actual operations (Bochtis, et al., 2010; Hansen, et al., 2003; Ntogkoulis, et al., 2014; Taylor., et al., 2002) as well as by using simulation models (Benson, et al., 2002; Bochtis, et al., 2009).

The non-working traffic not only causes high soil compaction due to the repetition of turning maneuvers (Ansorge and Godwin, 2007), but also increases fuel consumption, labor demands, and operators' workload. Therefore, selection of an optimized fieldwork pattern for a particular operation plays an important role in the reduction of the non-working distance and time.

In recent years, field coverage planning has become a research focus, striving to increase the field efficiency by reducing the non-working distance and time. It mainly consists of two distinctive problems: Geometrical field representation and route planning. The geometrical field representation uses geometrical primitives, such as points, lines and polygons to represent the field with headland, field body and tracks geometrically for further high-level operational planning. A number of methods have been developed for tow-dimensional and three-dimensional field geometrical representation (Hameed, et al., 2010; Hameed, et al., 2013; Hofstee, et al., 2009; Jin and Tang, 2011; Oksanen and Visala, 2009). Route planning regards finding an optimized route for the vehicle to follow within the geometrical field representation. Recently, a new type of optimal fieldwork pattern, B-pattern, has been introduced (Bochtis and Vougioukas, 2008) and defined ( Bochtis, et al., 2013). The B-pattern optimization criteria include the minimization of total or non-working distance, total operational time, and risk of soil compaction. In the case of minimization of a non-working distance, experimental results show a reduction of total non-working distance of up to 50% by implementing the B-patterns (Bochtis and Vougioukas, 2008).

Even though B-patterns can minimize the non-working distance, no commercial navigation-aiding system for agricultural vehicles exists at the moment that can implement these route plans. Moreover, no algorithmic procedures are commercially available that enables the farmers to generate the optimal track sequences and

embed them into currently available navigation-aiding systems by skipping the appropriate number of tracks in each headland turning. In contrast, predetermined standard motifs for fieldwork patterns can be followed by an operator using an auto-steering system or manual steering. For example, by selecting a simple standard motif fieldwork pattern consisting of consequently skipping the neighboring track may allow the driver to make the turns faster than the continuous fieldwork pattern and thereby reduce the total non-working time. So, the implementation of applicable standard motifs in real life operations can provide sub-optimal, yet improved solutions, compared to the operator's standard choice.

In order to investigate the benefits of using alternative fieldwork patterns compared with the operator's default patterns, a novel approach is presented, where five selected common fieldwork patterns are compared with the patterns used by farmers in real life and under similar conditions: Same fields, machines and crops. Three sequential operations for potato cultivation have been chosen for the case study: Bed forming, stone separation and planting. The remainder of our work is organized as follows: Section 2 describes the potato cultivation system and the machines used for the three operations of interest; in section 3 the involved materials and methods are described, consisting of a methodological overview (3.1), a description and mathematical formulation of the applied fieldwork patterns (3.2) and the turning models (3.3), a description of the fields and the equipment used for recording operational positioning data (3.4), and finally a description of the simulation model. Next, in section 4 the results are presented and discussed. First, the recorded GPS data for actual field operations are analyzed (4.1) and used to parameterize the turning models (4.2). The turning models are validated (4.3) and afterwards used to simulate and evaluate the total non-working time and distance for the five common fieldwork patterns (4.4). Finally, conclusions are made in section 5.

## 2   Potato cultivation System

Potato farmers all over Europe use a cultivation system where the potatoes grow in beds. In order to provide good (dry and warm) growing conditions for the potato three sequential operations are required for the establishment of the potato crop (Fig. 2): First the beds are formed, then oversized stones and clods are separated out of the beds, and finally the potato seeds are planted in the beds:
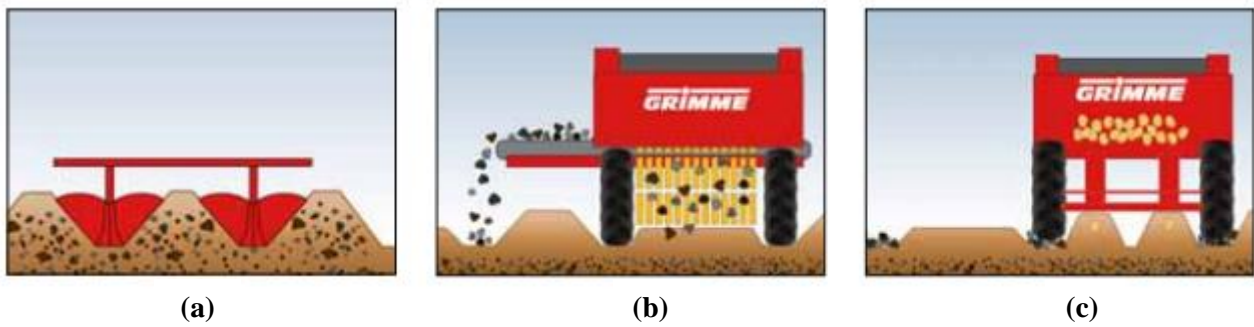
|  (a)  |  (b)  |  (c)  |

**Fig. 2 - Illustration of the three operations of potato crop establishment: (a) bed formation, (b) stone separation, and (c) planting (photo source: Grimme).**

1) Bed formation: Setting up perfectly formed beds is the first step towards successful establishment of a potato crop. The bed former uses shaped metal plates to lift up the soil and form it into one to more beds. This step is decisive, since the wheel tracks and bed width are determined for all subsequent field operations of the season (Fig 2.a).

2) Stone separation: This operation is also a part of the seedbed preparation in stony and cloddy soils which can provide ideal growing conditions for fast emergence of the potatoes and reduction of the picking cost in the harvesting. A stone separator uses a digging share and separating web through which the fine soil falls into the bed while the oversize stones and clods are transferred laterally through a cross-conveyor to an adjacent furrow between already formed beds where separation is not performed. The conveyor can be adjusted either to the right or left at the end of the current bed. In successive operations the machine's tires run on the rows of the processed stones and clods to bury them between alternate beds (Fig 2.b).

3) Planting: Potato planting starts immediately after the stone separation, normally by the use of automated planters. The planter is attached behind a tractor with the seed potatoes in a container, called the hopper. Special cups lift the seed potatoes from the hopper and place them with accuracy distance into the beds. The depth of sowing is about 5-10 cm and the distance between potato tubers along the rows are about 20-40 cm (Fig 2.c). Due to capacity constraints the hopper needs to be refilled occasionally. This is done by driving to the headland area where one or more reloading units

are located, refill the hopper and return to the location of the field where the hopper ran empty. The time spent for reloading is part of the non-working time.

# 3 Materials and methods

## 3.1 Methodology overview

The methodological approach of this paper is to develop a simulation model and apply it to assess the machinery performance with respect to non-working time and distance of the three operations described in section 2. The approach consists of four main stages (Fig. 3). Stage 1 is the data recording where GPS data of the different operations are recorded in three fields (section 3.4.1 and 3.4.2). Stage 2 analyses the GPS data and divides the operational driving into sequences of work elements: on-the-tracks work (productive), headland turnings, in-field transport and reloading (non-productive). The time and distance of each work element is extracted (section 3.4.3). Stage 3 defines theoretical models of four types of turnings (defined in section 3.3) and fits the models to the actual headland turnings determined in stage 2. Finally, stage 4 applies the fitted turning models together with a model for the planter refilling to simulate each of the three operations in each of the three fields applying each of the five fieldwork patterns (defined in section 3.2). In this way the optimal fieldwork pattern is determined for each combination of field and operation, and the corresponding non-working time and distance is compared to the actual measured values.
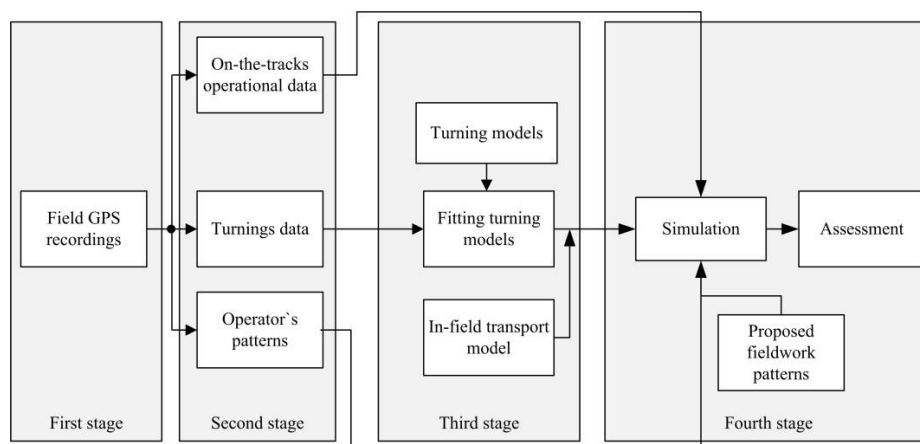


**Fig. 3 - Overview of the proposed methodology.**
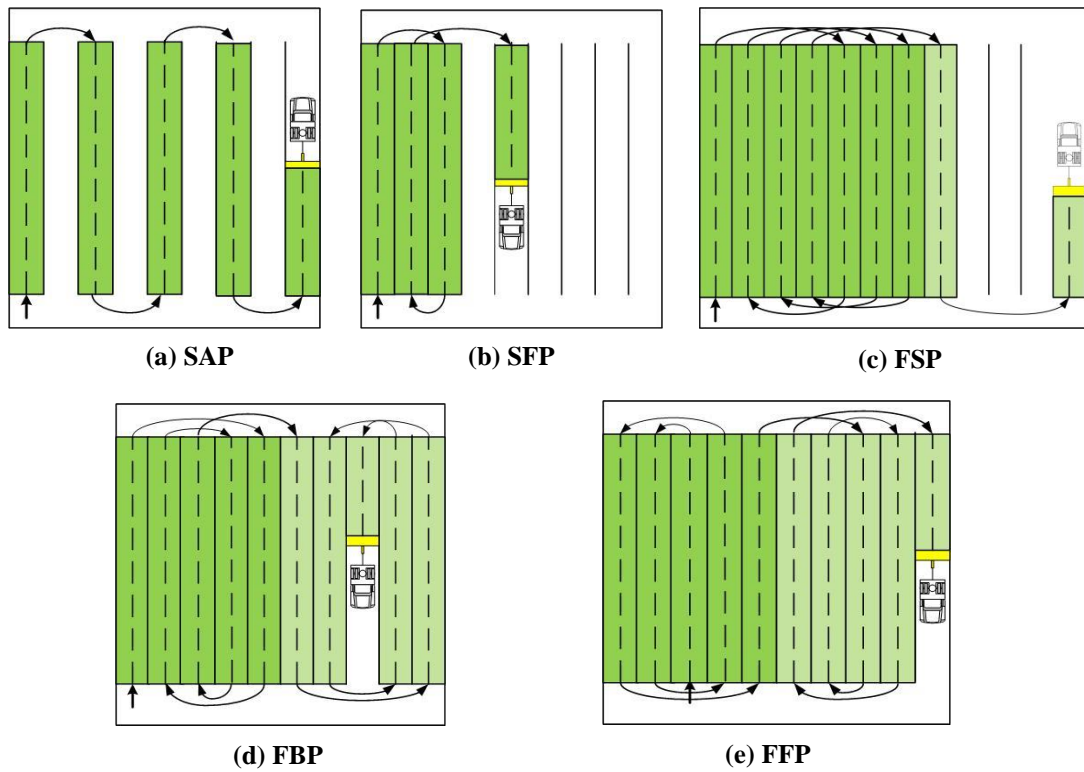
## 3.2   Fieldwork patterns



**Fig. 4 - Five selected common fieldwork patterns for field vehicles. Arrows show track sequences. Light and dark green indicate blocks with similar motifs of tracks.**

In this study, five common fieldwork patterns were selected (Hunt, 2008). Each fieldwork pattern is represented mathematically with the traversal function, which yields the traversal sequence of the field tracks. The traversal function is expressed as a sequence of integers $q_i$ with $i \in T$, where T is the set of tracks in the geometrical representation of the field coverage. For instance, $q_4 = 7$ indicates that the 4th track traversed by the vehicle is track number 7. The traversal function is the inverse of the bijective function $p$ defined by Bochtis and Vougioukas (2008).

In the following each selected fieldwork pattern is explained and described mathematically with the traversal function:

a) **Straight Alternation Pattern (SAP)**: In this pattern the vehicle skips a fixed number of tracks, $s$, when reaching the headland area. In practice the skip number is almost always 1, as illustrated in Fig. 4.a, such that the vehicle traverses the first track, then skips the second, traverses the third and subsequently the remaining odd numbered tracks. Finally, the even numbered tracks are traversed in reverse order, resulting in the track sequence $\rho = (1,3,5,7,...,8,6,4,2)$. The traversal function for the SAP pattern can be written as:

$$q_i = \begin{cases} 1, & i = 1 \\ q_{i-1} + 2, & 1 < i \leq \lceil N/2 \rceil \\ q_{i-1} + 1, & \mod(N,2) = 0 \wedge i = \lceil N/2 \rceil + 1 \\ q_{i-1} - 1, & \mod(N,2) = 1 \wedge i = \lceil N/2 \rceil + 1 \\ q_{i-1} - 2, & \lceil N/2 \rceil + 1 < i \leq N \end{cases}$$

Where mod is the modulus operator and $\lceil \ \rceil$ denotes the ceiling function that rounds a real number up to the smallest larger integer. $N$ is the number of tracks, i.e. the cardinality of $T$, $N = |T|$.

b) **Skip and Fill Pattern (SFP)**: This pattern mainly consists of repetitions of a standard motif of three tracks where first two tracks are skipped, and then the previous track is traversed. The first two and possibly the last tracks are exceptions to this motif, depending on the number of tracks. This results in the track sequence $\rho = (1,3,2,5,4,7,6,9,8,...)$. The traversal function can be written as:

$$q_i = \begin{cases} 1, & i = 1 \\ 3, & i = 2 \\ q_{i-1} - 1, & \mod(i,2) = 1 \wedge i \neq 1 \\ q_{i-1} + 3, & \mod(i,2) = 0 \wedge i \neq 2 \wedge i < N \\ i, & \mod(i,2) = 0 \wedge i \neq 2 \wedge i = N \end{cases}$$

c) **First turn Skip Pattern (FSP):** In this pattern the field tracks are grouped into blocks and the blocks are covered sequentially by following the same motif inside each block. The common motif is to skip a predetermined number of tracks, $s > 1$, in one headland and $s - 1$ tracks in the opposite headland. Fig. 4.c illustrates FSP with $s = 3$ resulting in a block size of 7 and the track

sequence $\rho = ((1,5,2,6,3,7,4),(8,12,9...),...)$. In general, the skip number $s$ defines the number of tracks in a block to $B = 2 \cdot s + 1$. The number of blocks in a field with $N$ tracks is $n = \lfloor N/B \rfloor$. In case $\mod(N,B) > 0$ the remaining tracks are simply covered sequentially. The overall track sequence is the combined sequences of each block: $\rho = (\rho_1, \rho_2, ..., \rho_n)$, where $\rho_j$ is the track sequence of block $j$, determined by the following traversal function for $1 \le i \le B$:

$$q_{i,j} = \begin{cases} B \cdot (j-1) + 1, & i = 1 \\ q_{i-1,j} + s + 1, & \mod(i,2) = 0 \\ q_{i-1,j} - s, & \mod(i,2) = 1 \end{cases}$$

d) **From Boundary Pattern (FBP)**: Like with FSP, this pattern has the field tracks grouped into blocks, which are covered sequentially. In each block, the vehicle covers the field tracks inwardly from the boundary. For instance, if the field has 10 tracks divided into 2 blocks with 5 tracks in each block (as illustrated in Fig.4.d), then the track sequence is $\rho = (\rho_1, \rho_2) = ((1,5,2,4,3),(6,10,7,9,8))$. In this pattern it is not required that the blocks have the same size, so in general, assuming that the field is divided into $n$ blocks with $B_j$ denoting the size of the $j^{th}$ block, then it is only required that $B_j > 0$ and $\sum_{j=1}^{n} B_j = N$. The track sequence $\rho_j$ of block $j$ can be expressed with the following traversal function, where $B_0 = 0$:

$$q_{i,j} = \begin{cases} \sum_{k=0}^{j-1} B_k + 1, & i = 1 \\ q_{i-1,j} + B_j - 1, & i = 2 \\ q_{i-2,j} + 1, & \mod(i,2) = 1 \wedge i \ne 1 \\ q_{i-2,j} - 1, & \mod(i,2) = 0 \wedge i \ne 2 \end{cases}$$

Then the track sequence for covering the entire field is $\rho = (\rho_1, \rho_2, ...., \rho_n)$.

e) **From back Furrow Pattern (FFP)**: This pattern is similar to the FBP pattern, except that the vehicle covers the field tracks outwardly from the central track of the block. For instance, in a

field with 10 tracks grouped into 2 blocks with 5 tracks in each block the track sequence

becomes: $\rho = ((3, 4, 2, 5, 1), (8, 9, 7, 10, 6))$, see Fig. 4.e. Assuming that $B_j$ is the size of the

$j^{th}$ block and that the conditions that $B_j > 0$, $\sum_{j=1}^{n} B_j = N$ and $B_0 = 0$ are satisfied, then the track

sequence $\rho_j$ of block $j$ can be written as:

$$q_{i,j} = \begin{cases} \sum_{k=0}^{j-1} B_k + \lceil B_j / 2 \rceil, & i = 1 \\ q_{i-1,j} + 1, & i = 2 \\ q_{i-2,j} - 1, & \mod(i,2) = 1 \wedge i \neq 1 \\ q_{i-2,j} + 1, & \mod(i,2) = 0 \wedge i \neq 2 \end{cases}$$

Then the track sequence for covering the entire field is $\rho = (\rho_1, \rho_2, ...., \rho_n)$.

## 3.3 The turning models

The four most common types of turns for agricultural vehicles operating in a headland pattern are the following: the forward turn ($\Omega$-turn), the double round corner turn ($\Pi$-turn), the reverse cross turn ($T_{cross}$-turn) and the reverse open turn ($T_{open}$-turn), illustrated in Fig. 5. (Hunt, 2008; Witney, 1996).

$\Pi$-turns are fast and need less headland space for turning. Their disadvantage, relative to the other turns, is that they require large distance between the exit and the entry tracks; at least twice the turning radius of machinery. $\Omega$-turns are fast and smooth for narrow manoeuvers, but they require more turning space, i.e. a wider headland. $T$-turns ($T_{cross}$ and $T_{open}$) are the most commonly used turns in bed formation and stone separation due to their low demand of space for maneuvering, but they are time demanding, because twice the vehicle needs to stop and change gear between forward and reverse direction. The field efficiency can be improved with minimal headland width by selecting $T$-turns instead of $\Pi$-turns. However, this requires skipping of tracks which is complicated for the driver, unless the tracks are clearly defined and the pattern is simple.

To calculate the turning length of these four turns, a geometrical turn model introduced by Bochtis and Vougioukas (2008) and Spekken (2015), was used. The model is written as follows:

$$L(w, r_{min}, d_{ij}) = \begin{cases} \Omega(d_{ij}) = r_{min} \cdot \left[ 3\pi - 4\sin^{-1}(\frac{2 \cdot r_{min} + d_{ij} \cdot w}{4r}) \right], d_{ij} < 2 \cdot r_{min} / w & (1) \\[2em] T_{cross}(d_{ij}) = r_{min} \cdot (2 + \pi) - d_{ij}.w + 2 \cdot l, d_{ij} < 2 \cdot r_{min} / w & (2) \\[2em] T_{open}(d_{ij}) = r_{min} \cdot (2 + \pi) + d_{ij}.w + 2 \cdot l, d_{ij} < 2 \cdot r_{min} / w & (3) \\[2em] \Pi(d_{ij}) = r_{min} \cdot (\pi - 2) + d_{ij}.w, d_{ij} \geq 2 \cdot r_{min} / w & (4) \end{cases}$$

where $r_{min}$ is the minimal turning radius of the vehicle with implement, $w$ is the operating width of the implement $d_{ij}$ is the turn degree defined as $|i - j|$, where $i$ and $j$ are the exit and entry track numbers, respectively. In other words, the number of skipped track in a headland equals to $d_{ij} - 1$. For modelling of the T-turns, a minimum distance $l$ is needed for a tractor attached with implement to become fully parallel to a field boundary before starting to drive backwards, which is the distance between the front axle of the tractor and the rear axle of either the implement or the tractor, in case the implement has no wheels.
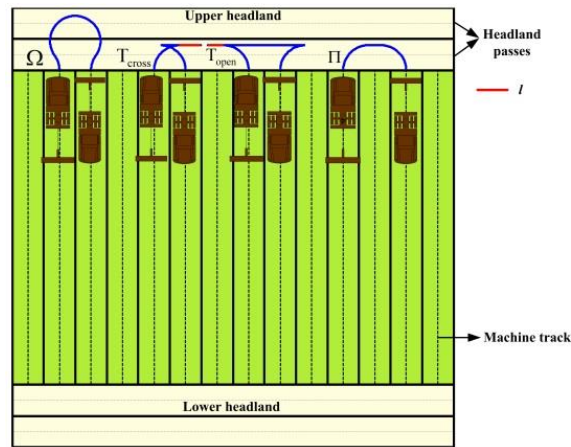


Fig.5 - Illustration of the geometrical representation of a field with three common turn types.

It has to be noted that these turn models calculate the minimal length of each individual turn for an Ackerman-steering machine. However, in actual operations, the driver cannot exactly follow this shortest turning path in the headland area, since the minimal turning radius cannot be implemented due to dynamic factors, hence the actual turning length is always longer than the turning length estimated by the models. It can be observed from the above turning model that the only factor that affects the turning length of each individual turn is the turning radius, $r$, since the turn degree $d_{ij}$ and operating width $w$ are fixed for a given turn with a specific vehicle. So, the task of the model fitting process is to estimate the actual turning radius $r$ from the measured turning lengths. In this study, all the measured turns in each operation are categorized into groups that have the same turn type and $d_{ij}$; each turn is treated as a data point in the model fitting terminology. For each measured turn, the actual turning radius $r$ can be calculated according to the formula of the corresponding turn type. For instance, if the measured turn is a $\Pi$ turn with $d_{ij} = 4$ and $w = 5.0$ and its length is 26.85, then the actual turning radius is obtained by formula (4): $r = (L - d_{ij}.w)/(\pi - 2) = (26.85 - 4*5.0) / (\pi - 2) = 6.0$. The average turning radius $r_{ave}$ of these actual turning radiuses is used as the input parameter of the turning models. Furthermore, due to the different maneuverability and specification of the machines in different operations, the $r_{ave}$ may vary, hence the fitting process for each turn type needs to be done separately.

## 3.4   Field operations recordings

### 3.4.1   Fields

The case study is based on three fields located at Lolland, Denmark. Field A [N 54°42´09´´, E 11°18´39´´] has an area of 3.24 ha; field B [N 54°44´37´´, E 11°12´42´´] has an area of 5.30 ha, while field C [N 54°44´23´´, E 11°12´33´´] has an area of 11.07 ha. The region is mainly flat, so machinery performance in these three fields was not affected by the slope of the fields. Figure 6 shows satellite images of the experimental fields.

|   (a) Field A   |   (b) Field B   |   (c) Field C   |

**Fig. 6 - Satellite images of the experimental fields.**

### 3.4.2 Machinery and GPS positioning system

Three types of tractor-implement combinations were involved in the experimental operations: A Fendt 928 for bed forming (length: 2 m), a Fendt 818 with separator (length: 6.8 m) for stone separation and a Fastrac 3200 with planter (length: 6 m) for planting (Figure 7). Besides, five operators were involved in these three operations (1 for bed forming; 2 for stone separation; and 2 for planting). The applied fieldwork patterns for each operation were based on the operators' own choice. The considered potato planting system consisted of 2.25 m wide beds which was the basic module width. For each field crossing the bed former can produce two beds (one complete and two half beds), while the stone separator and the planter can only process one bed. Hence, the operating width $w$ was 4.50 m for the bed former and 2.25 m for the stone separator and the planter.

Two types of GPS receivers were used for recording the positions of the vehicles involved. An AgGPS 162 Smart Antenna DGPS receiver (Trimble®, GA, 243 USA) was used for recording the trajectory of the bed former, and two Aplicom A1 TRAX Data loggers (Aplicom®, Finland) were used for recording the trajectory of the stone separator and planter. The recording frequency was set to 1Hz for all experimental recordings. Moreover, the tractor of the bed former was used to record the inner field boundary, which is the boundary between the headland and the cropping areas, by travelling along the inner field boundary. This boundary is used later to decompose the entire field coverage paths into sequences of turning paths, transport paths in headland and operating path on the beds in the cropping area.

**Fig. 7- The tractor-implement combinations used in the operations**

### 3.4.3    Decomposition of recorded GPS data

The recorded GPS data were analyzed and decomposed into sequences of productive and non-productive activities of the vehicles. This was done for each operation and field with a dedicated auxiliary tool developed using the MATLAB® technical programming language (The MathWorks, Inc., Natwick, Mass). The input parameters of the tool include the coordinates of the field boundary, the inner field boundary, the location of the reloading unit(s) and the coordinates of the machinery trajectories.

For the bed formation and the stone separation operations the motion sequences were categorized in two types: turning in the headland and effective working in the field body. A turn was defined as beginning with the first and ending with the last sequential data point inside the headland, determined by the recorded coordinates of the inner field boundary, and the remaining recorded data points inside the inner field boundary are considered as the effective on-the-tracks working. The planting operation has a third type of motion activity, namely reloading in the headland area. To distinguish the recorded points of turning and reloading motion in the headland area, circles were drawn with the radius of a given threshold value at the centers of the locations of the service units. If a machine stays inside the circle for a given period of time, then this can be considered as the reloading task. Otherwise, it can be considered as turning motion. In this work, the threshold values were defined to 6 meters for the circle radius and 3 minutes for the inactivity/servicing time.

## 3.5   Simulation model

This study focuses on the savings on the total operational time that can be achieved by minimizing the non-working distance. Therefore, the data for on-the-tracks working is extracted from the actual operation. In other words, in the simulation model, only the non-working distance and time is regenerated based on the specifically selected fieldwork pattern. The simulation model was developed using the MATLAB$^{®}$ technical programming language.

The input data to the simulation model includes the following:

- Number of beds (tracks) extracted from the field recording.

- Fieldwork pattern for vehicle.

- Machinery information: Turning radius $r_{ave}$, operating width $w$, maximum distance that a machine with full load capacity can cover.

- Operational information: turning speeds for $\Omega$-turn, $\Pi$-turn and $T$-turn corresponding to the operation and location of the reloading units.

The whole simulation process is presented in Figure 8. In brief, the simulation includes the following steps:

1. Generation of track sequence: Based on the number of tracks and the mathematical description of the selected fieldwork pattern the track sequence $\rho$ is generated.

2. Simulation settings: The simulation configuration is completed, such as determination of the operation type and the maximum distance that one full tank capacity can cover, etc. For material neutral operations, such as bed forming and stone separation, the maximum cover distance of the machine can be considered as infinite since there is no capacity constraint. For the material input operation, such as planting, the maximum cover distance is extracted from the field recording.

3. Simulation: In material neutral operations, according to the turn degree $d_{ij}$, operating width $w$ and $r_{ave}$, the total turning length can be calculated by using the corresponding formula described in section 3.3. The material input operations (e.g. planting) involve tank reloading and the reload event occurs at the headlands with the reloading unit(s) located. Hence, each time the vehicle reaches the headland with a reloading unit, the simulation model will estimate whether the current tank capacity is sufficient to cover the next tracks to reach a headland with a reloading units. If not, the reloading event is triggered, and then transport distance, time and reloading time are calculated, otherwise, the turn is executed to continue the operation and the turning length is calculated using the turn models.

4. Output: The total estimated non-working distance and time consisting of all the turns of the tested fieldwork pattern and the required reloads is calculated and output.
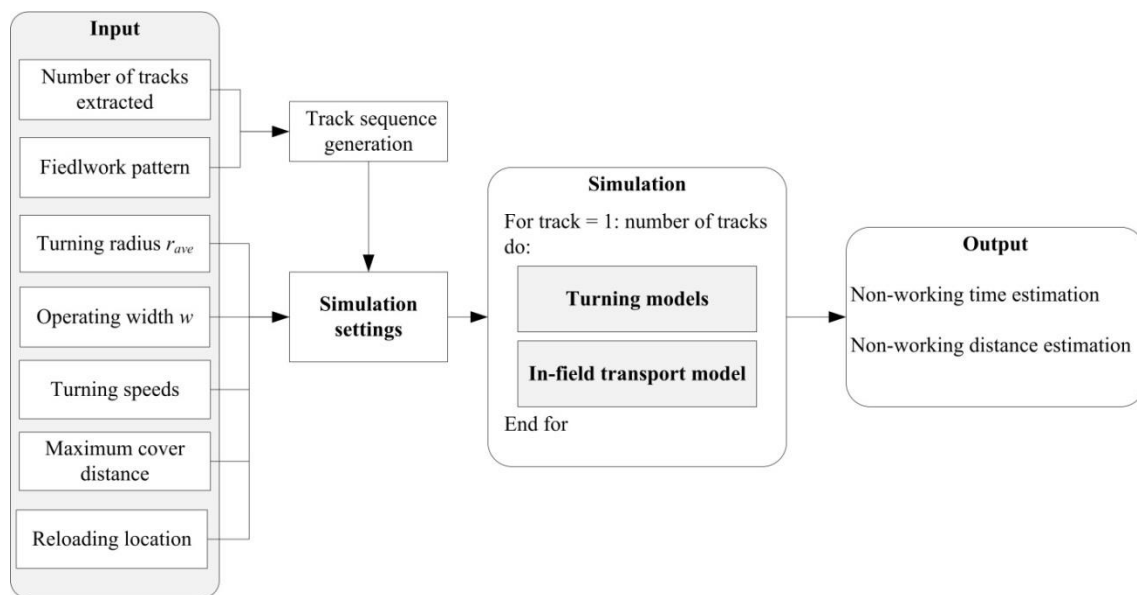


**Fig. 8 - Overall flow of the simulation model.**

# 4    Results and discussion

## 4.1    Analysis of field recordings

Figure 9 shows the GPS recordings of the bed former, stone separator, and planter in fields A, B, and C, respectively. The total number of the formed beds in fields A, B, and C were 34, 66, and 116, respectively.

The track sequence of each operation in the three fields is provided in Appendix A. The GPS recordings for each field and operation were decomposed into path segments (section 3.4.3) and the accumulated results are presented in Table 1 for time and distance with effective as well as non-effective parts (turning, transport and reload).In addition, the time based field efficiency also is presented in Table 1.
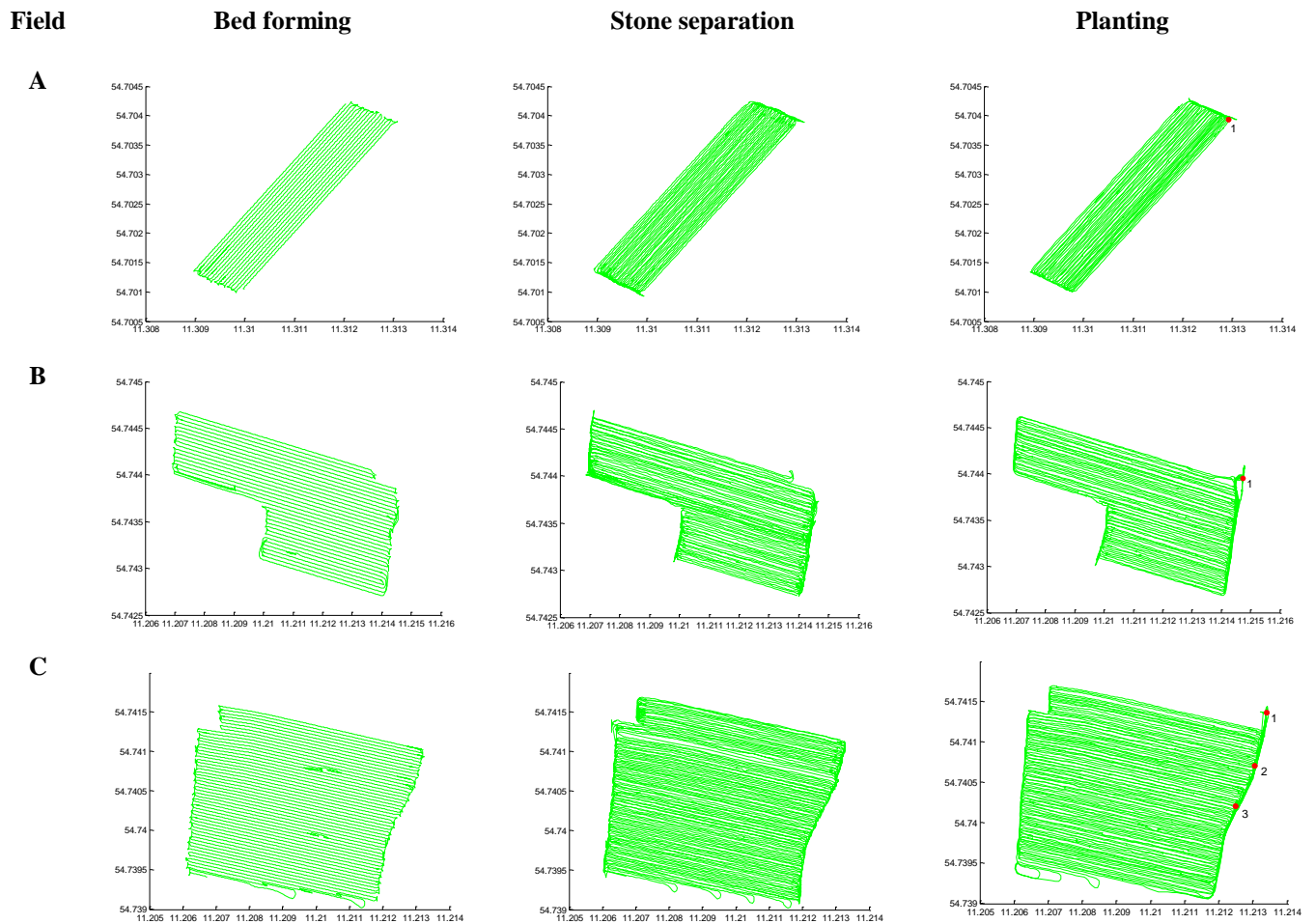


**Fig. 9 - Plot of GPS recordings for bed forming, stone separation and planting operations in field A, B and C, respectively. Red points show the locations of the reloading units.**

| | Track operating distance (m) | Turning distance (m) | Transport distance (m) | Track operating time (s) | Turning time (s) | Transport time (s) | Reload time (s) | Field efficiency (%) |
|---|---|---|---|---|---|---|---|---|
| **Table 1– Measured data for the experimental operations in field A, B and C.** | | | | | | | | |
| **Field A** | | | | | | | | |
| **Bed forming** | 6418.6 | 487 | - | 5840 | 452 | - | - | 92.8 |
| **Stone separation** | 12803.0 | 1431.5 | - | 17905 | 2204 | - | - | 89.0 |
| **Planting** | 12951.0 | 927.0 | 297.3 | 12215 | 940 | 343 | 3630 (4 reloads) | 71.3 |
| **Field B** | | | | | | | | |
| **Bed forming** | 12556.0 | 1058.4 | - | 11368 | 960 | - | - | 92.2 |
| **Stone separation** | 25162.0 | 2845.0 | - | 31746 | 4429 | - | - | 87.8 |
| **Planting** | 25261.0 | 1884.0 | 2163.0 | 18161 | 1957 | 2121 | 11475 (12 reloads) | 53.9 |
| **Field C** | | | | | | | | |
| **Bed forming** | 20718.0 | 1761.7 | - | 16407 | 1611 | - | - | 91.1 |
| **Stone separation** | 42981.0 | 4741.0 | - | 49781 | 7294 | - | - | 87.2 |
| **Planting** | 43049.0 | 2942.0 | 3937.0 | 40329 | 2901 | 3977 | 16729 (24 reloads) | 63.1 |

## 4.2 Fitting of the turning models

Onsite observation and analysis of the field GPS recordings showed a clear relationship for each operation between the driver's selected turning type and the number of skipped tracks. In the bed forming operation, two types of T turn: $T_{cross}$ and $T_{open}$ were used when $d_{ij}$ was 1 (non-skipped turn), the $\Omega$-turn was used when $d_{ij}$ was 2 (skip one track), otherwise the $\Pi$-turn was used. In both the stone separating and the planting operations the $T_{cross}$- turn was used for $d_{ij}$ values less than 5, the $\Omega$-turn was used for $d_{ij}$ values equal to 5 or 6, otherwise the $\Pi$-turn was used. Table 2 shows the selected turn types, in addition to the average calculated turning radius $r_{ave}$ and the average turning speeds for each turn type in the three operations. It should be mentioned that the differences in measured turning speeds for the same type of turns were

negligible with different values of turn degree, so the same value has been assumed in Table 2. The average values of turning radius and speed were used as parameters of the simulation model for calculating the turning distance and time. Figure 10 presents examples with the actual and simulated turns for the bed former, stone separator and planter, respectively.

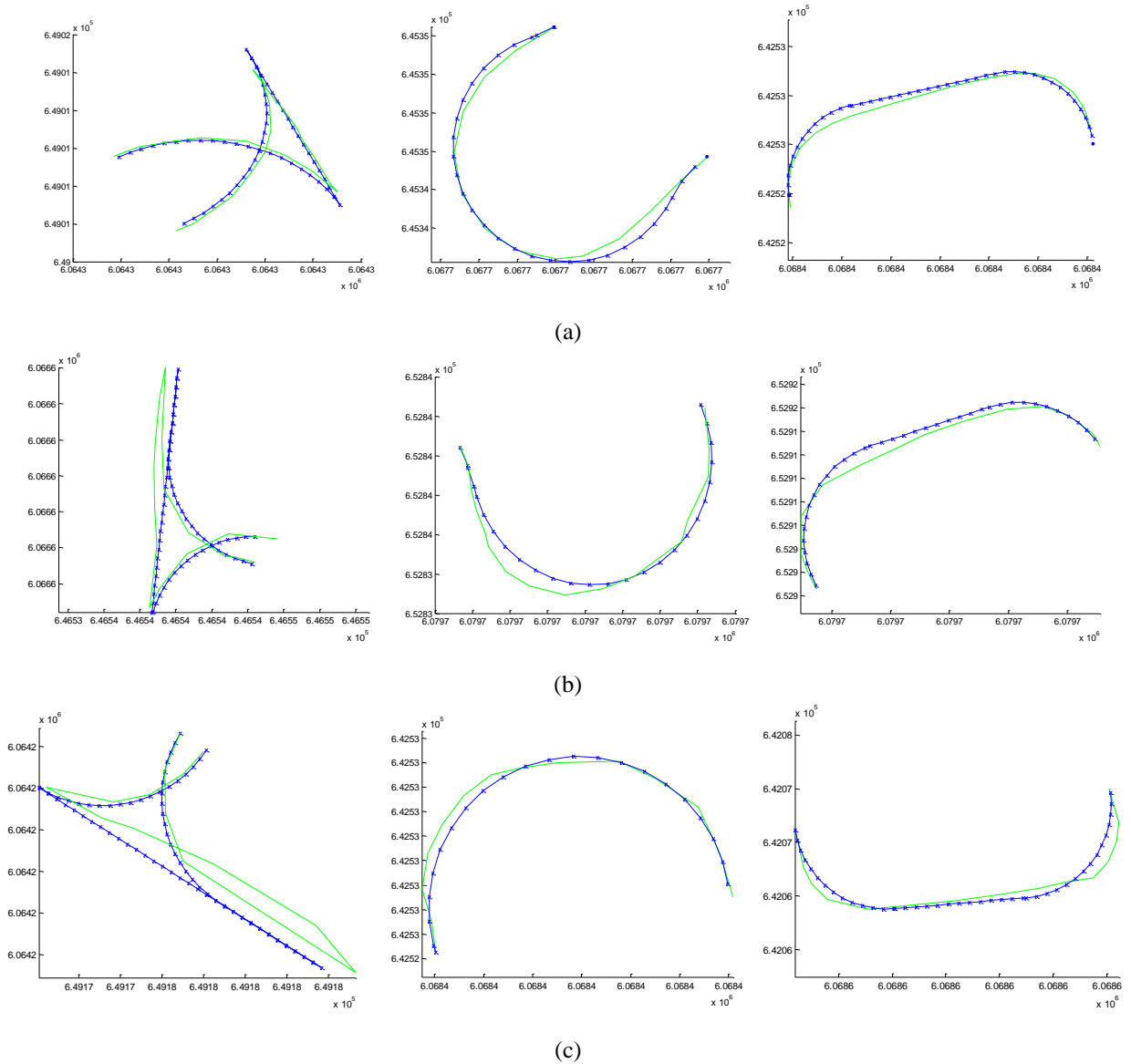| Table 2 – Calculated average turning radius for each turn type with the same turn degree for bed former, stone separator and planter and the corresponding speeds. | | | | | |
|---|---|---|---|---|---|
| Equipment | Turn type | $d_{ij}$ | number of observations | $r_{ave}$ (m) | Turn speed (m s$^{-1}$) |
| Bed former | $T_{cross}$ | 1 | 65 | 6.16 | 1.08 |
| | $T_{open}$ | 1 | 65 | 4.98 | |
| | $\Omega$ | 2 | 32 | 6.02 | 1.15 |
| | $\Pi$ | 3 | 20 | 8.24 | 1.35 |
| | $\Pi$ | 4 | 20 | 8.23 | |
| Stone separator | $T_{cross}$ | 1 | 65 | 5.93 | 0.64 |
| | $T_{cross}$ | 2 | 18 | 5.74 | |
| | $T_{cross}$ | 3 | 18 | 5.75 | |
| | $T_{cross}$ | 4 | 18 | 5.34 | |
| | $\Omega$ | 5 | 18 | 6.42 | 0.85 |
| | $\Omega$ | 6 | 18 | 7.12 | |
| | $\Pi$ | 7 | 23 | 8.21 | 1.16 |
| | $\Pi$ | 8 | 23 | 8.32 | |
| Planter | $T_{cross}$ | 1 | 65 | 6.07 | 0.65 |
| | $T_{cross}$ | 2 | 40 | 5.84 | |
| | $T_{cross}$ | 3 | 40 | 5.72 | |
| | $T_{cross}$ | 4 | 40 | 5.50 | |
| | $\Omega$ | 5 | 60 | 6.13 | 0.86 |
| | $\Omega$ | 6 | 60 | 7.08 | |
| | $\Pi$ | 7 | 60 | 8.23 | 1.20 |
| | $\Pi$ | 8 | 60 | 8.65 | |

**Fig. 10 - Examples of the actual ( ——— ) and simulated ( —✳— ) turns for the bed former (a), stone separator (b), and planter (c).**

## 4.3 Simulation model evaluation

In the previous section, the average turn radius $r_{ave}$ for each type turn with the same $d_{ij}$ in each operation was calculated based on measured turns. These values were used in the simulation model to simulate the exact driving patterns chosen by the operators of the nine field coverages (three operations in three fields). Table 3 compares the simulated and the measured data. The errors in predicting the turning distance and time for three operations in these three experimental fields are in the range of 0.66% - 3.60%, 0.88% - 3.83%,

respectively and the errors in predicting the transport distance and time are in the range of 1.92% - 3.70%, 2.04% - 3.68% respectively, which indicates that the turning models with the average turn radius $r_{ave}$ can predict the non-working distance and time with sufficient accuracy.

| | Turning distance (m) | | Turning time (s) | | Transport distance (m) | | Transport time (s) | | Error [c] (%) | | | |
|---|---|---|---|---|---|---|---|---|---|---|---|---|
| **Table 3 - Comparison between simulated and measured data of non-working for the experimental operations in fields A, B and C.** | | | | | | | | | | | | |
| | Simul[a] | Meas[b] | Simul | Meas | Simul | Meas | Simul | Meas | Turn | | Transport | |
| | | | | | | | | | Dist. | Time | Dist. | Time |
| **Bed forming** | | | | | | | | | | | | |
| **Field A** | 483.8 | 487 | 448 | 452 | - | - | - | - | 0.66 | 0.88 | | |
| **Field B** | 1021 | 1058.4 | 945 | 960 | - | - | - | - | 3.53 | 1.56 | - | - |
| **Field C** | 1715 | 1761.7 | 1588 | 1611 | - | - | - | - | 2.65 | 1.43 | | |
| **Stone separation** | | | | | | | | | | | | |
| **Field A** | 1380 | 1431.5 | 2156 | 2204 | - | - | - | - | 3.60 | 2.18 | | |
| **Field B** | 2791 | 2845 | 4378 | 4429 | - | - | - | - | 1.90 | 1.15 | - | - |
| **Field C** | 4808.7 | 4741 | 7383 | 7294 | - | - | - | - | 1.43 | 1.22 | | |
| **Planting** | | | | | | | | | | | | |
| **Field A** | 895 | 927 | 904 | 940 | 303 | 297.3 | 350 | 343 | 3.45 | 3.83 | 1.92 | 2.04 |
| **Field B** | 1866 | 1884 | 1916 | 1957 | 2083 | 2163 | 2043 | 2121 | 0.96 | 2.10 | 3.70 | 3.68 |
| **Field C** | 2863 | 2942 | 2876 | 2901 | 3854 | 3937 | 3893 | 3977 | 2.69 | 0.86 | 2.11 | 2.11 |

[a] simulated; [b] measured; [c] |measured – simulated| / measured*100%.

## 4.4 Fieldwork pattern assessment

For the planting operations the three fields were planting with three varieties of seed potato with different size; therefore, the maximal distance covered by a filled hopper differed accordingly. Based on the GPS recordings, the maximal distance that one full hopper can cover was set to 3800, 2900, and 2400 m, respectively for the simulations in fields A, B and C. The location of the reloading units were set as the same as the locations in the actual operations for operations in field A and B, while in field C the location of the

reloading unit was set at the location 3 in the actual operation. The transport speed and reloading time of planter in the simulation were set to be the average transport speed and reloading time in the actual operation in each field. In addition, as mentioned earlier, in bed forming, two types of T-turn were used, but in the simulation only the $T_{open}$ turn was applied since it is more often used during the operation.

Each of the five fieldwork patterns were tested with different parameters and only the best solutions are presented here. For instance, the FSP pattern for bed forming was tested with all integer values of skipped track numbers between 1 and 5. However, only the best solution (skipped 3 tracks) is presented. This was also applied to the FBP and FFP patterns to find the best size of the blocks. Figure 11 shows the simulated turning distance and time for the selected field-work patterns. It can be derived that for each operation in each field there exist fieldwork patterns that can provide better solutions in comparison with the operator-selected ones. By selecting these patterns the tuning distance and time could have been reduced significantly.

It can be concluded that the FSP pattern provides the largest savings in terms of distance and time among the selected patterns in all fields and all operations. Specifically, in the case of field A, the maximum savings in non-working distance are 70 m, 451.6 m, 28.0 m for bed forming, stone separation and planting, respectively,, while the corresponding time savings are 133 s, 1267 s and 61 s; for field B, the maximum savings in non-working distance are 194.4 m, 976.0 m and 891.6 m, while the savings in non-working time are 3292 s, 2667 s and 3825 s, for bed forming, stone separation and planting; for field C, the maximum savings in non-working distance are 258.4 m, 1663.7 m and 672.0 m, the savings in non-working time are 526 s, 4437 and 3576 s for bed forming, stone separation and  planting.

Fig. 12 provides the savings of non-working distance and time in percentage for these three operations in each field. For all three fields and all three operations the FSP fieldwork pattern turned out to be superior to the other patterns and to the farmer's selected pattern. It can be observed that the maximum savings in non-working distance are 14.4%, 32.7%, 2.3% and in time are 29.4%, 58.8%, 2.3% for bed forming, stone separation and planting in field A; for field B the maximum savings in non-working distance are 18.4%, 35.0% and 22.6%, and in time are 30.4%, 60.9%, 24.8%  for bed forming, stone separation and planting; in

field C the maximum savings in non-working distance are 15.1%, 34.6% and 10.0% and in time are 32.7%, 60.1% and 15.2% for bed forming, stone separation and planting.

The results in Fig. 12 show that the turning time can be reduced for bed forming and stone separation, regardless of field and fieldwork pattern. The savings were up to 32.7% for the bed forming and up to 60.9% for stone separation (using FSP in both operations). Also the distance was reduced for all fieldwork patterns, except for the SAP pattern in bed forming, where the turning distance reduced with values between 3.0% to 35.0%.

With respect to the planting operation, not all the tested fieldwork patterns could reduce the non-working distance and time in these three fields. In field A and C some fieldwork patterns resulted in longer non-working distances and in field A also in longer times than the operator's selected patterns. In field B, all fieldwork patterns saved non-working distance and time for planting. In contrast to this, in field A, all the tested field patterns except the FSP pattern increased the non-working distance and time. In the case of field B and C, the non-working distance and time could still be reduced, even for the SAP pattern, which is intuitively the worst of all the tested patterns for planting. The main reason is that the operator did not evaluate the combination of operating width, machine kinematics, headland length and location of the reloading unit properly. It can be seen from the planter's track sequence in field B that the operator skipped more than ten tracks to enter a new bed from the current one, which led to excessive turning distance. In addition, the transport distance, transport time and reload time are main contributions to the non-working distance and time in planting. During the operation, the operator could easily misjudge the amount of potato seed required for the next route, resulting in excessive reloading and transport, and subsequently reduced field efficiency. This fact was clearly demonstrated in the case of field B and C, where the simulated planter was able to save 3 reloads in field B and 4 reloads in field C, respectively, leading to improved field efficiency. For example, the simulated planter in field B spent 1957 extra seconds for turning when following the pattern SAP, but this loss was mitigated by savings of 564 and 2869 seconds for transport and reloading, respectively.

146

Fig. 13 presents the total savings of non-working distance and time per hectare in the three fields resulting from selecting the same fieldwork pattern in all three operations. It can be seen that fieldwork pattern (FSP) with maximum total estimated reduction of turning distance per ha were saving 28, 105 and 132.3 m/ha, and 75, 345 and 435 s/ha for all the operations in field A, B and C, respectively. These reduced turning distance and time lead to increased field efficiency. In the case of field A, the maximum estimated increase in time-based field efficiency for bed former, stone separator and planter are 2.0%, 6.5%, 0.9%, respectively. In the case of field B, the maximum estimated increase in field efficiency are 2.3%, 7.1%, 7.1%, while in the case of field C, the maximum increased field efficiency are 2.7%, 7.2%, 3.8%.

It can be concluded that it requires adequate experience from the operator to determine the best fieldwork pattern. If the operator cannot properly evaluate the combination of the operating width, machine kinematics as well as the number of tracks, the selected pattern will result in excessive turning distance and time, and consequently low field efficiency. The selected fieldwork pattern has additional effects, apart from decreased field efficiency, since the pattern may also affect the soil compaction in the headland area. For instance, the tested FSP pattern mainly consists of $\Pi$-turns and a few $T$-turns (if any). The smooth $\Pi$-turns lead to less lateral forces during turning and consequently result in less soil compaction. Moreover, the $\Pi$-turns require less headland space than the $\Omega$-turns, so the proportion of the field area used as headland can be decreased, consequently more field area can be used for cropping to obtain more economic benefits.
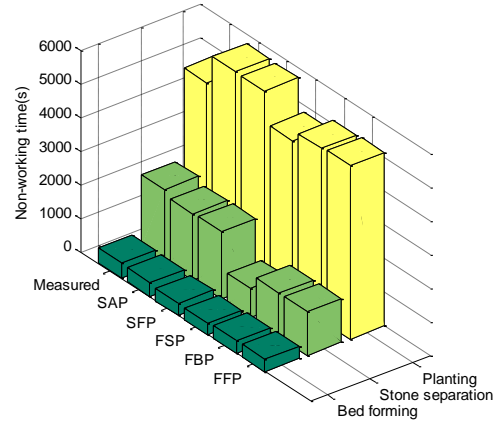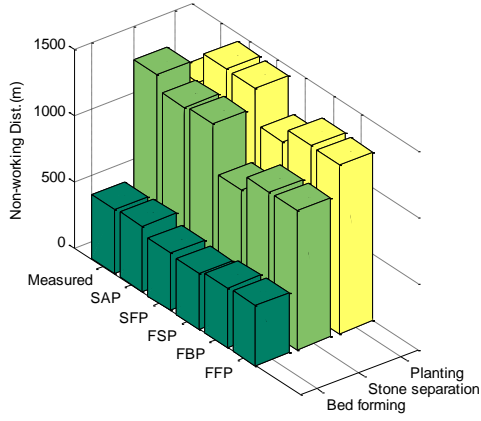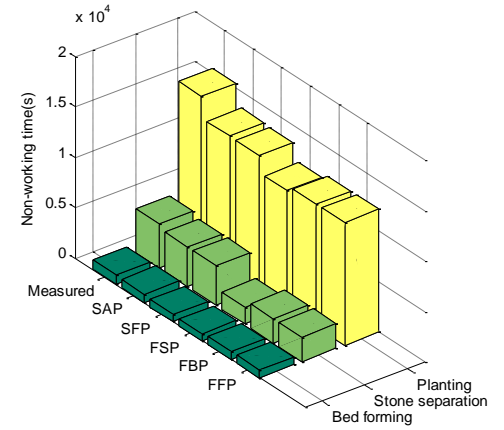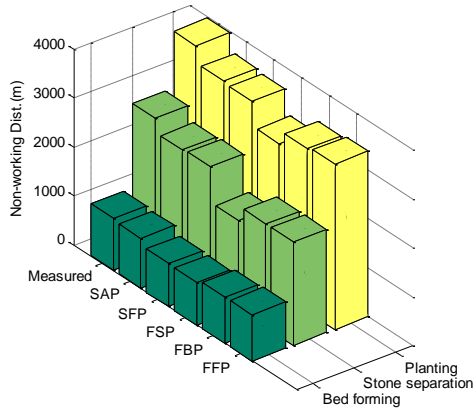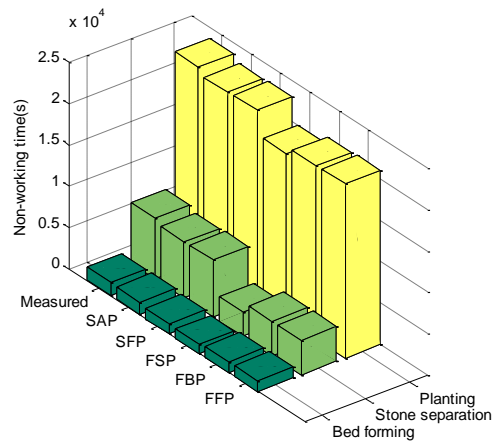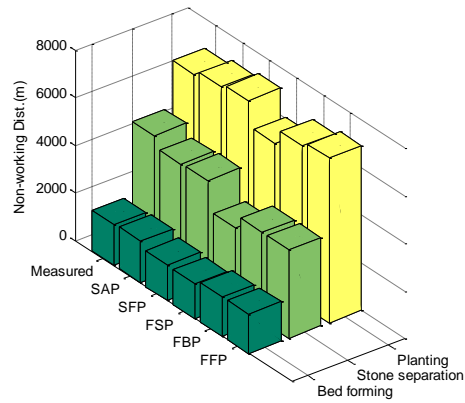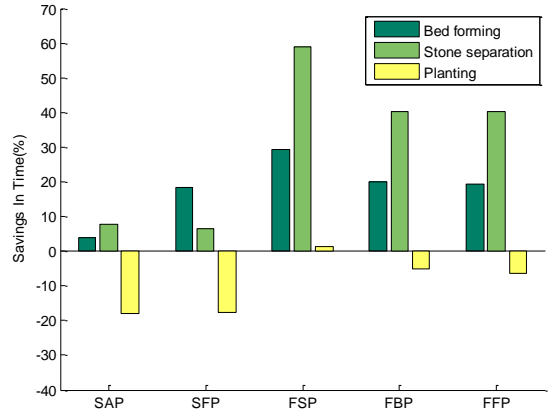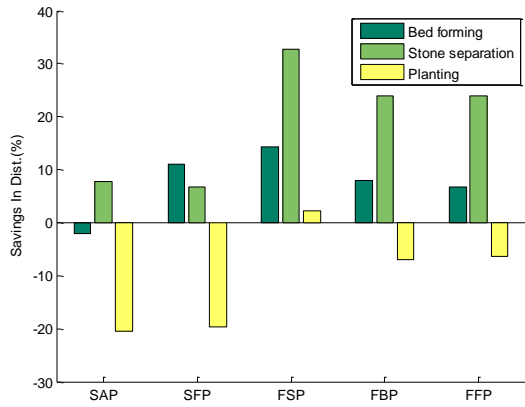
**Fig. 11 - Measured and simulated non-working distance and time of bed forming, stone separation and planting based on five field-work patterns in fields A, B and C.**
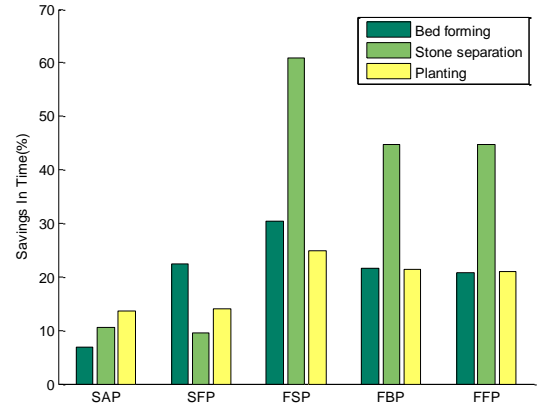
148
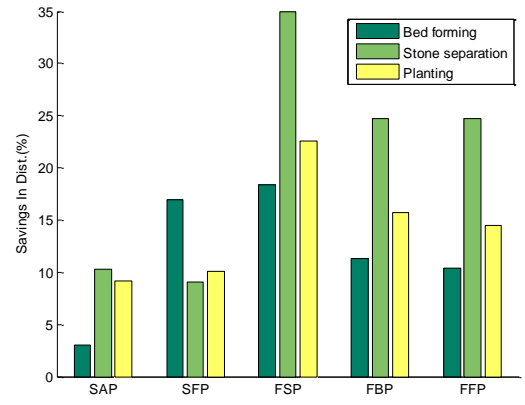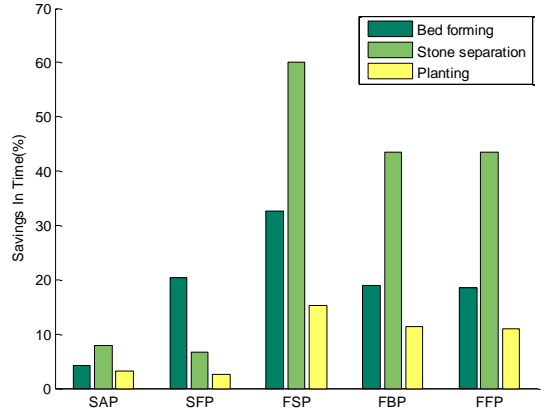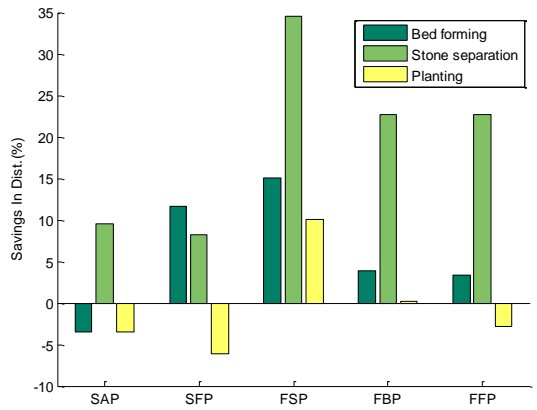
**Fig. 12 - Savings in non-working distance and time for bed forming, stone separation and planting in fields A, B and C.**
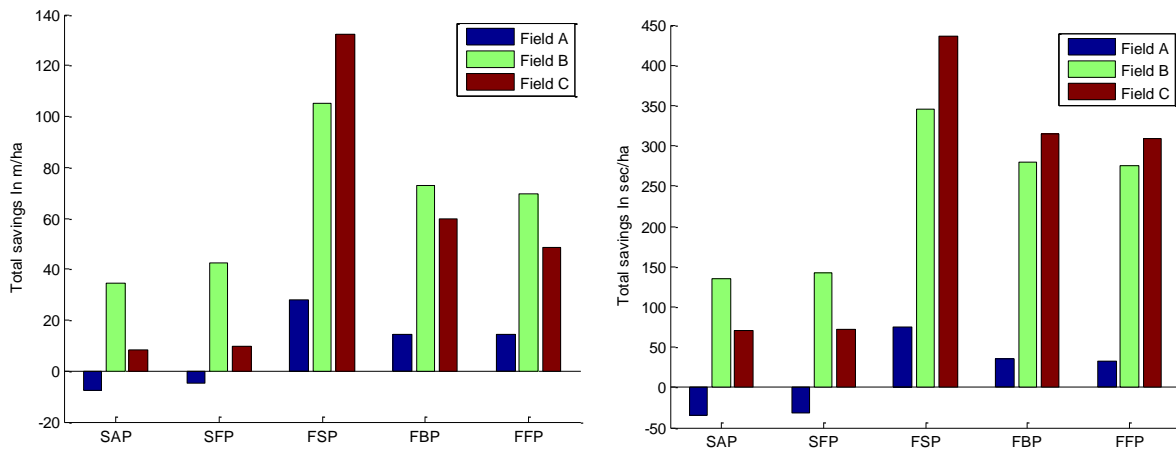
**Fig. 13 - Non-working distance and time per hectare in fields A, B and C.**

# 5   Conclusions

In this study, an assessment approach for the saving analysis in non-working distance and time of using five standard fieldwork patterns against farmer-used patterns for potato cultivation was carried out. Based on the simulated results for three case study fields, it was shown that by using the appropriate pattern for involved three operations the total non-working distance and time can be substantially reduced. The savings for bed former were up to 18.4% in turning distance and 32.7 % in turning time, the maximum savings for stone separator in terms of turning distance and time were 35.0 and 60.9% while for the planter the maximum savings were 22.6% in non-working distance and 24.8% in non-working time when compared with the actual operation in three case study fields. Regarding the time-based field efficiency, in the case of field A, the estimated increase in time-based field efficiency for bed former, stone separator and planter were 2.0%, 6.5%, 0.9%, respectively. In the case of field B, the estimated increase field efficiency were 2.3%, 7.1%, and 7.1%, while in the case of field C, the increased field efficiency were 2.7%, 7.2%, and 3.8%.

The proposed method can be used as an evaluation tool for the operator's performance against pre-determined field coverage track sequence motifs. The results of the evaluation can be used as the feedback

for the operations planning management in order to select a realizable field work pattern that improves the overall field efficiency for a specific combination of field and machinery characteristics.

## Reference

Ansorge, D., Godwin, R., 2007. The effect of tyres and a rubber track at high axle loads on soil compaction, Part 1: Single axle-studies. *Biosystems Engineering, 98*(1), 115-126.

Benson, E., Hansen, A., Reid, J., Warman, B., & Brand, M., 2002. Development of an in-field grain handling simulation in ARENA. ASAE Paper, 02-3104.

Bochtis, D. D., Vougioukas, S., 2008. Minimising the non-working distance travelled by machines operating in a headland field pattern. *Biosystems Engineering*, 101(1), 1-12.

Bochtis, D. D., Sørensen, C. G., Busato, P., Berruto, R., 2013. Benefits from optimal route planning based on B-patterns. *Biosystems Engineering*, 115(4), 389-395.

Bochtis, D. D., Sørensen, C. G., Green, O., Moshou, D., Olesen, J., 2010. Effect of controlled traffic on field efficiency. *Biosystems Engineering*, 106(1), 14-25.

Bochtis, D. D., Sørensen, C. G., Jørgensen, R. N., Green, O., 2009. Modelling of material handling operations using controlled traffic. *Biosystems Engineering*, 103(4), 397-408.

Hameed, I. A., Bochtis, D., Sørensen, C., & Nøremark, M., 2010. Automated generation of guidance lines for operational field planning. *Biosystems Engineering*, 107(4), 294-306.

Hameed, I. A., Bochtis, D. D., Sørensen, C. G., Jensen, A. L., Larsen, R., 2013. Optimized driving direction based on a three-dimensional field representation. *Computers and Electronics in Agriculture*, 91(0), 145-153.

Hansen, A., Hornbaker, R., Zhang, Q., 2003. Monitoring and analysis of in-field grain handling operations. Paper presented at the Proceedings of the International Conference on Crop Harvesting.

Hofstee, J., Spätjens, L., Ijken, H., 2009. Optimal path planning for field operations. Paper presented at the Proceedings of the 7th European conference on precision agriculture.

Hunt, D., 2008 . Farm power and machinery management: *Waveland Press*.USA.

Jin, J., Tang, L., 2011. Coverage path planning on three- dimensional terrain for arable farming. *Journal of Field Robotics*, 28(3), 424-440.

Ntogkoulis, P. A., Bochtis, D. D., Fountas, S., Berruto, R., Gemtos, T. A., 2014. Performance of cotton residue collection machinery. *Biosystems Engineering*, 119(0), 25-34.

Oksanen, T., Visala, A., 2009. Coverage path planning algorithms for agricultural field machines. *Journal of Field Robotics*, 26(8), 651-668.

Randal K. Taylor, M. D. S., Scott A. S., 2002. Extracting Machinery Management Information from GPS Data. ASABE,St. Joseph, Michigan .

Speken, M., Molin, J. P., Romanelli, T. L., 2015. Cost of boundary manoeuvres in sugarcane production. *Biosystems Engineering*, 129(1), 112-126.

Witney, B., 1996. Choosing and Using Farm Machines, 1996. Land Technology Ltd, Scotland, UK.

# Appendix A

**Tracks sequence of each operation**

**Field A:**

**Bed former:** 1 2 3 4 5 6 7 8 9 10 11 12 13 14 15 16 17.

**Stone-separator:** 1 2 3 4 5 6 7 8 9 10 11 12 13 14 15 16 17 18 19 20 21 22 23 24 25 26 27 28 29 30 31 32 33 34.

**Planter:** 1 7 2 9 3 11 5 4 13 6 15 8 17 10 19 12 21 14 23 16 26 18 29 20 32 24 31 22 34 25 27 30 33 28.

**Field B:**

**Bed former:** 4 5 3 6 2 7 1 8 9 10 11 12 13 14 15 16 17 19 18 20 21 22 23 24 25 26 27 28 29 30 31 32 33 34

**Stone separator:** 1 2 3 4 5 6 7 8 9 10 11 12 13 14 15 16 17 18 19 20 21 22 23 24 25 26 27 28 29 31 35 30 32 34 36 37 38 33 39 40 41 42 43 44 45 46 47 48 49 50 51 52 53 54 55 56 57 58 59 61 60 62 63 64 65 66

**Planter:** 3 5 7 9 11 4 6 13 8 15 10 17 12 19 14 21 16 23 18 25 20 27 22 29 33 39 41 37 35 43 24 28 26 31 34 45 36 47 30 32 49 38 51 40 53 42 56 44 58 1 2 46 59 48 60 50 61 52 65 55 63 57 62 64 54 66.

**Field C:**

**Bed former:** 1 2 3 4 5 6 7 8 9 10 11 12 13 14 15 16 17 18 19 20 27 28 29 30 31 32 33 34 35 36 37 38 39 40 41 42 43 44 45 46 47 48 49 50 51 52 53 54 55 56 57 58.

**Stone separator:** 1 2 3 4 5 6 7 8 9 10 11 12 13 14 15 16 17 18 19 20 21 22 23 24 25 26 27 28 29 30 31 32 33 34 35 36 37 38 39 40 41 42 43 44 45 46 47 48 49 50 51 52 53 54 55 56 57 58 59 60 61 62 63 64 65 66 67

68 69 70 71 72 73 74 75 76 77 78 79 80 81 82 83 84 85 86 87 88 89 90 91 92 93 94 95 96 97 98 99 100 101 102 103 104 105 106 107 108 109 110 111 112 113 114 115 116.

**Planter:** 2 8 5 1 10 3 12 4 14 7 6 16 9 15 11 17 13 23 19 25 21 26 18 28 20 30 22   32 24 35 27 37 33 29 39 31 41 34 43 36 45 47 38 48 40 50 42 52 44 54 46 56 49 58 51 61 53 62 55 64 57 66 59 68 60 70 63 72 65 74 75 76 67 78 69 80 71 82 73 84 77  86 79 88 81 90 83 92 85 94 87 96 89 98 91 100 101 107 93 103 95 105 97 109   99   111   102   110   104   108   106   116   115   117   114   113   112

# Chapter 7

# General discussion and conclusions

# 7 General discussion and conclusions

In this chapter, the developed methods and gained results from Chapter 2 to Chapter 6 are discussed.

## 7.1 General discussion

### 7.1.1 Monitoring and analysis of field operations

**Chapter 2** considers the operation monitoring and analysis involving a developed tool for automatic analysis of geo-referenced data and applying this tool on recorded GPS data from five sequential operations involved in potato production. The results of the analysis enable farmers to know exactly how efficient the machinery performed and which factors resulted in inefficiencies during the operations, subsequently to make better decisions on the operation planning in future cropping seasons. For example, the field shape may be one of the factors that affect the operational efficiency, and as illustrated in this study the fields with higher MBR values have higher field efficiency than fields with lower MBR values. MBR is a measure of the level of regularity of a field where a rectangular field has value 1 and an extremely irregular field has a value approaching 0. Other researchers also used other shape indices to estimate the operational efficiency. Witney (1996) presented that a rectangle field with a 4:1 ratio between the lengths of its borders has highest value of efficiency and Oksanen (2013) developed a formula for estimating the operational efficiency using multiple shape indices based on multivariate regression. However, there are no general shape indices or formulas for estimation of operational efficiency of any type of fields. Furthermore, based on these measured time/distance elements, the machinery variable cost, consisting of the labor, fuels and oil, repair and maintenance costs can be roughly estimated. The labor cost can be estimated by the labor rate (€ h$^{-1}$) times the total hours used. For estimation of the fuel consumption and accumulated repair and maintenance costs, the relevant equations in the Agricultural Machinery Management Data ASAE Standard (ASAE D497.6, 2009; ASAE EP496.3, 2009) can be used.

In the presented work, only the primary units that execute the main field task were monitored, while the in-field and out-of-field activities involving transport units, e.g. the tractor for transporting seed potato from the farm to the field in the planting operation, and for transporting the harvested potato from the field to the farm

in the harvesting operation, were not considered in the experiment. It has been reported in the literature that the transport units are equally important as the primary units for the whole production system's productivity (Busato *et al.*, 2013; P. Busato *et al.*, 2007; Jensen and Bochtis, 2013). For example, in the potato planting and harvesting operations, the locations of the transport units in the headland area affect the transporting distance of the planter and harvester. Therefore, recognition of the activities of all units involved in one crop production system can help farm managers make more precise plans, e.g. for and labor planning and for machinery assignment and scheduling.

### 7.1.2 Optimized field coverage planning

**Chapter 3** and **4** contributes to the area of field coverage planning. In **Chapter 3**, a three-stage planning method was developed to generate feasible coverage plans for agricultural machines to execute non-capacitated operations in fields with obstacle areas. The first two stages regard the generation of a geometrical representation of the field with its obstacle areas using geometric primitives and then decomposing the field into a set of blocks, where a block is a subfield without obstacles. The third stage regards the optimization of the block sequence to be traversed with minimum distance. The processing and categorization of the physical obstacles is an important step before the generation of geometrical fieldwork tracks and headland passes. In this step it is determined which of the physical obstacles in the field are of importance for the optimization. Depending on the driving direction, the working width and the shape, size and position of the obstacles, an obstacle may be merged with another obstacle or with the headland, or simply ignored in the optimization stage. Taking obstacles 2 and 3 in Fig. 2 as an example, when the minimum distance between these two obstacles, measured perpendicular to the driving direction, is less than the operating width of the implement, then there is no room for a fieldwork track between them. If without merge of these two obstacles, there may be a track generated through them, thus this track is impractical for an agricultural vehicle to follow to go through the area between obstacle 2 and 3. Furthermore, without the processing and categorization of the physical obstacles, it would be possible to generate small subfields that were impracticable to operate. In addition, the computational time increases dramatically with the number of blocks.
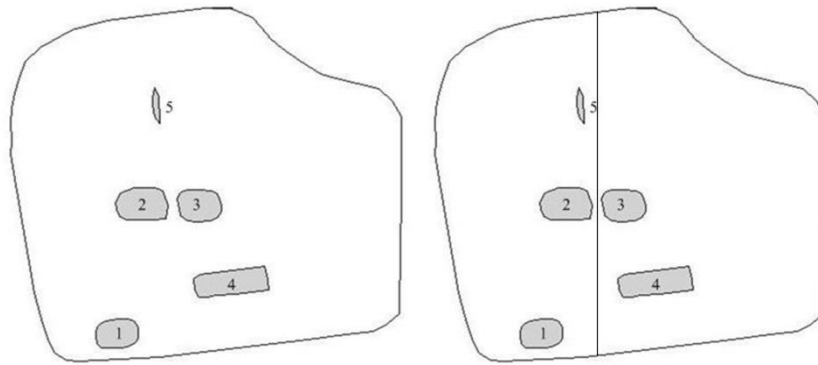
**Fig. 2 – A field track may be generated between unprocessed obstacle 2 and 3 and is impractical for agricultural machines.**

In the present study, after the decomposition into blocks, the driving direction is the same in each block. In other research works, however, the decomposition method, in general, consists of two procedures: First, finding the best reference line for field decomposition, second, obtaining the optimal driving direction in each block based on a cost function (e.g. turning time and distance, total travelled distance, overlapped area, etc.). But finding the optimal driving direction for each block potentially leads to another problem, namely that each subfield may need its own headland area for headland maneuvering. Fig. 3 is an example in the work of Zandonadi (2012) showing that more headland area (Fig. 3.b) was needed when a field was split into subfields. In this situation the cost function should take into account the fact that the headland area has lower production due to soil compaction resulted by excessive traffic maneuvering.
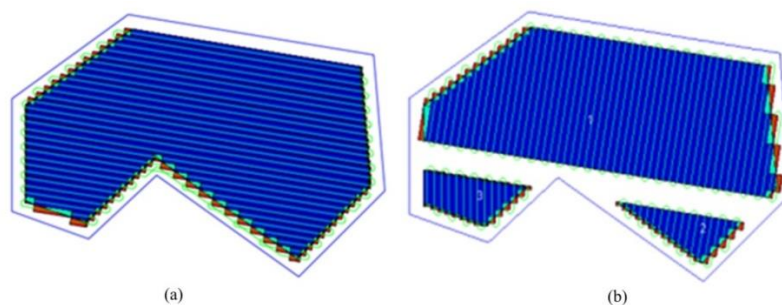


**Fig. 3 - An example of (a) a field with a driving direction, (b) a field divided into three subfields, with each subfield having its own driving direction and headland Zandonadi (2012).**

In the case of different driving direction in each subfield, the optimization approach in the third stage still can be directly applied for block sequence optimization, since the requirement of this optimization approach

is that the coordinates of the entry and exit tracks of each subfield should be known and used as parameters for the cost matrix generation. Furthermore, this planning method can also be incorporated in a navigation system for agricultural machines, since currently such systems cannot provide a complete route for covering fields with obstacles.

In **Chapter 4,** a web-based implementation of a tool for coverage planning demonstrates feasibility to be applied as an integral part of a decision support system, which enables users to easily access to test different alternative plans, e.g. in driving direction, working width, etc., providing the farmer a reference coverage plan prior to the execution of field operations. A web-based tool has the additional advantage that there is no need to install and update software for the farmer. The backend server program was developed using MATLAB technical programing language. The development focused more on the functionality of the tool than the computational time, so it requires a somewhat prolonged computational time to obtain the coverage plan. The problem of computational time can be solved using web dedicated programming language, such as JAVA, to implement the backend server program. Furthermore, this system needs further elaboration so that the user can input the field boundary as readable files (e.g. KML file), and can interactively split the field into subfields based on the user's own past experience, etc.

### 7.1.3 Simulation models as DSS

Simulation models can provide significant advantages for improving or optimizing the field operations, especially in complex operations involving multiple factors that affect the operational efficiency. In **Chapter 5**, a simulation model for simulating a complete set of operations in potato crop production was developed. The developed simulation model can be used to evaluate and optimize a variety of different user selected scenarios on infield operational decisions (e.g. driving direction, location of SUs, fieldwork pattern, etc.), and machinery dimension (e.g. working width, tank/hopper size, etc.) for an entire year's production. Based on the outputted time and distance from the simulation results, the farm managers can further estimate and calculate cost factors such as the labor cost, the cost of depreciation of the machines, and the cost of fuel consumption, and so on. For further development, these relevant formulas for estimating costs can be

embedded into the simulation model itself. In addition, the developed model can support strategic decisions for the production system transformation such as the purchase of a new set of machines.

As a demonstration of the capability of the simulation as a DSS, it has been applied to quantitatively assess the benefits of using different fieldwork patterns in terms of non-working distance and time, subsequently select an optimal one among these tested fieldwork patterns for field operation in **Chapter 6**. The assessment results showed that adopting an appropriate pattern can substantially reduce the non-working distance and time in the operations of bed forming, stone separating and planting. Besides, there are additional potential advantages of using an optimal standard fieldwork pattern suggested by the presented approach: In general, the optimal fieldwork pattern mainly consists of easy steering turns (e.g. $\Omega$-turns and $\Pi$-turns), which not only reduce the operational cost but also reduce the fatigue of the operator (Holpp *et al.*, 2013) making it possible for the operator to work efficiently for longer periods and at a consistently high level of work quality. Other existing routing methods, such as the B-pattern introduced by Bochtis and Vougioukas, (2008), which computes the optimal track sequence towards minimization of the total non-working turning distance, requires developing a dedicated tool for each agricultural vehicle to implement this type of pattern in each operation. Nevertheless, these standard fieldwork patterns can be directly implemented in the currently available navigation-aiding systems (e.g. iTEC Pro®, John Deere) and it is not even necessary to mount navigation-aiding systems on tractors for each operation in the case of bed crop production, because operators of the subsequent operations after bed forming can easily distinguish the next track to be followed, since the beds are already clearly formed. In this way, the farmers do not need to purchase extra and multiple navigation-aiding systems.

## 7.2  Future perspectives

This thesis mainly focused on two issues: field coverage planning and simulation development. In this study, a field coverage planning method for agricultural machines operating in fields with obstacles was developed, but the problem of finding the optimal routing track sequence in fields with multiple obstacles is still unsolved. Another research point is to include the capability of handling servicing of capacitation of

machines in the routing algorithm, which is a very important aspect in the realm of machine routing in operations such as planting, harvesting, etc.

As a future work for the simulation model development, the in-field and out-field activities of transport units in operations of a cropping system as well as the economic aspects throughout all involved field operations also should be incorporated into the model. In this way, a complete and comprehensive simulation model can help the farm managers or advisors to make more accurate decisions.

The web-based prototype described in Chapter 4 demonstrates promising perspectives, both for online route planning and simulation modelling. Pre-calculated plans rarely hold in reality, especially when the interdependent driving of multiple vehicles (PU and SUs) is involved. Therefore, online and real-time systems, where the plan can be updated continuously during the operation and as a result of the actual observed progress of the operation, are very interesting.

## 7.3   General conclusions

The main contributions of this thesis are:

1) The developed method extends the state-of-the-art method by providing a complete route for coverage fields with multiple obstacles either for agricultural machines or for future field robots executing non-capacitated operations. The optimization methodology in this approach can also be used for finding the optimal sequence of blocks using different driving directions.

2) A web-based field coverage path planning tool is proposed. On the webpage, the user can interactively select the field to be used as the basis for calculating the path planning by zooming to the field and drawing the field border on Google Maps. After selecting the field of interest the user specifies the input parameters, e.g. working width, and selects between a range of objective functions. In real time, the tool generates the specific output parameters, such as total working distance, overlapped area, total turning distance etc., and it produces a visualization of the coverage plan on top of the aerial map image of Google Maps.

3) A simulation-based approach for decision support targeting the derivation of fieldwork pattern was developed to estimate the benefits of using different standard auto-guidance based fieldwork patterns and then enable the machine operator to choose a proper fieldwork pattern to save operational costs and improve field efficiency.

4) A unified simulation model for sequential operations in potato production was developed. This model extends the capabilities of the state-of-the-art models from simulating one operation to all sequential field operations like those involved potato production.

5) Analysis of GPS motions of the in-field machinery involved in all operations of an entire growing season in potato production led to the determination of performance measures for these operations. For some of these operations, namely potato bed forming and stone separation, the expected performance has not been published before, and they are not part of the norm data supplied by ASABE.

# References

Ali, O., Verlinden, B., Van Oudheusden, D., 2009. Infield logistics planning for crop-harvesting operations. *Engineering Optimization, 41*(2), 183-197.

Benson, E. R., Hansen, A. C., Reid, J. F., Warman, B. L., Brand, M. A., 2002. Development of an in-field grain handling simulation in ARENA. *ASAE Paper*, 02-3104.

Bochtis D. D., Sorensen, C. G., 2009. The vehicle routing problem in field logistics part I. *Biosystems Engineering, 104*(4), 447-457.

Bochtis D. D., Sorensen, C. G., Green, O., Moshou, D., Olesen, J., 2010. Effect of controlled traffic on field efficiency. *Biosystems Engineering, 106*(1), 14-25.

Bochtis D. D., Sørensen, C. G., Jørgensen, R. N., Green, O., 2009. Modelling of material handling operations using controlled traffic. *Biosystems Engineering, 103*(4), 397-408.

Bochtis, D. D., Oksanen, T., 2009. *Combined coverage and path planning for field operations.* Paper presented at the Precision Agriculture, In: EJ van Henten, D. Goense, C. Lokhorst (Eds.), Proceedings of the 7th European conference on precision agriculture.

Bochtis, D. D., Sorensen, C. G., Busato, P., Hameed, I. A., Rodias, E., Green, O., Papadakis, G., 2010. Tramline establishment in controlled traffic farming based on operational machinery cost. *Biosystems Engineering, 107*(3), 221-231.

Bochtis, D. D., Sørensen, C. G., Busato, P., Berruto, R., 2013. Benefits from optimal route planning based on B-patterns. *Biosystems Engineering, 115*(4), 389-395.

Bochtis, D. D., Sørensen, C. G. C., Busato, P., 2014. Advances in agricultural machinery management: A review. *Biosystems Engineering, 126*(0), 69-81.

Bochtis, D. D., Vougioukas, S. G., 2008. Minimising the non-working distance travelled by machines operating in a headland field pattern. *Biosystems Engineering, 101*(1), 1-12.

Bochtis, D. D., Vougioukas, S. G., Griepentrog, H. W., 2009. A Mission Planner for an Autonomous Tractor. *Transactions of the ASABE, 52*(5), 1429-1440.

Busato, P., Berruto, R., 2014. A web-based tool for biomass production systems. *Biosystems Engineering, 120*(0), 102-116.

Busato, P., Sørensen, C. G., Pavlou, D., Bochtis, D. D., Berruto, R., Orfanou, A., 2013. DSS tool for the implementation and operation of an umbilical system applying organic fertiliser. *Biosystems Engineering, 114*(1), 9-20.

Busato, P., 2015. A simulation model for a rice-harvesting chain. *Biosystems Engineering, 129*(0), 149-159.

Busato, P., Berruto, R., Saunders, C., 2007. Optimal Field-Bin Locations and Harvest Patterns to Improve the Combine Field Capacity: Study with a Dynamic Simulation Model.

Cariou, C., Lenain, R., Berducat, M., Thuilot, B., 2010. *Autonomous Maneuvers of a Farm Vehicle with a Trailed Implement in Headland.* Paper presented at the ICINCO.

Choset, H., 2001. Coverage for robotics–A survey of recent results. *Annals of mathematics and artificial intelligence, 31*(1-4), 113-126.

de Bruin, S., Lerink, P., J. La Riviere, I., Vanmeulebrouk, B., 2014. Systematic planning and cultivation of agricultural fields using a geo-spatial arable field optimization service: Opportunities and obstacles. *Biosystems Engineering, 120*(0), 15-24.

Dubins, L. E., 1957. On Curves of Minimal Length with a Constraint on Average Curvature, and with Prescribed Initial and Terminal Positions and Tangents. *American Journal of Mathematics, 79*(3), 497-516.

Edwards, G., Brøchner, T., 2011. A method for smoothed headland paths generation for agricultural vehicles. Paper presented at the CIGR/NJF seminar 441–Automation and system technology in plant production.

Galceran, E., Carreras, M., 2013. A survey on coverage path planning for robotics. *Robotics and Autonomous Systems, 61*(12), 1258-1276.

Grisso, R. D., Jasa, P. J., Rolofson, D. E., 2002. Analysis of traffic patterns and yield monitor data for field efficiency determination. *Applied Engineering in Agriculture, 18*(2), 171-178.

Grisso, R. D., Kocher, M. F., Adamchuk, V. I., Jasa, P. J., Schroeder, M. A., 2004. Field efficiency determination using traffic pattern indices. *Applied Engineering in Agriculture, 20*(5), 563-572.

Hameed, I. A., 2014. Intelligent Coverage Path Planning for Agricultural Robots and Autonomous Machines on Three-Dimensional Terrain. *Journal of Intelligent & Robotic Systems, 74*(3-4), 965-983.

Hameed, I. A., Bochtis, D. D., Sorensen, C. G., 2011. Driving Angle and Track Sequence Optimization for Operational Path Planning Using Genetic Algorithms. *Applied Engineering in Agriculture, 27*(6), 1077-1086.

Hameed, I. A., Bochtis, D. D., Sorensen, C. G., Noremark, M., 2010. Automated generation of guidance lines for operational field planning. *Biosystems Engineering, 107*(4), 294-306.

Hameed, I. A., Bochtis, D. D., Sorensen, C. G., Vougioukas, S., 2012. An object-oriented model for simulating agricultural in-field machinery activities. *Computers and Electronics in Agriculture, 81*(0), 24-32.

Hameed, I. A., Bochtis, D. D., Sørensen, C. G., Jensen, A. L., Larsen, R., 2013. Optimized driving direction based on a three-dimensional field representation. *Computers and Electronics in Agriculture, 91*(0), 145-153.

Holpp, M., Kroulik, M., Kviz, Z., Anken, T., Sauter, M., Hensel, O., 2013. Large-scale field evaluation of driving performance and ergonomic effects of satellite-based guidance systems. *Biosystems Engineering, 116*(2), 190-197.

Hunt, D., 2001. *Farm Power and Machinery Management* (Tenth ed.). Ames, Iowa Iowa State Press.

Jensen, M. A. F., Bochtis, D. D., 2013. Automatic Recognition of Operation Modes of Combines and Transport Units based on GNSS Trajectories. Paper presented at the Agricontrol.

Jin, J., 2009. Optimal field coverage path planning on 2D and 3D surfaces. *Graduate Theses and Dissertations.* Paper 11054.

Jin, J., Tang, L., 2010. Optimal Coverage Path Planning for Arable Farming on 2d Surfaces. *Transactions of the ASABE, 53*(1), 283-295.

Jin, J., Tang, L., 2011. Coverage Path Planning on Three-Dimensional Terrain for Arable Farming. *Journal of Field Robotics, 28*(3), 424-440.

Ntogkoulis, P. A., Bochtis, D. D., Fountas, S., Berruto, R., Gemtos, T. A., 2014. Performance of cotton residue collection machinery. *Biosystems Engineering, 119*(0), 25-34.

Oksanen, T., 2007. Path planning algorithms for agricultural field machines. Helsinki University of Technology.

Oksanen, T., 2013. Shape-describing indices for agricultural field plots and their relationship to operational efficiency. *Computers and Electronics in Agriculture, 98*(0), 252-259.

Oksanen, T., Visala, A., 2007. Path planning algorithms for agricultural machines. Agricultural Engineering International: the CIGR Ejournal. Manuscript ATOE 07 009. Vol. IX. July, 2007.

Oksanen, T., Visala, A., 2009. Coverage path planning algorithms for agricultural field machines. *Journal of Field Robotics, 26*(8), 651-668.

Palmer, R. J., Wild, D., Runtz, K., 2003. Improving the efficiency of field operations. *Biosystems Engineering, 84*(3), 283-288.

Renoll, E., 1981. Predicting Machine Field-Capacity for Specific Field and Operating-Conditions. *Transactions of the Asae, 24*(1), 45-47.

Sabelhaus, D., Roben, F., Helligen, L. P. M. Z., Lammers, P. S., 2013. Using continuous-curvature paths to generate feasible headland turn manoeuvres. *Biosystems Engineering, 116*(4), 399-409.

Spekken, M., de Bruin, S., 2013. Optimized routing on agricultural fields by minimizing maneuvering and servicing time. *Precision Agriculture, 14*(2), 224-244.

Spekken, M., Molin, J. P., Romanelli, T. L., 2015. Cost of boundary manoeuvres in sugarcane production. *Biosystems Engineering, 129*, 112-126.

Sørensen, C. G., Bochtis, D. D., 2010. Conceptual model of fleet management in agriculture. *Biosystems Engineering, 105*(1), 41-50.

Sørensen, C. G., Møller, H. B., 2006. Operational and economic modeling and optimization of mobile slurry separation. *Applied Engineering in Agriculture, 22*(2), 185-193.

Sørensen, C. G., Nielsen, V., 2005. Operational analyses and model comparison of machinery systems for reduced tillage. *Biosystems Engineering*, 92(2), 143-155.

Taylor, R. K., Schrock., M. D., Staggenborg., S. A., 2002. Extracting Machinery Management Information from GPS Data. *ASABE,St. Joseph, Michigan.*

Witney, B., 1996. Choosing and Using Farm Machines, 1996. *Land Technology Ltd, Scotland, UK*.

Zandonadi, R. S., 2012. Computational Tools for Improving Route Planning in Agricultural Field Operations. Theses and Dissertations-Biosystems and Agricultural Engineering. Paper 11.